University of Salerno

Department of Chemistry and Biology "A. Zambelli"

and

University of Basilicata

Department of Science

Ph.D. in Chemistry

Cycle XXXIII 2017-2020

Thesis on

CAPSICUM ANNUUM L. cv SENISE AND
SOLANUM AETHIOPICUM L. cv ROTONDA:
PHYTOCHEMICAL PROFILE
AND CELL-BASED ASSAYS

Ph.D. Student: Chiara Sinisgalli

Matriculation number 8800100041

Chiara Sinisgalli

TUTOR
Prof. Angela Ostuni

Angela Ostuni

CO-TUTOR
Prof. Maria Antonietta
Castiglione Morelli

MA Castiglione Morelli

COORDINATOR
Prof. Claudio
Pellecchia

Academic Year 2019/2020

Il bene supremo al quale l'uomo
deve tendere è la conoscenza.
È grazie alla conoscenza
se si è giunti fin qui e senza di essa
non possono affermarsi
tutti gli altri valori fondamentali
dei quali l'uomo sente il bisogno
per vivere con consapevolezza.
L'umanità dunque non deve smettere
di conoscere e di indagare
lasciando che la conoscenza
vada in ogni direzione e in ogni luogo,
tendendo verso l'uomo
e non in direzione contraria.
In particolare, in un mondo
governato dal benessere,
dobbiamo preoccuparci e occuparci
di quelle parti del nostro pianeta
in cui si lotta quotidianamente
per la sopravvivenza.
La felicità non esiste, è solo un attimo,
ma per il resto bisogna sforzarsi
di vivere con la serenità di chi
apprezza e ama la vita,
cercando di far prevalere sempre
l'ottimismo sul pessimismo
che è un sentimento sterile.
La serenità si raggiunge
con l'amore verso noi stessi,
verso il prossimo, nella comprensione
e nell'accettazione dei nostri errori.
Lasciatevi travolgere
dalla dedizione verso il prossimo
e otterrete la serenità.

La conoscenza - Rita Levi Montalcini

Alla fenice che rinasce….

sempre*!*

Summary

LIST OF FIGURES

LIST OF TABLES

ACKNOWLEDGEMENTS

Thanks to Professoressa Angela Ostuni and Professoressa Maria Antonietta Castiglione Morelli, for allowing me to carry out this path.

Thanks to Professor Luigi Milella, Dani, Imma and all Millelliani's group

Thanks to all people of Professor Bisaccia Lab without forgetting the cell chamber and my cells.

Thanks to my family, my love and my friends for their presence and support.

Thanks to myself and my madness

ABBREVIATIONS

ABCA1, ATP-binding cassette transporter A1

ABCG2, ATP-binding cassette transporter G2

ABCG5, ATP-binding cassette transporter G5

ABCG8, ATP-binding cassette transporter G8

AMPK, AMP-activated protein kinase

BIP, binding immunoglobulin protein

Caco-2 cell line, colorectal adenocarcinoma cell line

CAE, *Capsicum annuum* extract

CAT, catalase

CHOP, C/EBP homologous protein

COX-1, cyclooxygenase-1

CPT1A, carnitine palmitoyl transferase 1A

CTRL, control

ER, endoplasmic reticulum

GLUT1, glucose transporter type 1

GPX, glutathione peroxidase

GSK, glycogen synthase kinase

HepG2 cell line, human hepatoma cell line

HMG-CoA reductase, 3-hydroxy-3-methyl-glutaryl-CoA reductase

IFN-γ, interferon-γ

IL-4, interleukin-4

IL-6, interleukin-6

IRS-1, insulin receptor substrate-1

LC-MS/MS, Liquid chromatography-mass spectrometry

LDLr, low density lipoprotein receptor

NQO1, NADPH-quinone oxidase 1

Nrf2, nuclear factor erythroid 2-related factor 2

OA, oleic acid

ORAC, Oxygen Radical Absorbance Capacity assay

PTP1B, protein tyrosine phosphatase 1B

ROS, reactive oxygen species

RT-PCR, Real Time Polymerase chain reaction

SAE, *Solanum aethiopicum* extract

SOD, superoxide dismutase

SREBP-1, sterol regulatory element-binding protein 1

UCP2, uncoupling protein-2

ABSTRACT

Natural products rich in health-promoting compounds could represent new potential therapy strategy in many diseases.

In the present study we focus our attention on *Capsicum annuum* L. cv Senise and *Solanum aethiopicum* L. cv Rotonda, two typical products of Basilicata region and source of health-promoting compounds. Particularly, we investigated molecular pathways involved in anti-obesity activity demonstrated in mice fed with high fat diet.

Firstly, antioxidant activity of samples was evaluated in HepG2 cell line. Cells were pre-treated with different doses of the extracts and ROS generation was measured by flow cytometry. Expression of several markers involved in antioxidant defence was evaluated by qRT-PCR in order to understand molecular mechanism responsible of the activity.

Oxidative stress characterized several pathology conditions. About obesity, prolonged exposure of excess of fat induced weight gain but also ROS and pro-inflammatory cytokines generation. Hypolipidemic, antioxidant and anti-inflammatory activity of the extracts were evaluated in HepG2 and Caco-2 cell line used as model. Lipid accumulation was morphologically evaluated by Oil red O staining and the expression of several markers involved in lipid metabolism, antioxidant defense and inflammatory status was measured by qRT-PCR. Both extracts reduced fat accumulation in OA-treated HepG2 cell line by reducing *de novo* lipogenesis and improved intestinal lipid absorption. Moreover, both extracts enhance the activity of antioxidant enzymes severely compromised in obesity.

Obesity is also associated with diabetes type 2 and cardiovascular risk. Senise pepper influenced the expression of some gene involved in insulin signalling pathway improving glucose uptake as demonstrated by 2-NBDG assay and ^{1}H-NMR analysis. In addition, Senise pepper demonstrated cardioprotective effect by improving endothelial dysfunction in obese mice (in collaboration with Universidad de Granada) due to inhibition of NADPH oxidase and antioxidant and anti-inflammatory activity demonstrated in OA-treated cells and splenocytes (in collaboration with Laboratory of Immunotherapy, Institute of Microbiology of the Academy of Science Czech in Prague).

Finally, LC-MS was performed in order to identify the specialized compounds responsible of biological activity of *C.annnum* L. cv Senise and *S. aethiopicum* L. cv Rotonda

Chapter 1

INTRODUCTION

Nowadays, medicinal plants and nutraceuticals or functional foods have witnessed great interest in treatment of human diseases due to the presence of health promoting compounds (Brandt et al. 2004). They are products of secondary metabolism not essential for life sustaining process such as energy acquisition or photosynthesis. For a long time they are known as "*secondary metabolites*" but for their structural diversity and their specificity for certain cell types, development stages or environmental stimuli, now they are defined also "*specialized metabolites*" (Zhao et al. 2020). They are classified in different classes like terpenes or terpenoids, phenolic compound (as flavonoids, anthocyanins, lignins, tanins, phenolic acids), and nitrogen containing compounds (as alkaloids). Secondary metabolites present in fruits and in plants increase their attractiveness to seed dispersers and protect against biotic and abiotic stresses. Moreover, many organoleptic characteristics like aroma, color and fruit nutritional value depends on secondary metabolite content. Polyphenols are found largely in the fruits, vegetables, cereals. Epidemiological studies reported as diets rich in plant and food polyphenols protect against development of cancers, cardiovascular diseases, diabetes, obesity, neurodegenerative diseases (Lamorte et al. 2018). It is well known that polyphenols exert antioxidant activity directly by acting as electron acceptor and indirectly by promoting the expression of several markers involved in antioxidant defense. In this way polyphenols counteract the oxidative stress which characterizes several human diseases. In addition, they exert cardio-protective, anti-inflammatory, anti-cancer, anti-diabetic, anti-aging effect by acting on different molecular pathways. For example, resveratrol, an abundant stilbene found in red wine, protects from atherosclerosis by preventing platelet aggregation via preferential inhibition of cyclooxygenase-1 (COX-1) activity, which synthesizes thromboxane A2, an inducer of the platelet aggregation and vasoconstrictor (Wiciński et al. 2018). In addition, resveratrol promotes vasodilatation by enhancing nitric oxide signaling pathway, reducing in this way cardiovascular disease (Xia et al. 2017). Thus, in contrast to synthetic pharmaceuticals based upon single chemicals, many phytomedicines exert their beneficial effects through the additive or synergistic action of several chemical compounds acting at single or multiple target sites associated with a physiological process. In addition, natural products could solve adverse effects associated with the predominance of a single xenobiotic compound in the body and could represent new and safe therapeutic strategies (Briskin 2000).

In the present work thesis, we focus our attention on different molecular pathways involved in a complex disease as obesity and on the search of new therapeutic strategies. Obesity is the results of a sustained imbalance between energy intake and energy expenditure. A chronic excess of nutrients induces an adaptive change in adipose tissue, the main organ involved in the accumulation of excess energy in the form of triglycerides. In addition to adipocyte hypertrophy, there is a functional change with impaired secretion of adipokines. Furthermore, the cellular composition changes with infiltration of activated macrophages, T lymphocytes and dysfunctional adipocytes. This results in increased expression and secretion of pro-inflammatory adipokines capable of determining a systemic level of low-grade inflammation, worsening insulin sensitivity and helping the development of metabolic and cardiovascular complications associated to obesity.

Thus, different are the mechanisms involved which could represent targets for drug therapy. Currently, anti-obesity drugs act through the inhibition of the digestion and absorption of nutrients. Example Orlistat reduces triglyceride digestion and absorption by inhibiting pancreatic lipase activity. In addition to anti-obesity drugs focused on reduction of fat absorption, there are other categories of drugs acting by suppressing appetite, by increasing energy expenditure or by redistributing adipose tissue. For example, sibutramine is a central inhibitor of monoamine uptake but side effects outweigh the beneficial effects. However, side effects often outweigh the beneficial effects.

Natural products could be a good and alternative option in prevention and treatment of obesity. Many studies reported as polyphenols and other bioactive compounds can reduce food intake and appetite by acting on digestive enzyme and central nervous system. Unlike synthetic drugs, natural compounds are widely recognized for their antioxidant and anti-inflammatory properties which could play an important to counteract the systemic low grade of inflammation in obese tissue.

Source of health-promoting compounds are two typical food of Basilicata region:
Capsicum annuum L. cv Senise and *Solanum aethiopicum* L. cv Rotonda.

Figure 1.1 *Capsicum annuum* L.cv Senise

***Capsicum annuum* L. cv Senise** (Solanaceae) is a sweet pepper cultivated in Basilicata region. It is typical of the culture and gastronomical tradition of the valley between Sinni and Agri rivers. It is similar to hot pepper but it is sweet. It has a conical shape and a medium length of 15cm. The ripe fruit is deep-red. The peppers are planted between March and February and they are harvested at the begin of August. Traditionally it is sun-dried threaded onto strings called *"serte"* and then eaten fried ("*cruschi peppers*") or powdered and used as spice. Pepper powder is similar to saffron, red and precious, indeed are known also as *"Safràn"*. For this reason, it is known also as "the red gold of Basilicata region". In 1996 it gained the protected geographical identification (IGP).

In addition to being a typical product, it is also a source of health-promoting compounds responsible of *in vitro* antioxidant and potential hypoglycemic activity (Loizzo et al. 2008, Pascale et al. 2020), but also of anti-obesity activity demonstrated in our previous study (Sinisgalli, et al. 2020). Molecular pathways involved as well as health promoting compounds responsible for the activity are not yet known and will be investigated in the present work.

Figure 2.2 *Solanum aethiopicum* L.cv Rotonda

Solanum aethiopicum L. (Solanaceae) or Scarlet eggplant is one of the most commonly consumed vegetable in tropical Africa. At the beginning of last century some Lucanian emigrants in Africa decided to return to their native land carrying with them the seeds of this plant, with the complicity of the World War, the already poor people of the area find an important food in this particular eggplant with red fruits like tomatoes but with a spicy slightly bitter taste. It is cultivated in Rotonda and other countries of National Pollino Park. It is part of the Slow Food Foundation catalogue and entered the Protected Designation of Origin category (DOP).

In indigenous medicine *S.aethiopicum* has a wide range of utilization like weight reduction, asthma, allergic diseases, gastro-esophageal reflux disease, constipation and dyspepsia. Root and fruits have been used as a carminative and sedative and to treat colic

and high blood pressure. Scientific studies supported the use of this plant in the treatment of inflammation, diabetes, excessive weight gain.

Up to now no study evaluate biological activity and chemical composition of *Solanum aethiopicum* cv Rotonda.

chapter 2

AIM OF THE THESIS

The general goal of this thesis was:

To investigate phytochemical profile and biological activity of two local foods of Basilicata region *Capsicum annuum* L. cv Senise and *Solanum aethiopicum* cv Rotonda.

Oxidative stress characterizes many pathological conditions and different studies report as the consumption of food and vegetables rich in antioxidants play a protective and preventive role in several diseases. Therefore, the first specific aim of this work was:

1. *To investigate the antioxidant activity of Senise pepper and Rotonda eggplant on HepG2 cell line used as model identifying biological markers and bioactive compounds involved in the observed effect.*

Among different diseases characterized by an excess of free radicals, there is the obesity. Prolonged exposure to excess of fat induces fat accumulation in adipose tissue and then in liver, the main organ involved in lipid metabolism and trafficking. Excess of fatty acids also causes pro-inflammatory cytokines production and ROS generation involved in several metabolic disorders associated to obese condition. For this reason, the second aim was:

2. *To study the hypolipidemic effect of the extracts in OA-treated HepG2 and Caco-2 cell lines. Particularly, we evaluated the effect on markers of lipid metabolism but also markers involved in oxidative stress and inflammatory status associated to fat accumulation.*

ROS and pro-inflammatory cytokines can affect other tissues like vascular endothelium and other pathways like insulin signaling cascade. In this way, excess of fat, ROS and pro-inflammatory cytokines induced type 2 diabetes and cardiovascular diseases often associated to obesity. Thus, the third aim was:

3. *To evaluate the protective effect of Capsicum annuum cv Senise in splenocytes and vascular endothelium and its potential ability to reduce insulin resistance and improve hyperglycemia.*

Finally,

4. *Senise pepper and Rotonda eggplant extract were encapsulated in liposomes, promising drug carriers by enhancing the membrane penetration of drugs, delivering the entrapped drugs across cell membranes, and improving extract stability and bioavailability.*

Chapter 3

EXPERIMENTAL DESIGN

A work-flow was reported to describe the different step of this thesis. Different experimental techniques were used to evaluate biological activities of *Capsicum annuum* L. cv Senise and *Solanum aethiopicum* L. cv Rotonda. Spectrophotometry assays were used carried out to preliminary investigate the biological activity of the extracts, then confirmed by cell models.

For the investigation, different cell-based assays were performed. Cell cultures are widely used as model system to study cellular biochemistry and physiology, the effects of drugs and toxic compounds on the cells, mutagenesis and carcinogenesis, drug screening and development and large-scale manufacturing of biological compound (vaccines, grow factors, monoclonal antibody). Although they are different from *in vivo* conditions, cell culture represent a simplified and reproducible experimental model.

Immortalized cell lines were used in this work thesis since they are easier to handle and of broader use than primary cells which live shortly in culture and have low reproducibility. Human hepatoma cell line (HepG2) and colorectal adenocarcinoma cell line (Caco-2) were used as experimental models to study biomarkers and different pathways affected by the excess of fat in liver and intestine, the main organs involved in lipid metabolism, absorption and secretion. HepG2 cell line shows many of the specialized functions that characterize human hepatocytes and treated with oleic acid is traditionally used as steatosis model (Kanuri and Bergheim 2013). Caco-2 cell line express several morphological and functional properties characteristic of normal human intestinal epithelium and these cells are used for studies on the absorption of drugs and other compounds after oral intake in humans (Lea 2015).

Quantitative real time polymerase chain reaction (qRT-PCR) was performed to study the expression of several markers and identify molecular pathways involved in biological activity together with metabolome analysis through ^{1}H-NMR.

The experimental procedure will be described in detail in the material and methods of each section of Chapter 4.

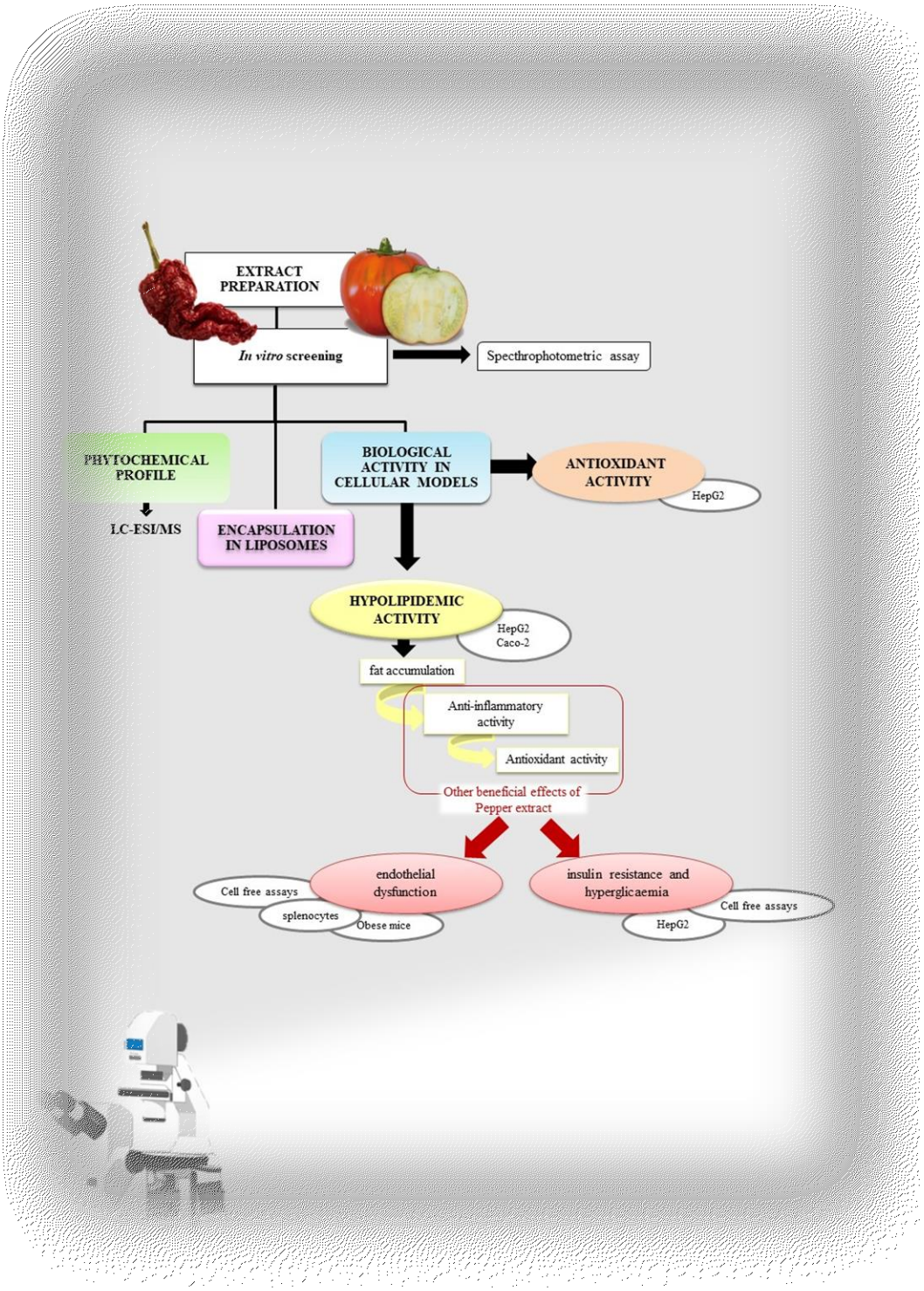

Figure 3.1 Experimental design

Chapter 4

RESULTS

4.1 Phytochemical profile and antioxidant activity

4.1.1 Phytochemical Profile of *Capsicum annuum* L. cv Senise, incorporation into Liposomes, and evaluation of cellular antioxidant activity

Published online 2020 May 15. doi: 10.3390/antiox9050428.
Sinisgalli, C., Faraone, I., Vassallo, A., Caddeo, C., Bisaccia, F., Armentano, M. F., ... & Ostuni, A. (2020). Phytochemical profile of Capsicum annuum L. cv Senise, incorporation into liposomes, and evaluation of cellular antioxidant activity. Antioxidants, 9(5), 428.

Introduction

Every day, several factors, such as pollution, cigarette smoking, drugs, physical inactivity, and excessive alcohol consumption, can increase the production of free radicals and alter the homeostasis of the body (Flora, 2007). The increase in free radicals, resulting in oxidative stress, is implicated in the aetiology of several major human ailments, including cancer, cardiovascular diseases, neural disorders, diabetes, and arthritis.

Many studies have reported that a high intake of fruits, spices, and vegetables rich in polyphenols is linked to lower risk of chronic and degenerative diseases (Faraone et al. 2018; Zhang et al. 2016). The biological activities of polyphenols have been attributed to their chemical structures, which make these compounds good electron or hydrogen atom donors capable of neutralizing free radicals (Zhang et al. 2016) and thus restoring redox homeostasis. Moreover, they promote the expression of antioxidant enzymes involved in organism defences such as catalase (CAT) superoxide dismutase (SOD) and glutathione peroxidase (GPX) (Kaulmann et al. 2014; Mignet et al 2013).

Despite their health-promoting properties, polyphenols have a weak oral bioavailability due to their low water solubility, poor absorption, and rapid metabolism (Mignet et al 2013). These problems can be tackled by using different drug delivery approaches, which can enhance polyphenols bioavailability and thus their therapeutic efficacy. Liposomes represent an optimal delivery system due to the morphological similarity with cell

membranes and the ability to entrap both lipophilic and hydrophilic compounds that should be delivered to a specific target site (Bozzuto et al. 2015).

Capsicum annuum L. cultivar Senise (Solanaceae) is a sweet pepper cultivated in the Basilicata region (Italy). Traditionally, it is sun-dried and eaten fried ("cruschi peppers") or powdered and used as a spice. The "red gold of the Basilicata region", as it is called for its similarity with saffron, is a very precious and important source of health-promoting compounds. Until now, few studies have investigated the biological activity and chemical composition of this pepper cultivar (Loizzo et al. 2013; Speranza et al. 2019). Particularly, they reported the antioxidant activity and potential hypoglycemic activity *in vitro* (Loizzo et al. 2013), which were ascribed to the presence of health-promoting compounds, such as carotenoids, polyphenols, terpenes, and ascorbic acid (Loizzo et al. 2013; Speranza et al. 2019; Moudache et al. 2016).

The aim of this study was to investigate the phytochemical profile of an ethanol extract of *Capsicum annuum* L. cultivar Senise and its antioxidant activity on cells. The HepG2 cell line was used as a model in the present work because its cells show many of the specialized functions that characterize human hepatocytes and they live longer than primary hepatocytes, improving the reproducibility (Aversano et al. 2017; Tuberoso et al. 2018). The advantage provided by liposomal incorporation was evaluated. Furthermore, the molecular signalling pathways involved in the antioxidant activity of the extract were assessed. As far as we are aware, this is the first study that reports the biological activity of *C. annuum* extract in cells or incorporated in a vesicular carrier system.

Materials and Methods

Chemicals

Absolute ethanol, sodium phosphate monobasic (NaH_2PO_4), fluorescein, 2,2′-azobis (2-amidinopropane) dihydrochloride (AAPH), Dulbecco's Modified Eagle Medium (DMEM), dimethyl sulfoxide (DMSO), [3-(4,5-dimethyl-2-thiazolyl)-2,5-diphenyl-2H-tetrazolium bromide] (MTT), 2′,7′-dichlorodihydrofluorescein diacetate (DCFH-DA), *N*-acetyl-*L*-cysteine (NAC), and *tert*-butyl hydroperoxide (*t*-BuOOH) were purchased from Sigma Aldrich S.p.A. (Milan, Italy). Trypsin-EDTA solution, fetal bovin serum (FBS), glutamine, penicillin-streptomycin, and phosphate saline buffer (PBS) were purchased from Euroclone (Milan, Italy). Reagents used for RT-PCR were purchased from Euroclone (Milan, Italy). Solvents used for LC-ESI/LTQOrbitrap/MS extraction and

water were purchased from VWR (Milan, Italy), while acetonitrile and formic acid were purchased from Merck (Merck KGaF, Darmstadt, Germany). Standards for LC-MS/MS were purchased either from Sigma Aldrich S.p.A. (Milan, Italy). Milli-Q water was obtained from Mill-Q purification system (Millipore, Bedford, MA, USA).
Phospholipon 90G (>90% phosphatidylcholine; P90G) was purchased from Lipoid GmbH (Ludwigshafen, Germany).

Extract Preparation

Sun-dried red peppers were kindly provided by "Azienda agricola Casata del Lago" (Senise, Potenza, Italy; 40°08′35.1"N 16°18′55.3"E) during October 2016. Dried fruits (500 g) without seeds and petiole were cut into small pieces and extracted by maceration with absolute ethanol (1.2 L) in the dark at room temperature for 48 h. The extraction procedure was repeated three times. *C. annuum* extract (CAE) (yield of 11.70% *w*/*w*) was filtered with filter paper and dried by means of a rotary evaporator (IKA RV 10). Then, it was stored in the dark at room temperature.

LC-ESI/LTQOrbitrap/MS

The phytochemical characterization of CAE was carried out by an in-house HPLC method coupled with a mass spectrometer, which associates the linear trap quadrupole with an OrbiTrap mass analyzer. LC-ESI/LTQOrbitrap/MS analyses were performed in positive and negative ion modes using an Accela 600 HPLC system (Thermo Scientific, Bremen, Germany) coupled to an LTQ OrbiTrap XL mass spectrometer (Thermo Scientific, Bremen, Germany). Separation was achieved using a Luna 2.5 μm C18 (100 mm × 2.10 mm) column (Phenomenex, Aschaffenburg, Germany).
The employed mobile phases were water + 0.1% formic acid (solvent A) and acetonitrile (solvent B). The flow rate was 0.2 mL/min, and the gradient was as follows: 2% of B at 0 min until 1 min, 40% at 21 min, 95% at 22 min until 25 min, returning to 2% of B at 26 min until 35 min.
MS settings were as follows: in positive ion mode, source voltage 3 kV, capillary voltage 49 V, tube lens voltage 120 V; in negative ion mode, source voltage 5 kV, capillary voltage −48 V, tube lens voltage −176.47 V. Capillary temperature for both positive and negative ion modes was 280 °C. MS spectra were acquired by full range acquisition covering *m/z* 150–1000.

Data were acquired using Xcalibur software version 2.1, and for fragmentation studies, a data dependent scan experiment was carried out selecting precursor ions as the most intensive peaks in the LC-MS analysis.Identification of compounds was based on retention times, accurate mass measurements, MS/MS data, exploration of specific spectral libraries and public repositories for MS-based metabolomic analysis (*MassBank MoNA, MassBank NORMAN, PubChem*), and comparison with data reported in the literature (Muhammad et al. 2012; Muhammadet al. 2016; Cottiglia et al. 2005; Wahyuni et al. 2011; Xavier et al. 2014; Devari et al. 2014; Yogendrarajah et al. 2013; Kawaguchi et al. 2004; Marín et al. 2004; Sricharoenet al. 2017; Marincaş et al. 2018).

Oxygen Radical Absorbance Capacity (ORAC) assay

According to Moudache et al. 2016, 25 µL of different concentrations of (0.01-0.2 mg/mL) CAE were incubated in a 96-well microplate with 125 µL of fluorescein (10 nM in 75 mM NaH_2PO_4 buffer at pH 7.4) for 30 min at 37 °C. Then, 25 µL of 10 mM AAPH was added to each well and fluorescence was recorded (λ_{ex} 485 nm and λ_{em} 520 nm) every 2 min for 90 min using a GLOMAX Multidetection System (Promega, Madison, WI, USA). Trolox (0–100 µM) was used as the reference standard. Results were calculated on the basis of differences in areas under the fluorescence decay curve between the blank, samples, and standards. Final oxygen radical absorbance capacity (ORAC) values were expressed as µmol of Trolox equivalents (TE)/100 g of dried extract.

Liposome Preparation and Characterization

For the preparation of liposomes, 90 mg/mL of P90G and 2 mg/mL of CAE were weighed in a glass vial, dispersed in water, and sonicated (25 cycles, 5 s on and 2 s off; 13 µm of probe amplitude) with a high intensity ultrasonic disintegrator (Soniprep 150, MSE Crowley, London, UK). Empty liposomes (i.e., without extract) were prepared under the same conditions as extract-loaded liposomes.

The average diameter (i.e., the intensity weighed mean hydrodynamic size), polydispersity index (P.I., a dimensionless measure of the broadness of the size distribution), and zeta potential of the liposomes were determined by dynamic and electrophoretic light scattering using a Zetasizer nano-ZS (Malvern Instruments, Worcestershire, UK). Samples (n > 10) were diluted with bidistilled water (1:100 *w/v*) and analyzed at 25 °C.

The stability of liposomes was evaluated by long-term stability tests, i.e., by analyzing vesicle average diameter, P.I., and zeta potential over two months at 25 °C.

Cell Line and Culture Conditions

Human hepatocellular carcinoma cell line (HepG2) cells were cultured in DMEM (supplemented with 10% fetal bovine serum, 2 mM glutamine, 100 U/mL penicillin, and 100 µg/mL streptomycin) and maintained at 37 °C in a humidified atmosphere containing 5% CO_2. The CAE was dissolved in EtOH/DMSO and different concentrations were tested (10–200 µg/mL). EtOH/DMSO-treated cells were used as the control (CTRL) in all the experiments.

MTT Assay

Cell viability was evaluated on HepG2 cells by the MTT assay, a colorimetric assay based on the conversion of the yellow tetrazolium salt MTT into purple insoluble formazan by the succinate dehydrogenase enzyme of viable cells. HepG2 cells were seeded in a 96-well plate (1.5×10^4 cells/well), incubated overnight, and treated with different concentrations (10-200 µg/mL) for 24 and 48 h. After removal of the medium, the cells were washed with PBS and incubated with 0.75 mg/mL of MTT solution in PBS for 4 h. Then, the solution was removed and the cells were lysed using a solubilization solution (1:1 DMSO:isopropanol). The solubilized formazan product was spectrophotometrically quantified at 560 nm using a UV–Vis spectrophotometer (SPECTROstar^{Nano} BMG Labtech, Ortenberg, Germany).

Measurement of Intracellular Reactive Oxygen Species (ROS)

The intracellular reactive oxygen species (ROS) level was measured by DCFH-DA (Chercar et al. 2019). HepG2 cells were plated at a density of 1×10^4 cells/well in a 24-well plate, incubated with different concentrations of CAE *(*10-200 µg/mL), liposomes, or 10 mM NAC for 24 h, and stressed with 5 mM *t*-BuOOH for 1 h. Finally, the cells were stained with 10 µM DCFH-DA for 30 min at 37 °C in the dark, and fluorescence was measured by BD FACSCanto II (BD Pharmingen, San Jose, CA, US) (λ_{ex} 485 nm and λ_{em} 515–540 nm).

Quantitative RT-PCR

HepG2 cells were treated with different concentrations of CAE (200–100 µg/mL) for 24 h. RNA was extracted using Quick-RNA MiniPrep kit (Zymo Research, Irvine, CA, USA) and then was transcribed to cDNA using random primers and a High-Capacity cDNA Reverse Transcription Kit (ThermoFisher scientific, Waltham, MA, USA, Life Technologies Corporation, Carlsbad, CA USA). The cDNA was amplified via real-time PCR using iTaqTM Universal SYBR® Green Supermix (Bio-Rad) by the 7500 Fast Real-Time PCR System (Applied Biosystems, Foster City, CA, USA). Primers were designed for spanning exon–exon junctions, eliminating undesirable genomic DNA amplification. The comparative threshold cycle method (ΔΔCt) was used to quantify the relative amounts of product transcripts with *β*-actin as the housekeeping gene (Armentano et al. 2018). The specificity of amplicons was confirmed by melting-curve analysis. Each test was performed in triplicate.

Statistical Analysis

Data were expressed as mean ± standard deviation (Mean ± SD). Statistical analysis was performed using GraphPad Prism 5 Software, Inc. (San Diego, CA, USA) and p values $\leq$ 0.05 were considered as statistically significant.

Results

Phytochemical Profile of C. annuum Extract

Qualitative analysis of CAE was performed by LC-ESI-Orbitrap-MS and LC-ESI-Orbitrap-MS/MS analyses. The use of the Luna C18 column and LC-ESI-MS/MS (alternating positive and negative ionization modes) allowed for the simultaneous separation and identification of all compounds (non-polar and polar compounds) in the ethanol extract. With a short interscan delay of 0.3 s, a number of scans in each mode across each chromatographic peak were obtained.

This procedure allowed us to save time and use a lower amount of sample, recording injection positive and negative ion data. The developed LC-ESI-MS/MS method can easily be utilized as a fast and sensitive analytical tool for analysis of phytochemical profiles of Senise pepper. Data are showed in **Figure 4.1**. Individual components were identified by comparison of their *m/z* values in the total ion current profile with those of the selected compounds described in the literature. In particular, 24 compounds were

identified in CAE (**Table 4.1**) belonging to a wide variety of structurally different metabolic classes: phenols (*caffeic acid* and *2,4-di-tert-butylphenol*); capsinoids (*capsiate* and *dihydrocapsiate*); carotenoids (*β-carotene, capsorubin, antheraxanthin* and *β-cryptoxanthin*); sesquiterpenoids (*canusesnol F*); flavones (*luteolin, luteolin-apiosylacetyl–glucoside, apigenin-6,8-di-C-glucoside, and vitexin*); flavonols (*isoquercetin, rutin, kaempferol-3-O-glucoside, kaempherol* and *myricetin*); flavan-3-ols (*catechin*); vitamins (*ascorbic acid and tocopherol*); and capsaicinoids (*nordihydrocapsaicin, capsaicin, and dihydrocapsaicin*).

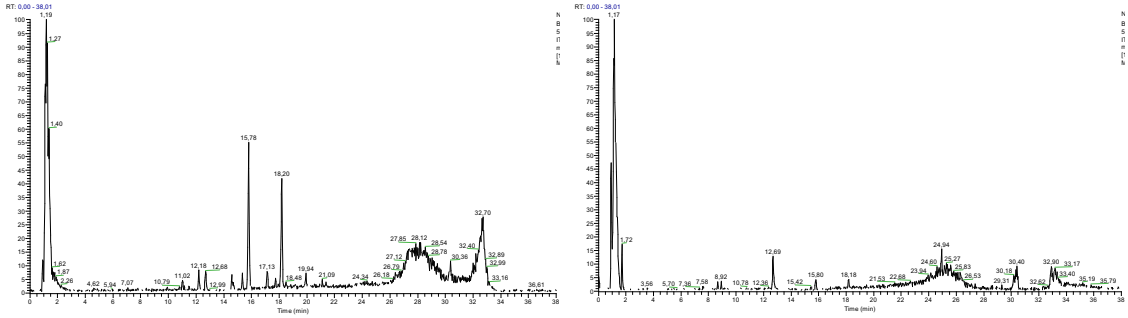

A) **B**)

Figure 4.1. LC-MS profile of *C. annuum* ethanol extract in negative (A) and positive (B) ion mode.

Table 4.1. Metabolites identified in *C. annuum* ethanol extract using LC-ESI/Orbitrap/MS/MS.

Compounds	**Rt**	**Molecular Formula**	**MW**	**$[M-H]^-$**	**$[M-H]^+$**	**MS/MS**
Caffeic acid	1.19	$C_9H_8O_4$	180. 0422	179		174, 135
Luteolin (apiosyl acetyl) glucoside	1.33	$C_{28}H_{30}O_{16}$	622.1533	621		327
Apigenin-6,8-di-*C*-glucoside	1.99	$C_{27}H_{30}O_{15}$	594.1584	593		473
Vitexin	2.34	$C_{21}H_{20}O_{10}$	432.1056	431		311, 283
Isoquercetin	4.95	$C_{21}H_{20}O_{12}$	464.0954	463		301
Rutin	5.64	$C_{27}H_{30}O_{16}$	610.1533	609		300, 179, 151
Kaempferol- 3-*O*-glucoside	6.01	$C_{21}H_{20}O_{11}$	448.1005	447		285
Catechin	33.08	$C_{15}H_{14}O_6$	290.0790	289		203
2,4-Di-tert-butylphenol	33.10	$C_{14}H_{22}O$	206.1670	205		189
Capsiate	33.11	$C_{18}H_{26}O_4$	306.1831	305		289, 151
Ascorbic acid	33.14	$C_6H_8O_6$	176.0320	175		157, 115, 112, 87
Dihydrocapsiate	1.10	$C_{18}H_{28}O_4$	308.1987		309	295, 278
Luteolin	1.29	$C_{15}H_{10}O_6$	286.0477		287	171, 153
Kaempherol	1.39	$C_{15}H_{10}O_6$	286.0477		287	241
Nordihydrocapsaicin	1.72	$C_{17}H_{27}NO_3$	293.1990		294	152
Tocopherol	7.80	$C_{29}H_{50}O_2$	430.3810		431	416
Myricetin	12.53	$C_{15}H_{10}O_8$	318.0375		319	227, 207
Capsaicin	15.56	$C_{18}H_{27}NO_3$	305.1990		306	227, 137

Dihydrocapsaicin	17.43	$C_{18}H_{29}NO_3$	307.2147	308	207, 122
β-carotene	18.22	$C_{40}H_{56}$	536.4382	537	353, 277
Canusesnol F	19.47	$C_{15}H_{22}O_4$	266.1518	267	247, 207
Capsorubin	26.62	$C_{40}H_{56}O_4$	600.4178	601	582, 411
Antheraxanthin	27.77	$C_{40}H_{56}O_3$	584.4229	585	145
β-cryptoxanthin	32.98	$C_{40}H_{56}O$	552.4331	553	461

Antioxidant Activity: ORAC Assay

The antioxidant activity of CAE was evaluated by the ORAC assay. As shown in **Figure 4.2**, the extract slowed fluorescein degradation by quenching the peroxyl radicals in a dose-dependent manner. An ORAC value of 38,144 µmol TE/100 g of DE was obtained by using the Trolox standard curve ($y = 0.48x - 3.38$; $R^2 = 0.99$).

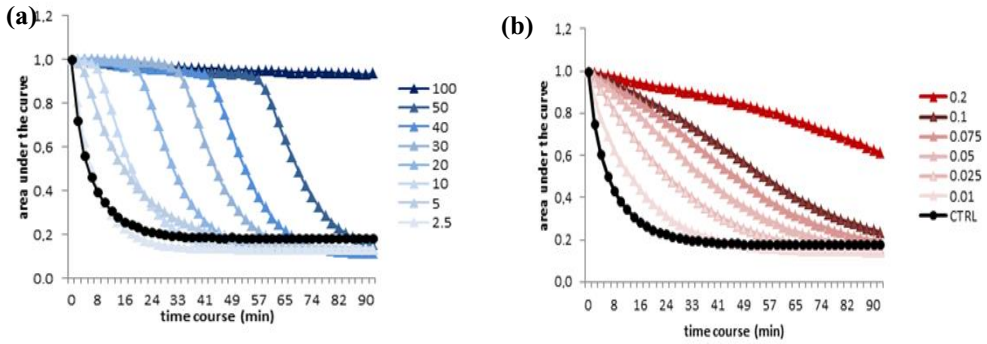

Figure 4.2 (**a**) Oxygen radical absorbance capacity (ORAC) assay for different concentrations (2.5–100 µM) of Trolox used as a standard. (**b**) ORAC assay for different concentrations (0.01–0.2 mg/mL) of CAE. Changes in the fluorescence intensity of fluorescein were monitored for 90 min.

Liposome Characterization

Liposomes were prepared by a simple, organic, solvent-free method involving the sonication of a phospholipid (P90G) and CAE in water. To evaluate the effect of the incorporation of the extract into the vesicle arrangement, empty liposomes (i.e., without extract) were also prepared and characterized.

Light scattering results, summarized in **Table 4.2**, showed that empty liposomes were small in size, around 80 nm, with good homogeneity (P.I. 0.28) and negative zeta potential (~-17 mV). The incorporation of CAE did not alter these values ($p > 0.05$), which points to a negligible effect of the extract on the vesicle assembly.

It is well known that the stability of liposomes is dependent on both formulation and manufacturing method parameters, and it is critical to establish safe and effective use of the liposomes. Therefore, the stability of the prepared liposomes was evaluated by monitoring the size, P.I., and zeta potential over two months of storage. The results showed no significant variations ($p > 0.05$) of the parameters examined, which indicates a good stability of the vesicle formulations.

Table 4.2. Characteristics of empty liposomes and *C. annuum*-loaded liposomes: intensity-weighed mean hydrodynamic diameter, polydispersity index (P.I.), and zeta potential.

	Mean Diameter (nm)	**P.I.#**	**Zeta Potential (mV)**
Empty liposomes	81.6 ± 6.8	0.28	−16.7 ± 3.7
C. annuum liposomes	83.8 ± 4.7	0.26	−17.5 ± 4.2

Each value represents the mean ± SD, $n > 10$; # SD for P.I. values was always < 0.03.

Effect of C. annuum extract on cell viability and intracellular ROS

The cell viability of CAE was evaluated on the HepG2 cell line, used as model cells, by the MTT assay. The extract was dissolved in EtOH/DMSO and the final concentrations (1.6% and 0.4%, respectively) of solvent used for HepG2 cell assays had no effect on cell viability. As shown in **Figure 4.3a**, the extract showed no cytotoxic effect after 24 and 48 h.

The protective effect of the extract against intracellular ROS was also investigated (**Figure 4.3b**). HepG2 cells were treated with different concentrations of extract (10–200 μg/mL) for 24 h and then oxidative stress was induced by *t*-BuOOH, known as a source of ROS. HepG2 cells stressed with *t*-BuOOH showed a 2-fold increase in fluorescence, as compared to untreated cells. The pre-treatment with the extract for 24 h reduced ROS levels dramatically, restoring the basal level similar to that of cells treated with NAC, a known antioxidant.

CAE was incorporated in liposomes to evaluate the effect of the formulation on its biological activity. More specifically, the protective effect of extract-loaded liposomes was evaluated in *t*-BuOOH–stressed HepG2 cells after 24 h of treatment (**Figure 4.3b**). The liposomes were tested at the same concentrations of the raw extract (10–200 μg/mL). It is interesting to note that when the extract was incorporated into liposomes, the ROS levels were significantly decreased (by 6 times vs. *t*-BuOOH control cells), already at 10 μg/mL, the lowest concentration tested, thus being twice as potent in comparison with both the raw extract and NAC (**Figure 4.3b**).

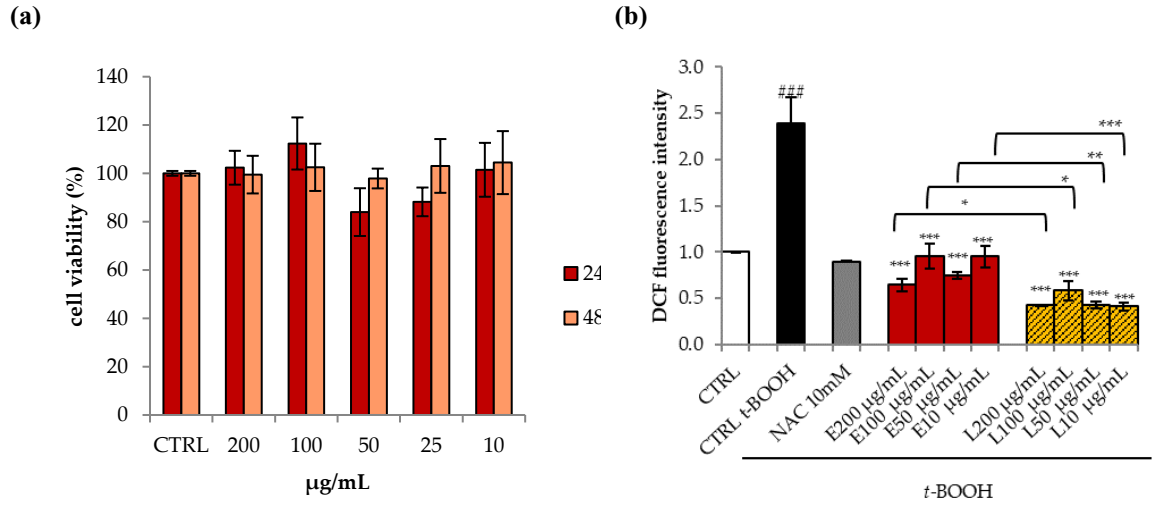

Figure 4.3. (a) Cell viability, evaluated by MTT assay, of HepG2 cells treated for 24 and 48 h with different concentrations of *C. annuum* extract (CAE). **(b)** Effects of CAE (E) and liposomes on *t*-BuOOH-induced intracellular reactive oxygen species (ROS) generation in HepG2 cells. Cells were pre-treated with the extracts or liposomes at different concentrations (10, 25, 50, 100, 200 µg/mL) for 24 h and subsequently incubated with 5 mM *t*-BuOOH for 1 h. ROS generation was measured by DCFH-DA staining with flow cytometry analysis. Data are expressed as the mean ± SD of three independent experiments ($n = 3$). $^{###}$ $p < 0.001$ *vs* CTRL, *** $p < 0.001$ *vs* *t*-BuOOH-treated cells, * $p < 0.05$, ** $p < 0.01$.

Effect of C. annuum extract on Gene Expression

HepG2 cells were treated with CAE (200 and 100 µg/mL) and the expression of some genes involved in antioxidant defense was evaluated by qRT-PCR. After 24 h of treatment, the extract did not affect the expression of genes, as compared to the control (CTRL) (**Figure 4.4**). In contrast, the extract upregulated the expression of SOD-2 and GPx-1 after 48 h, as well as the nuclear factor erythroid 2-related factor 2 (Nrf2) and ATP-binding cassette transporter G2 (ABCG2) (**Figure 4.4**). No statistical differences were found in the expression of catalase (CAT) and NADPH-quinone oxidase 1 (NQO1) (**Figure 4.4**).

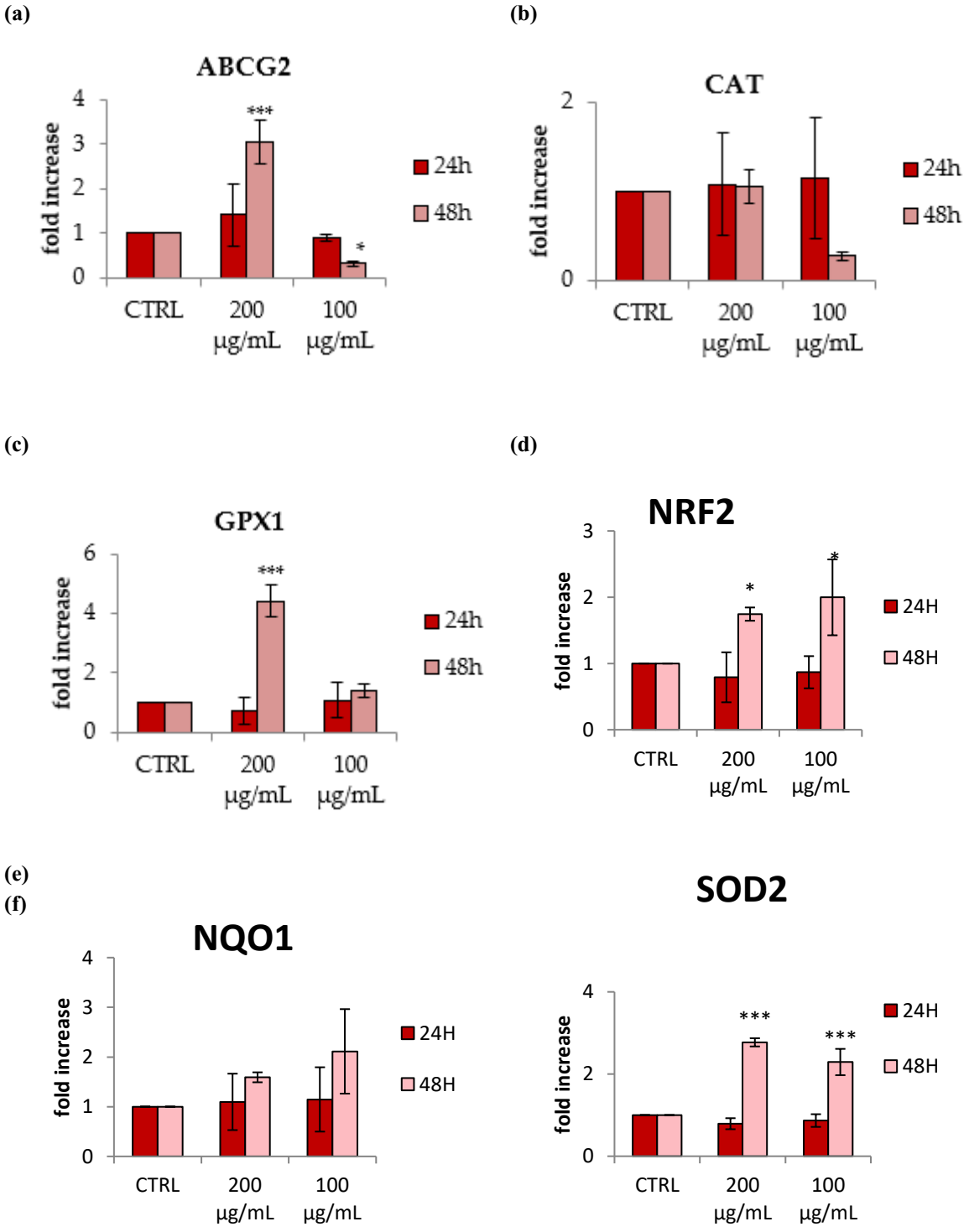

Figure 4.4 Effect of CAE (200 and 100 µg/mL) on the gene expression of (**a**) ATP-binding cassette transporter G2 ABCG2, (**b**) catalase (CAT), (**c**) glutathione peroxidase (GPx-1), (**d**) nuclear factor erythroid 2-related factor 2 (Nrf-2), (e) NADPH-quinone oxidase (NQO1), (**f**) superoxide dismutase (SOD-2) analysed by real-time q-PCR and normalized with the housekeeping gene, actin, in HepG2 cell line. Data are expressed as mean ± SD of three independent experiments (n = 3). * $p<0.05$, *** $p<0.001$ *vs* control (CTRL).

Discussion

Fruits of *C. annuum* cv Senise were extracted by exhaustive maceration with absolute ethanol achieving an extraction yield of 11.70% *w*/*w*, similar to that reported by Loizzo et al. 2013 who showed that ethanol improved the yield of pepper extract compared to exane (9.8 ± 0.8% vs. 0.5 ± 0.06%).

The potential health benefits of *C. annuum* L. cv Senise dried pepper was demonstrated previously by Loizzo et al. 2013. In particular, the authors demonstrated the good radical scavenging activity of an ethanol extract against two synthetic radicals, DPPH and ABTS (IC_{50} = 55.0 ± 1.8 μg/mL, TEAC value = 12.6 ± 1.1, respectively) (Loizzo et al. 2013). In the present study, the antioxidant activity of CAE extract was confirmed, reporting an ORAC value of 38,144 μmol TE/100 g of dried extract. The result was comparable with other cultivars of red sweet pepper (Wu et al. 2013) and other known antioxidant foods, such as *Olea europeae* L. (ORAC value of leaf extract = 69,639 μmol TE/100g of dried weight) (Wu et al. 2013). To the best of our knowledge, this is the first work that reports the biological activity of *C. annuum* cv Senise extract in cells. The extract was demonstrated to protect cells from oxidative stress, reducing intracellular ROS, by activating transcription factors that induce the expression of antioxidant enzymes. These beneficial effects could be ascribed to the presence of health-promoting compounds that were evaluated for the first time in Senise dried pepper. In particular, qualitative analysis performed with LC-MS/MS identified 24 compounds belonging to polyphenols, carotenoids, capsinoids, and vitamins.

Many studies have reported that polyphenols and carotenoids promote the expression of Nrf-2 (Kaulmann et al. 2014), a redox sensitive transcription factor that provokes an antioxidant response by inducing the expression of cytoprotective enzymes, such as glutathione *S*-transferase (GST), superoxide dismutase (SOD), heme oxigenase-1 HO-1, and NADPH-quinone oxidase NQO1 (Jigorel et al. 2006; Brechbuhl et al. 2010; Higashikuni et al. 2012). The cells treated with CAE showed a higher level of Nrf-2, as well as of SOD-2 and Gpx-1 expression, suggesting that the extract exerts its antioxidant activity by acting through this pathway. Previous studies evidenced that Nrf-2 expression also influences the expression of ABCG2, a transmembrane transporter protein responsible of GSH transport (Tuberoso et al. 2018; Higashikuni et al. 2012; Shen et al. 2010) and associated with redox regulation in some pathological conditions such as Alzheimer's and cardiovascular diseases (Bonomo et al. 2018; Brechbuhl et al. 2010; Higashikuni et al. 2011; Shen et al. 2010). In our study, both Nrf-2 and ABCG2 increased after 48 h of treatment with the extract. Moreover, the

polyphenols present in the extract can interact directly with this transporter, as reported in previous studies (Cooray et al. 2004).

In addition, the extract was incorporated into liposomes to explore their potential in favoring the internalization in cells, with a consequent enhancement of the efficacy of the extract. Liposomes have been demonstrated to increase the solubility and stability of polyphenols and carotenoids, which results in improved bioavailability and therapeutic benefit (Mignet et al 2013; Bozzuto et al. 2015). As reported by Caddeo et al.2016, cellular uptake of quercetin and resveratrol improved when they were incorporated in liposomes, ameliorating the biological activity in vitro and in vivo. In this study, liposomes were found to improve the antioxidant activity of *C. annuum* extract. More specifically, the cells treated with extract-loaded liposomes showed lower levels of ROS than cells treated with the extract, with liposomes being twice as active in comparison with the raw extract at equal concentrations. This means that the same beneficial effect, or even a stronger one, can be achieved with a lower dose, thus reducing costs and possible side effects. Probably this is due to a higher quantity of compounds that reach the cells when the extract is encapsulated into the liposomes, but further investigations are needed to understand the mechanistic aspects related to the measured CAE biological effects.

Conclusions

In this study, the effects of ethanolic extract of *Capsicum annuum* L. cv Senise were studied with particular regard to gene expression and ROS generation in cell models. It is clear that several genes involved in the redox cell system are activated during treatment with the extract, with an evident impact on SOD-2 and GPX-1 as well as Nrf2 and ABCG2. Overall, this study suggests that a typical food of the Basilicata region could represent a new strategy in nutraceutical and pharmaceutical fields. For the first time, the protective effect of *Capsicum annuum* L. cv Senise against oxidative stress was investigated in cells, and twenty-four compounds were identified with LC-MS. Results obtained demonstrated the activity of CAE, but further experiments are needed to understand if some of the identified compounds are responsible for the measured synergist effect. Moreover, interesting results were obtained by formulating the extract into liposomes, which potentiated its antioxidant activity. These findings support the association of antioxidants of natural origin with nanocarriers to develop health-promoting systems.

4.1.2 Phytochemical profile and antioxidant activity of *Solanum aethiopicum* L. cv Rotonda peel extract selected after *in vitro* screening

Introduction

Reactive oxygen species (ROS) are physiologically produced in our body as by-products of the cellular metabolism. The largest part of the radicals is generated at mitochondrial level where taken place the chemical processes connected with the electron transport of aerobic respiration and the organic compounds oxidation. Moreover, a countless number of exogenous agents such as solar and ionizing radiations, air pollutants, inhalation of chemicals, heavy metals in food and water could trigger free radical formation, initiating a cascade of oxidation reactions once gaining access to the human body and taking contact with tissue cells. ROS are highly reactive species and they are responsible of the oxidative damage of biological macromolecules, phospholipid membrane and DNA lesions. Our body could counteract and solve the damage through enzymatic or non-enzymatic defense system. Moreover, many bioactive compounds founded in plant and food possess antioxidant activity which could solve oxidative damage.

Solanum aethiopicum L. is a source of polyphenols and its extracts demonstrated antioxidant activity which was evaluated by different *in vitro* assay and also in several cell model. To the best of our knowledge *Solanum aethiopicum* cv Rotonda phytochemical profile and biological activity have not been reported yet.

Materials and methods

Chemicals

Absolute ethanol, Dulbecco's Modified Eagle Medium (DMEM), dimethyl sulfoxide (DMSO), [3-(4,5-dimethyl-2-thiazolyl)-2,5-diphenyl-2H-tetrazolium bromide] (MTT) and 2′,7′-dichlorodihydrofluorescein diacetate (DCFH-DA), Folin-Ciocalteu reagent, sodium carbonate (Na_2CO_3), 2,2-diphenyl-1-picrylhydrazyl (DPPH), sodium nitrate ($NaNO_3$), aluminum chloride ($AlCl_3$), sodium acetate anhydrous, ferric chloride hexahydrate ($FeCl_3 \cdot 6H_2O$), 2,4,6-tripyridyl-s-triazine (TPTZ), fluorescein, sodium phosphate monobasic (NaH_2PO_4), 2,2'-Azobis (2-amidinopropane) dihydrochloride (AAPH), 6-hydroxy-2,5,7,8-

tetramethylchroman-2-carboxylic (Trolox), quercetin, were purchased from Sigma Aldrich S.p.A. (Milan, Italy). Trypsin-EDTA solution, fetal bovin serum (FBS), glutamine, penicillin-streptomycin, and phosphate saline buffer (PBS) were purchased from Euroclone (Milan, Italy). Reagents used for RT-PCR were purchased from Euroclone (Milan, Italy). Solvents used for LC-ESI/LTQOrbitrap/MS extraction and water were purchased from VWR (Milan, Italy), while acetonitrile and formic acid were purchased from Merck (Merck KGaF, Darmstadt, Germany).

Extract preparation

The fruits of *S. aethiopicum* used in this study were provided by Consorzio tutela di Rotonda (Pz-Italy). Whole fruit, peel and pulp were cut into small pieces and extracted by exhaustive maceration technique. The plant material (peel 234 g, pulp 219 g and entire fruit 124 g) was placed in dark bottles with absolute ethanol (plant material:solvent ratio 1:20) in the dark at room temperature for 48h. Extraction procedure was repeated for three times. The obtained extracts were filtered with filter paper and the solvent was evaporated under reduced pressure by using a rotary evaporator. The extracts were kept dried in the dark until their use.

In vitro cell-free assays

*Total phenol content (TPC***)**

The total phenol content (TPC) was determined by Folin-Ciocalteu method (Braca et al. 2018). Briefly, 75µL of diluted extract were mixed with 425µL of distilled water, 500µL of Folin-Ciocalteau reagent and 500µL of Na_2CO_3 (10% w/v). The solution was mixed and incubated for 1h in the dark at room temperature. After incubation, the mixture absorbance was measured at 723 nm using a UV-Vis spectrophotometer (SPECTROstarNano, BMG Labtech, Ortenberg, Germany). The total phenolic content was expressed as mg of Gallic Acid Equivalent (GAE)/g of extract.

Total Flavonoid Content (TFC)

An aliquot (150 µL) of extract was added to 45 µL of 5% $NaNO_3$ into a microcentrifuge tube. After 5 min, 90 µL of 1% $AlCl_3$ was added and at then 1 minute, 300 µL of 1M NaOH solution was added and the total volume was made up to 1.5 mL with distilled water. The solution was mixed well and the absorbance was measured against reagent blank at 510 nm after 10 min of incubation at room temperature. Quercetin was used as standard to plot the

calibration curve. The total flavonoid content was expressed as mg of quercetin equivalent/g of extract (mg QE/g of extract).

2,2-diphenyl-1-picrylhydrazyl (DPPH) scavenging assay

The radical-scavenging ability of samples was evaluated by *in vitro* DPPH neutral radical as reported by Faraone et al. 2019. Briefly, 50 µL of various concentrations of extract or Trolox, used as standard, were added to 200 µL of a methanol solution of DPPH (0.0476 mg/mL) in a 96-well plate. The plate was incubated at room temperature for 30 minutes in the dark. The reaction was monitored at 515 nm and the data were expressed as milligrams of Trolox equivalents per gram of dried extract (mg TE/g).

Ferric Reducing Antioxidant Power Assay (FRAP)

The FRAP assay was carried out as described by Faraone et al. 2019. The FRAP reagent was prepared by mixing 38 mM sodium acetate anhydrous buffer in distilled water, pH 3.6, with 20 mM $FeCl_3 \cdot 6H_2O$ in distilled water and 10 mM TPTZ (2,4,6-tripyridyl-s-triazine) in 40 mM HCl in a ratio of 10 : 1 : 1. 20 µL of each extract dilutions and 180 µL of FRAP reagent were mixed in a 96-well plate and incubated at 37°C for 40 min in the dark. In the case of the blank, 20 µL methanol was added to 180 µL FRAP reagent. The absorbance of the resulting solution was measured at 593 nm using a plate reader. Trolox was used as reference antioxidant standard and results were expressed as milligrams of Trolox equivalents per gram of dried extract (mg TE/g).

Oxygen Radical Absorbance Capacity (ORAC) Assay

According to Sinisgalli et al. 2020 25 µL of different concentrations of SAE (0.01–0.2 mg/mL) were incubated in a 96-well microplate with 125 µL of fluorescein (10 nM in 75 mM NaH_2PO4 buffer at pH 7.4) for 30 min at 37 °C. Then, 25 µL of 10 mM AAPH was added to each well and fluorescence was recorded (λex 485 nm and λem 520 nm) every 2 min for 90 min using a GLOMAX Multidetection System (Promega, Madison, WI, USA). Trolox (0–100 µM) was used as the reference standard. Results were calculated on the basis of differences in areas under the fluorescence decay curve between the blank, samples, and standards. Final oxygen radical absorbance capacity (ORAC) values were expressed as µmol of Trolox equivalents (TE)/kg of dried extract (DE).

LC-ESI/LTQOrbitrap/MS

Phytochemical profile of peel extract was investigated by LC-MS method as described for *Capsicum annuum* in the 4.1.1 section.

Liposome preparation and characterization

Peel extract was encapsulated in liposomes following the same procedure described for CAE in section 4.1.1.

Biological activity of peel extracts in cell model

Cell viability

Human hepatocellular carcinoma cell line (HepG2) was cultured in DMEM (supplemented with 10% fetal bovine serum, 2 mM glutamine, 100 U/mL penicillin, and 100 µg/mL streptomycin) and maintained at 37°C in a humidified atmosphere containing 5% CO_2. HepG2 cells were seeded ($1.5*10^3$ cells/well) in a 96-well plate and treated with different doses (200-10 µg/mL) of *Solanum aethiopicum* cv Rotonda extract (SAE) for 24 and 48h. Then, cell viability was evaluated by MTT assay as reported in the 4.1.1 section.

Intracellular ROS

Reactive oxygen species (ROS) were quantified with a fluorescent probe DCFH-DA, as described by Sinisgalli et al. 2020. Briefly, HepG2 cells were seeded ($1.5*10^5$ cells/well) in a 24-well plate and treated with different doses of SAE (200-10 µg/mL), liposomes or NAC (10mM). After 24h, cells were stressed with 5 mM of *tert*-butilhydroperoxide (*t*-BuOOH) for 1h. Finally, the cells were stained with 10 µM DCFH-DA for 30 min at 37 °C in the dark, and fluorescence was measured by BD FACSCanto II (BD Pharmingen, San Jose, CA, USA) (λ_{ex} 485 nm and λ_{em} 515–540 nm).

Quantitative RT-PCR

HepG2 cells were treated with different concentrations of SAE (200–100 µg/mL) for 24 h. RNA extraction and qRT-PCR were performed as reported in section 4.1.1.

Table 4.3 Forward and reverse primers

Gene	Forward primer	Reverse primer
β-actin	5′-CCTGGCACCCAGCACAAT-3′	5′-GCCGATCCACACGGAGTACT-3′
ABCG2	5′-ATCACTGATCCTTCCATCTTG-3′	5′-GCTTAGACATCCTTTTCAGG-3′
CATALASE	5′-ATACCTGTGAACTGTCCCTACCG-3′	5′-GTTGAATCTCCGCACTTCTCCAG-3′
GPx-1	5‘-CAGTCGGTGTATGCCTTCTCG-3′	5′-CTCGTTCATCTGGGTGTAGTCC-3′
NQO1	5'-AGGGTCCTTCAGTTTACCTGTG-3'	5'-GGTGGTGGAGTCGGACCTCTA-3'
NRF2	5'-CATTGTCATCTACAAACGGGAA-3'	5'-AACTACTCCCAGGTTGCCCA-3'
SOD2	5'-CTACTCTCAAATCTGTTCTGG-3'	5'-GGATTCAATGAGGAGACTTG-3'

Statistical analysis

Data were expressed as mean ± standard deviation (Mean ± SD). Statistical analysis was performed using GraphPad Prism 5 Software, Inc. (San Diego, CA, USA) and p values ≤ 0.05 were considered as statistically significant.

Results

Extraction yield, total polyphenol and flavonoid content and antioxidant activity

Peel, pulp and whole fruit of *S. aethiopicum* cv Rotonda were extracted with absolute ethanol for 48h by exhaustive maceration as extraction technique.

The extraction yield was calculated (**Table 4.4**) and the total polyphenol and flavonoid content of three *S. aethiopicum* extracts were evaluated. Peel extract reported the highest value of polyphenols (20.94±0.83 mgGAE/g) and flavonoids (255.57±22.40 mgQE/g) followed by whole fruit and pulp (**Table 4.4**).

Table 4.4. Extraction yield, total polyphenol content (TPC), total flavonoid content (TFC) and antioxidant activity of *Solanum aethiopicum* extracts

	EXTRACTION YIELD (%)	TPC* (mg GAE/g)	TFC** (mgQE/g)	DPPH*** (mg TE/g)	ORAC (µmol TE/kg)	FRAP (mg TE/g)
PEEL	5.82[a]	20.94±0.83[a]	255.57±22.40[a]	16.96±0.57[a]	4477.22±330.64[a]	21.52±0.58[a]
PULP	4.72[b]	6.38±0.19[c]	154.21±17.09[b]	4.73±0.14[c]	700.37±125.56[c]	6.30±0.12[c]
WHOLE FRUIT	5.65[a]	9.41±0.17[b]	119.46±10.13[c]	8.03±0.16[c]	1565.31±374.65[b]	9.80±0.58[b]

* TPC: total polyphenol content expressed as milligrams of gallic acid per grams of extract; **TFC: total flavonoid content expressed as milligrams of quercetin equivalent per gram; ***DPPH:2,2-diphenyl-1-picrylhydrazyl expressed as milligrams of trolox equivalent per gram; ****ORAC: oxygen radical absorbance capacity (ORAC) assay expressed as micromoles of trolox equivalent per kg; *****FRAP: ferric reducing antioxidant power expressed as milligrams of Trolox equivalents per grams of extract;
Experiments were carried out in triplicate and data were reported as mean ± SD. Significant differences ($p < 0.05$) are highlighted with different letters (a, b and c).

Polyphenols are a wide class of compounds which act as radical scavengers, oxygen quenchers and chelating the metal ions involved in the generation of free radicals. Thus, polyphenols amount influenced antioxidant activity. It is well known that a single test cannot fully assess the antioxidant activity of an extract since antioxidants are a composite class of substances and each of them depending on its chemical structure is able to counteract a specific category of radical and/or oxidizer. Therefore, more than one technique is needed to fully understand the antioxidant characteristics of a product. For this reason, we evaluated antioxidant activity of the extract through three different spectrophotometric assays as DPPH, ORAC and FRAP. All extracts showed the antioxidant activity (**Table 4.4**), in particular peel extract reported the highest reducing power (21.52±0.58 mgTE/g of dried extract) evaluated by FRAP assay and radical scavenging activity (16.96±0.57 mgTE/g of dried extract). All three extracts quenched peroxyl radical produced by AAPH in a dose dependent manner in ORAC assay, a method of measuring capacities in food samples *in vitro*. Peroxyl radicals are the predominant free radicals in lipid oxidation in foods and biological systems under physiological conditions. In ORAC assay peroxyl radicals produced by AAPH react with fluorescence probe resulting in the loss of fluorescence. Different fluorescence decay curves were obtained for different extracts (**Figure 4.5**). Pulp extract curve was steeper than that of the trolox used as standard and of the other two extracts meaning that the fluorescence is lowered faster over time due to the greater quantity of radical present. In contrast, peel extract strongly slowed fluorescein degradation and reported the highest ORAC value (4477.22±330.64 µmolTE/kg of dried extract), three times and six times higher than whole fruit and pulp, respectively (**Table 4.4**).

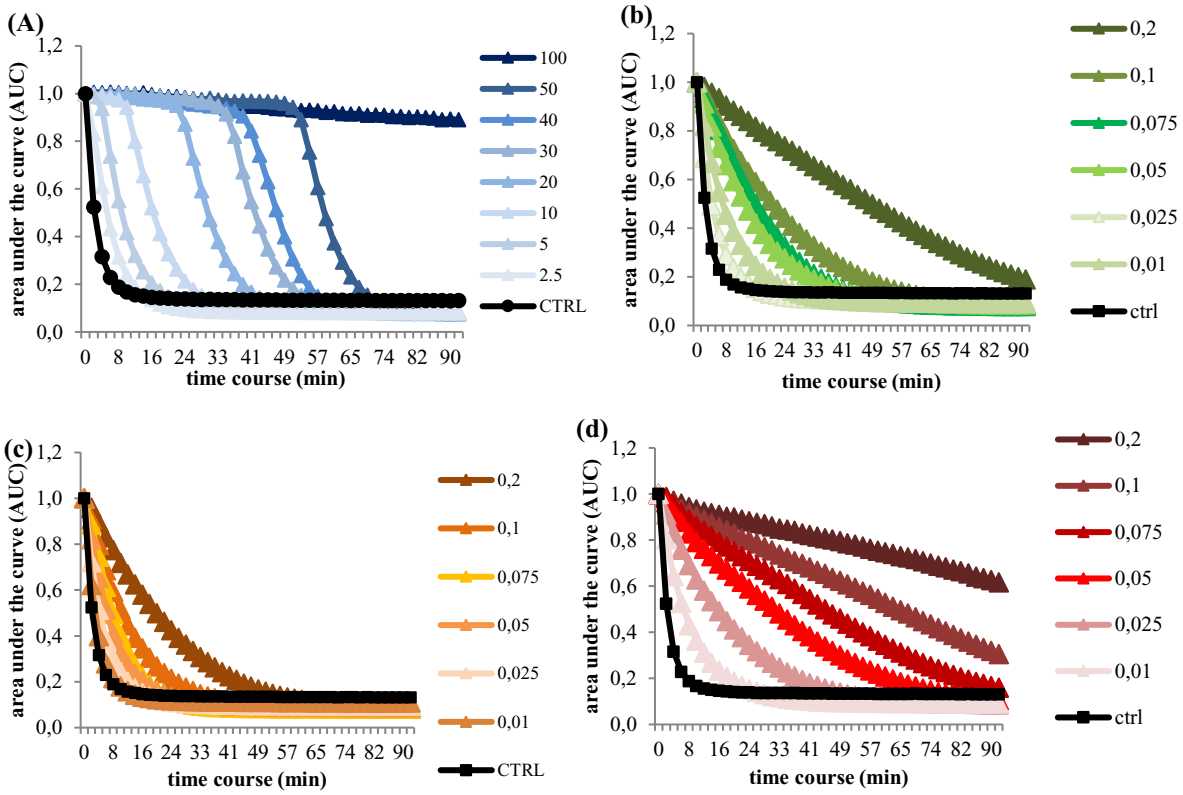

Figure 4.5. Oxygen radical absorbance capacity (ORAC) assay for different concentrations (2.5–100 µM) of Trolox used as a standard (**a**) and (0.01–0.2 mg/mL) of whole fruit (**b**), pulp (**c**) and peel (**d**). Changes in the fluorescence intensity of fluorescein were monitored for 90 min.

Relative antioxidant capacity index (RACI), an adimensional index, was calculated to compare results of different samples from different tests (Faraone et al. 2019). In the present work, RACI has been used to have a clear comparison among the antioxidant activity results obtained from DPPH, FRAP and ORAC. It has been calculated using Excel software (2010, Microsoft, Redmond, WA, USA) where the values of antioxidant capacity in each data set are transformed into standard scores, derived by subtracting the mean from the raw data divided by standard deviation. The mean of standard scores was used for RACI calculation. TPC method was also included in RACI calculation. The TPC method was recently proposed for the determination of total reducing capacity of samples which reflects the cumulative of both phenolic and non-phenolic compounds to reduce the Folin-Ciocalteu reagent. According with previous results, peel extract had the highest RACI value (0.91) followed whole fruit and pulp (**Figure 4.6**).

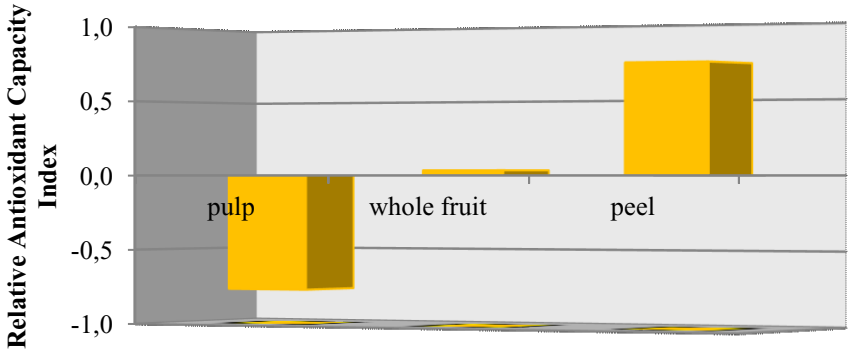

Figure 4.6 Relative Antioxidant Capacity Index (RACI) values obtained comparing Total Polyphenol Content (TPC), 2,2-diphenyl-1-picrylhydrazyl (DPPH) Ferric Reducing Antioxidant Power (FRAP) and Oxygen Radical Absorbance Capacity (ORAC) results.

Phytochemical profile of Solanum aethiopicum peel extract

Qualitative analysis of *S. aethiopicum* peel extract was performed by LC-ESI-Orbitrap-MS/MS analysis. Data are showed in **Figure 4.7**. Individual components were identified by comparison of their *m/z* values in the total ion current (TIC) profile with that of the selected compounds described in literature (Mbondo et al. 2018; Anosike et al. 2012; Watanabe et al. 2001; Plazas et al. 2014; Nwanna et al. 2019). Thirteen compounds were identified in SAE (**Table 4.5**) belonging to a wide variety of structurally different metabolic classes: phenols (*caffeic acid*, *gallic acid*, *ellagic acid*, *chlorogenic acid*), flavonols (*quercetin, rutin, kaempherol*), flavanols (e*picatechin*), anthocianins (*delphinidin-3-rutinoside*), vitamins (*ascorbic acid*), carotenoids (*β-carotene, lycopene*), sesquiterpenoids (*solavetivone*).

The identified compounds showed the typical ion peaks reported by several studies; for example, the ellagic acid demonstrated $[M\text{-}H]^-$ ion peak at m/z 301 and fragment ions at m/z 257 and 150 (Jiang et al. 2017). Moreover, *β*-carotene and lycopene exhibited molecular ions in positive ionization mode with characteristic fragmentation patterns (444/429 for *β*-carotene and 444/375 for lycopene) (Zhang et al 2019). Among the compounds identified, there is also the sesquiterpenoid solavetivone, a phytoalexin characteristic of the Solanaceae family (Sabater-Jara,et al 2010).

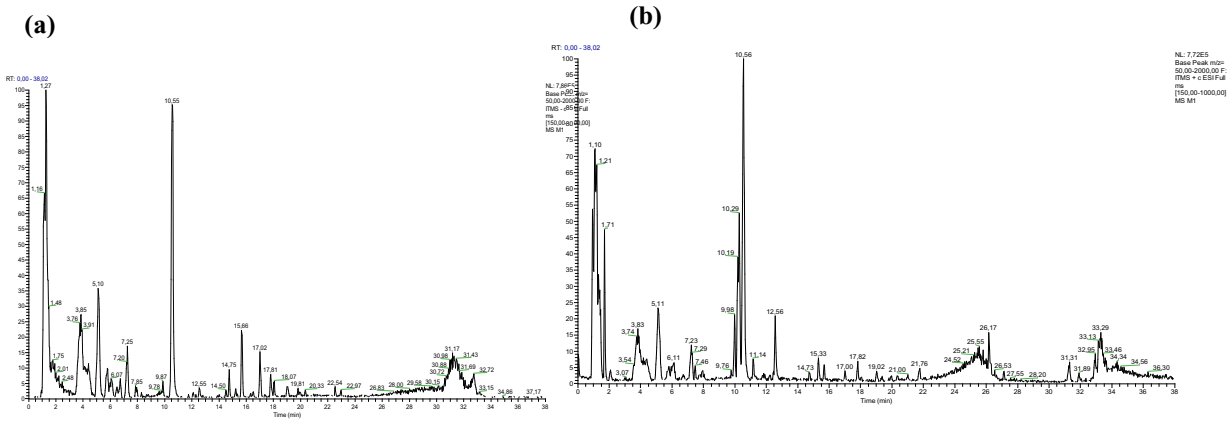

Figure 4.7 LC-MS profile of *Solanum aethiopicum* peel ethanol extract in negative (**a**) and positive (**b**) ion mode**.**

Table 4.5. Metabolites identified in *Solanum aethiopicum* L. cv Rotonda peel ethanol extract using LC-ESI/Orbitrap/MS/MS.

Compounds	Rt(min)	Molecular Formula	MW	$[M+H]^+$	$[M-H]^-$	Product ions (*m/z*)
Caffeic Acid	1.25	$C_9H_8O_4$	180.0422		179.0344	174, 135
Kaempferol	1.91	$C_{15}H_{10}O_6$	286.0477		285.0399	267, 191, 165
Delphinidin-3-rutinoside	3.82	$C_{27}H_{31}O_{16}$	611.1612		610.1533	609, 300, 125
Rutin	5.85	$C_{27}H_{30}O_{16}$	610.1533		609.1455	300, 179, 151
Ellagic acid	8.48	$C_{14}H_6O_8$	302.1991		301.1970	257, 150
Quercetin	10.72	$C_{15}H_{10}O_7$	302.0426		301.0348	287, 151, 121
Epicatechin	33.12	$C_{15}H_{14}O_6$	290.0790		289.0712	245, 227, 165, 161
Ascorbic acid	33.31	$C_6H_8O_6$	176.0320		175.0242	157, 115, 112, 87
Gallic Acid	1.41	$C_7H_6O_5$	170.0215	171.0287		157, 110, 82
Chlorogenic acid	17.03	$C_{16}H_{18}O_9$	354.0950	355.1029		338, 273, 227, 197, 173, 163, 147
β-carotene	18.18	$C_{40}H_{56}$	536.4382	537.4460		457, 444, 429, 391, 338, 273, 199, 171
Lycopene	18.20	$C_{40}H_{56}$	536.4382	537.4460		444, 375, 344, 309, 273, 207, 199, 171
Solavetivone	25.42	$C_{15}H_{22}O$	218.1670	219.1748		207, 199, 198, 182, 171, 166, 163

Biological activity of Solanum aethiopicum peel extract (SAE) in HepG2 cell used as model

Effect of SAE on cell viability and ROS generation in HepG2 cell line

HepG2 cells were treated with different doses of SAE and cell viability was evaluated by MTT assay. The extract showed no cytotoxic effect after 24 and 48h and the lowest doses (50 and 25μg/mL) enhanced cell proliferation about 30-60% compared to untreated cells (CTRL) (**Figure 4.8a**).

The antioxidant activity of SAE was evaluated in HepG2 cells exposed to *t*-BuOOH a known source of ROS. As shown in Figure 1b, *t*-BuOOH increased intracellular ROS reporting a double fluorescence value compared to untreated cells (CTRL). SAE counteract ROS generation induced by *t*-BuOOH restoring basal conditions with no statistically differences compared to NAC, a known antioxidant (**Figure 4.8b**).

Moreover, SAE was incorporated in liposomes (prepared as indicated in Chapter 1) and the effect of this formulation on biological activity was evaluated. HepG2 cells were pretreated with SAE liposomes for 24h at the same doses used for raw extract (200-1μg/mL). After 24h, cells were stressed with *t*-BuOOH and antioxidant activity was analyzed. The formulation improved biological activity of the extract at low doses (10-1μg/mL) which reported fluorescence intensity lower than that of the raw extract (**Figure 4.8b**).

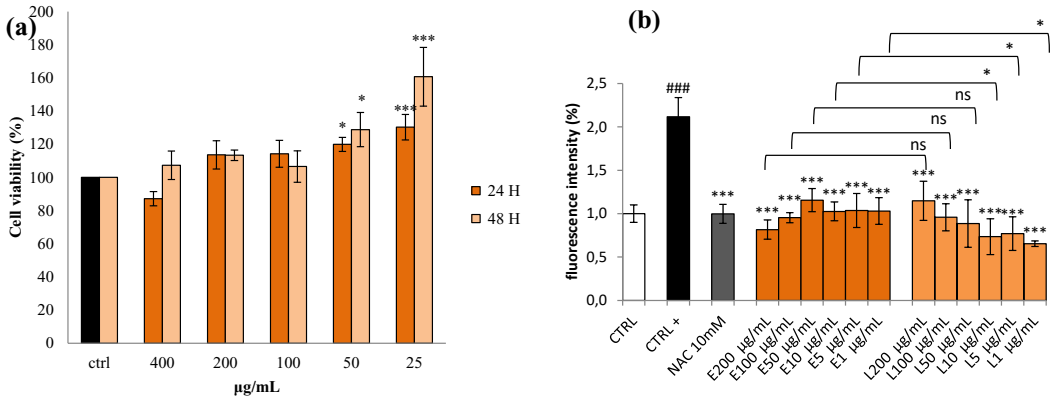

Figure 4.8 (**a**) Cell viability, evaluated by MTT assay, of HepG2 cells treated for 24 and 48 h with different concentrations of *S. aethiopicum extract* (SAE). Data are expressed as the mean ± SD of three independent experiments (n = 3). (**b**) Effects of SAE (E) and liposomes (L) on *t*-BuOOH-induced intracellular reactive oxygen species (ROS) generation in HepG2 cells. Cells were pre-treated with the extracts or liposomes at different concentrations (200-1 µg/mL) for 24 h and then incubated with 5 mM *t*-BuOOH for 1 h. ROS generation was measured by DCFH-DA staining with flow cytometry analysis. Data are expressed as the mean ± SD of three independent experiments (n = 3). $^{###}$ $p < 0.001$ vs. CTRL, *** $p < 0.001$ *vs* *t*-BuOOH-treated cells, * $p < 0.05$, ns not statistically different

Effect of SAE on several markers involved in antioxidant defense

HepG2 cell line was treated with different doses (200-100µg/mL) of SAE for 24h and qRT-PCR was performed in order to evaluate molecular pathways involved in antioxidant activity (**Figure 4.9**). The extract up-regulated expression of ATP-binding cassette transporter G2 (ABCG2), NADPH-quinone oxidase (NQO1), catalase and nuclear factor erythroid 2-related factor 2 (Nrf-2). In contrast, the extract decreased glutathione peroxidase (GPx-1) expression. No statistically effect was shown on superoxide dismutase (SOD-2) expression.

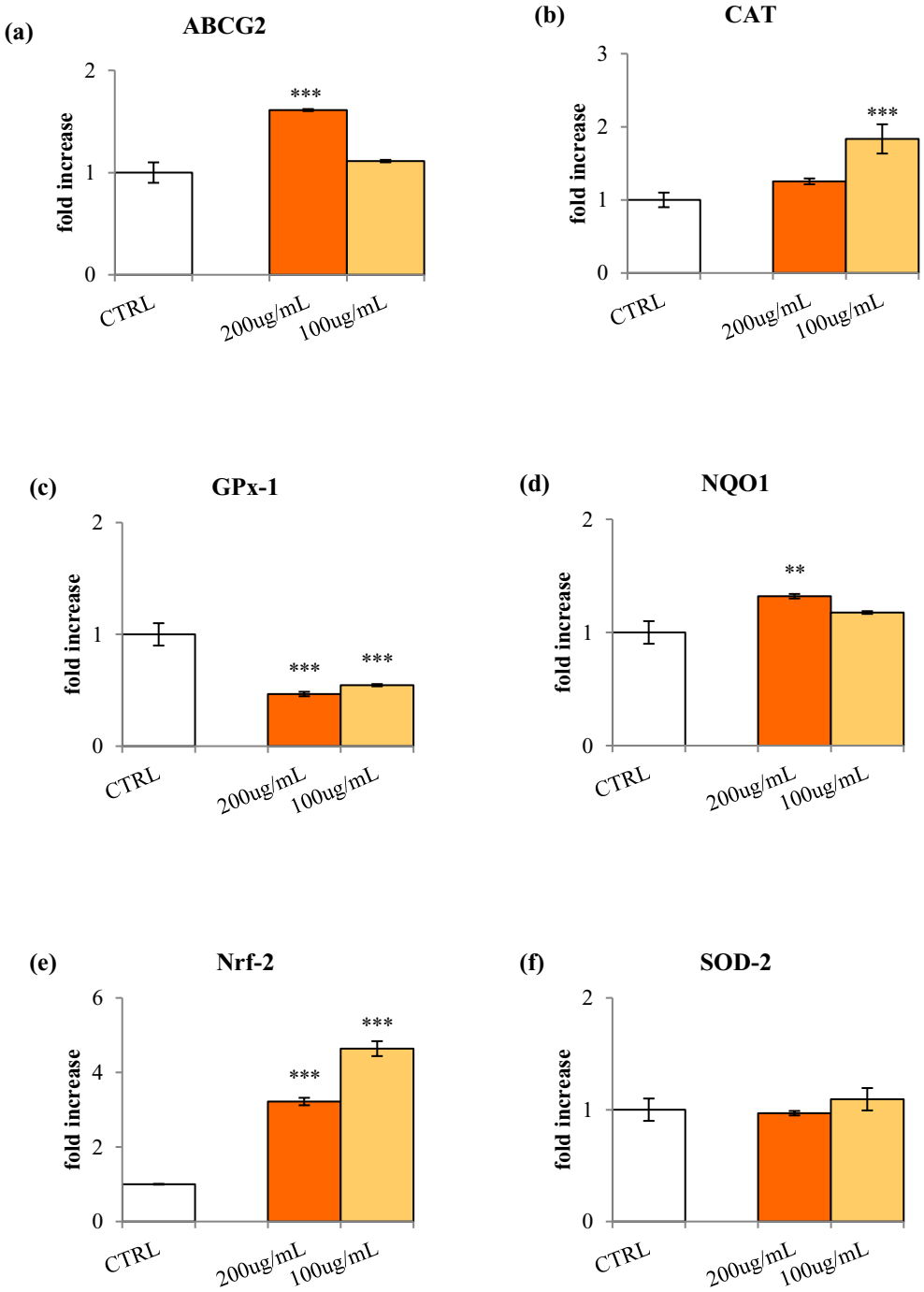

Figure 4.9 Effect of SAE (200 and 100 µg/mL) on the gene expression of (**a**) ATP-binding cassette transporter G2 ABCG2, (**b**) catalase (CAT), (**c**) glutathione peroxidase (GPx-1), (**d**) NADPH-quinone oxidase (NQO1), (**e**) Nuclear factor erythroid 2-related factor 2 (Nrf-2), (**f**) superoxide dismutase (SOD-2) analyzed by real-time q-PCR and normalized with the housekeeping gene, *β*-actin, in HepG2 cell line. Data are expressed as mean ± SD of three independent experiments ($n = 3$). $^{**}p < 0.01$, *** $p < 0.001$ *vs* control (CTRL)

Discussion

In the present study whole fruit, peel and pulp of *Solanum aethiopicum* L. cv Rotonda were extracted by exhaustive maceration in absolute ethanol and antioxidant activity was evaluated by different *in vitro* assays. Peel extract reported the best antioxidant activity due to the highest content of polyphenols and flavonoids. For this reason, it was selected for further investigation. LC-MS identify the presence of thirteen compound in peel extract of *S. aethiopicum* known as antioxidant indeed responsible of biological activity of the extract. SAE reported no cytotoxic activity on HepG2 cell line used as model. *Plazas et al 2014* demonstrated as *S. macrocarpon* was more toxic than *S. aethiopicum* that showed no toxicity on RAW 264.7 macrophage due to higher glycoalkaloid content. Moreover, eggplant varieties with highest content of chlorogenic acid significantly reduce LPS-induced NO production in RAW 264.7 macrophage. Alterations in NO production are related to many inflammatory status; chlorogenic acid inhibits NO production by inhibiting the inducible nitric oxide synthase (iNOS) without any cytotoxicity (Plazas et al. 2014). *Akanitapichat et al. 2010* demonstrated as flavonoids and phenolic acids are mainly correlated with hepatoprotective effect of different varieties of *S. melongena* and *S.aethiopicum* in *t*-BuOOH exposed HepG2 cells. Flavonoids and phenolic acids were found also in *S. aethiopicum* peel and affected its biological activity. Particularly, peel extract reduced intracellular ROS in *t*-BuOOH-stressed HepG2 cell line promoting the expression of the transcription factor Nrf-2 and, consequently, of catalase, NQO1, ABCG2, markers involved in antioxidant defense.

Herbal extracts are valuable components with great therapeutic potential. Low solubility, absorption and bioavailability limit their pass-through membrane. Liposomes are promising carrier systems for the delivery of natural extracts by making them available at the side of action. In the present study peel extract was incorporated in liposomes in order to enhance cell interaction and thus improve biological activity. Interestingly to note that raw and liposome loaded extract protected cells from oxidative stress at all doses. When extract was incorporated in liposome exerted strong antioxidant activity especially at lower doses by halving ROS amount compared to control. In contrast to raw extract, liposomes demonstrated better antioxidant activity compared with NAC, a known antioxidant. This means that we can obtain the same or stronger effect reducing the dose and consequently also costs and side effects.

Conclusions

The present study evaluated, for the first time, biological activity and chemical characterization of *Solanum aethiopicum* L. cv Rotonda extracts. Among fruit tissues, peel extract demonstrated the best antioxidant activity *in vitro,* demonstrated also in cellular model. The extract protected the cells from oxidative stress and enhanced the expression of several antioxidant enzymes like ABCG2, catalase NQO1 via Nrf2 pathway. Liposome formulation improved antioxidant activity of the extract representing a good strategy to have strong activity with low doses of the extract.

4.2 Effects of *Capsicum annuum* L. cv Senise and *Solanum aethiopicum* L. cv Rotonda extracts on fat accumulation, oxidative stress and inflammation in OA-treated HepG2 and Caco-2 cell lines

Introduction

Proteins, carbohydrates and lipids from the diet are metabolized in our organism through different enzymes and pathways to produce energy. Our body can use this energy right away or store it as glycogen or lipids. Normally, the entire metabolic process is finely controlled so that there is a balance between the incoming energy and the outgoing energy. A positive energy balance, due to excessive caloric consumption and inadequate physical activity induce fat accumulation firstly, in adipose tissue, and then in liver, the main organ involved in regulation of lipid metabolism and trafficking (Stefan 2020). AMP-activated protein kinase (AMPK) is a key regulatory molecule that modulates hepatic lipid metabolism via regulating the transcription factors sterol regulatory element-binding protein 1/2 (SREBP1/2) and peroxisome proliferator activated receptor α (PPARα). The isoform, SREBP1 preferentially regulates *de novo* lipogenesis by activating the genes, fatty acid synthase (FAS) and acetyl-CoA carboxylase (ACC), required for lipid synthesis whereas SREBP2 controls the cholesterol homeostasis via activating the gene, 3-hydroxy-3-metylglutaryl-CoA Reductase (HMGCR), required for cholesterol synthesis. PPARα, on the other hand, regulates the genes carnitine palmitoyl transferase (CPT1) and uncoupling protein 2 (UCP2), which are involved in fatty acid oxidation. *De novo* lipogenesis or de novo fatty acids (FA) synthesis is the metabolic pathway that synthesizes fatty acids from excess carbohydrates. These fatty acids can then be incorporated into triglycerides (TGs) for energy storage. In normal condition *de novo* lipogenesis takes place in liver and in adipose tissue, the major metabolic tissues. Liver is more efficient, in fact FAS, a marker for lipogenesis has been categorized as a housekeeping protein in the liver. High-carbohydrate or high fat

diets activate a lipogenic response in the liver thus via SREBP-1c. This transcription factor regulates the expression of many genes that code for enzyme involved in fatty acid and lipid biosynthesis as ATP-citrate lyase (ACLY), acetyl-CoA carboxylase (ACC) and fatty acid synthase (FAS) for lipogenesis, stearoyl CoA desaturase (SCD) and long-chain elongase (Elovl6; LCE) catalyzing fatty acid elongation and desaturation steps, and glyceraldehyde-3-phosphate acyltransferase (GPAT). ACLY catalyzes the conversion of citrate to acetyl-CoA which is carboxylated to malonyl-CoA by ACC. FAS converts malonyl-CoA into palmitate which after a series of reactions is further converted into complicated fatty acids. Elevated malonyl-CoA concentrations inhibit CPT1, the rate-limiting enzyme of β-oxidation which regulates the transfer long-chain-acyl-CoAs from the cytosol into the mitochondria. This results in a shift from an oxidative pathway to a reesterification pathway with triglycerides synthesis. SREBP1 is negatively regulated by AMPK.

In addition, diets high in fatty acids increase plasma total cholesterol and low-density lipoprotein (LDL) concentrations. Plasma cholesterol homeostasis in the body is controlled mainly by endogenous synthesis, intestinal absorption and hepatic excretion. Dietary cholesterol is absorbed from micelles with fatty acids and phospholipids in the proximal parts of the small intestine, re-esterified into cholesteryl esters for the assembly into lipoproteins, and transported to the lymph and then to the circulations. It has been shown that cholesterol transport-related proteins play important roles in cholesterol metabolism by regulating the cholesterol absorption in enterocytes. Among key proteins involved in dietary cholesterol uptake in the enterocytes have been identified, the cholesterol uptake transporter, Niemann-Pick C1-Like 1 (NPC1L1), the cholesterol efflux transporters, ATP-binding cassette (ABC) proteins ABCG5 and ABCG8, ABCA1. ABCG5 and ABCG8 represent apical sterol export pumps that promote active efflux of cholesterol and plant sterols from enterocytes back into the intestinal lumen for excretion. ABCA1 is localized on basolateral membrane of enterocytes and facilitate the efflux of cholesterol to circulation as constituent of HDL. It is involved in Reverse cholesterol transport (RCT), a process that involves the net movement of cholesterol from the peripheral tissues to the liver for reuse or for the final elimination via excreting into the bile.

Prolonged exposure to excess of lipid can influence all tissues and induce several disease like obesity, diabetes, dyslipidemia, atherosclerosis and non-alcoholic fatty acid disease (NAFLD) (Liu et al. 2010). Regulation of lipid metabolism is essential for treatment and prevention of several chronic diseases.

Many studies reported as food and vegetable normally present in the diet can represent new and alternative therapeutic strategies (Wong et al. 2014). Polyphenols, carotenoids and capsinoids known for their antioxidant activity can also influence the expression of lipogenic genes (Forbes-Hernández et al. 2017). Some of these health-promoting compounds have been found in *Capsicum annuum* L. cultivar Senise (Solanaceae) (Pascale et al. 2020; Sinisgalli, Faraone, et al. 2020; Loizzo et al. 2008) and also in *Solanum aethiopicum* cv Rotonda (section 4.1.2) which could represent a new potential strategy in treatment of metabolic disorders. Our previous study demonstrated anti-obesity activity of Senise pepper extract in mice fed with high fat diet based on anti-inflammatory effect and the modulation of the gut microbiota (Sinisgalli et al. 2020). Epidydimal and abdominal fat together with LDL/HDL ratio decreased with treatment but the molecular signaling pathway involved are unknown (Sinisgalli, Vezza, et al. 2020). Previous studies reported as methanolic leaf extracts of *S. aethiopicum* reduced plasma LDL cholesterol and triglycerides in diabetic male wistar rats (Okafor et al. 2016). No study investigated on biological activity of *S. aethiopicum* cv Rotonda. Phytochemical profile and *in vitro* antioxidant activity, together with studies on other cultivars suggest as this local food could have potential application in some metabolic disorders.

The aim of the present study was to investigate the hypolipidemic activity of *Capsicum annum* L. cv Senise and *Solanum aethiopicum* L. cv Rotonda extracts in HepG2 and Caco-2 cell line treated with oleic acid (OA) used as model.

Materials and methods

Chemicals

Absolute ethanol, Dulbecco's Modified Eagle Medium (DMEM), dimethyl sulfoxide (DMSO), [3-(4,5-dimethyl-2-thiazolyl)-2,5-diphenyl-2H-tetrazolium bromide] (MTT) and 2′,7′-dichlorodihydrofluorescein diacetate (DCFH-DA) were purchased from Sigma Aldrich S.p.A. (Milan, Italy). Trypsin-EDTA solution, fetal bovin serum (FBS), glutamine, penicillin-streptomycin, and phosphate saline buffer (PBS) were purchased from Euroclone (Milan, Italy). Reagents used for RT-PCR were purchased from Euroclone (Milan, Italy).

Cell culture

Human hepatocellular carcinoma cell line (HepG2) and human colorectal adenocarcinoma cell line (Caco-2) were cultured in DMEM (supplemented with 10% fetal bovine serum,

2 mM glutamine, 100 U/mL penicillin, and 100 µg/mL streptomycin) and maintained at 37°C in a humidified atmosphere containing 5% CO_2.

Cell viability

Cell viability was evaluated in Caco-2 cell line following the same procedure used for HepG2 cell line in previous setion 4.1. Briefly, Caco-2 cells were seeded ($1.5*10^3$ cells/well) in a 96-well plate and treated with different doses (200-10 µg/mL) of *Capsicum annum* L. cv Senise extract (CAE) or *Solanum aethiopicum* L. cv Rotonda peel extract (SAE) for 24 and 48h. Then, cell viability was evaluated by MTT assay.

Determination of total lipid accumulation in HepG2 cell line by Oil Red O Staining

HepG2 cells were seeded in 24 well ($1.8*10^5$/well) and treated with different doses of CAE or SAE (200-100 µg/mL) and oleic acid (0.3mM OA/BSA solution) for 24h. Subsequently, cells were washed twice with phosphate buffer saline (PBS) and they were fixed with 4% paraformaldehyde for 30 minutes. Then cells were stained with Oil red O working solution for 20 min at room temperature. The Oil Red O stock solution was prepared by dissolving 0.35 g of Oil Red O (Sigma Aldrich,Milan, Italy) in 100 mL of isopropanol by gentle heating and then cooled and filtered through a 0.45 µm filter. The working solution was prepared by diluting three parts of the stock solution in two parts of water (stock solution: water; 3:2 v/v) (Hwang et al. 2014). After several washings, cells were observed using fluorescence microscopy Floid Cell™ Imaging Station (Thermo Fisher Scientific).

Intracellular ROS determination

HepG2 cells were plated at a density of 1.8 x 10^5 cells/well in 24-well plate and treated with different concentrations of SAE or CAE (200-100µg/mL) and oleic acid (0.3mM) for 24 h. Then, ROS was determined by flow-cytometry as reported in section 4.1.

Quantitative RT-PCR

HepG2 or Caco-2 were seeded in 6-well plates ($8.5*10^5$/well) and treated with different doses of CAE or SAE (200-100µg/mL) and oleic acid (OA 0.3Mm) for 24h. RNA extraction and qRT-PCR were performed as reported in section 4.1.1.

Table 4.6. Reverse and forward primers used for qRT-PCR

Gene	Forward primer	Reverse primer
β-actin	5′-CCTGGCACCCAGCACAAT-3′	5′-GCCGATCCACACGGAGTACT-3′
AMPK	5'-TTCAAAAGGCTAATCACAGAAG-3'	5'-TTCAGGAAGATTGTATGCAGG-3'
ABCA1	5′-GGACATGCACAAGGTCCTGA-3′	5′-CAGAAAATCCTGGAGCTTCAAA-3′
ABCG2	5′-ATCACTGATCCTTCCATCTTG-3′	5′-GCTTAGACATCCTTTTCAGG-3′
ABCG5	5'-GCTCCAGGATCCTAAGG-3'	5'-GAAAAAGCTCAGAACGG-3'
ABCG8	5'-TTCTATGTGGACCTGAC-3'	5'TCAAGATCCTTCGTCTCT-3'
BIP	5'-GTTTGCTGATAATTGGTTGAACA-3'	5'-GAATCGCCTGACACCTGAAGA-3'
CHOP	5'-TCTCCTTCATGCGCTGCTTTC-3'	5'-GTACCTATGTTTCACCTCCTG-3'
CATALASE	5′-ATACCTGTGAACTGTCCCTACCG-3′	5′-GTTGAATCTCCGCACTTCTCCAG-3′
CPT1A	5'-TTTGCAGTGCCCATCCTCCG-3'	5'-ACAGGTGGTTTGACAAGTCG-3'
e-CADHERIN	5'-AAGAAGCTGGCTGACATGTACG-3'	5'-CCACCAGCAACGTGATTTCTGCAT-3'
GPx-1	5'-CAGTCGGTGTATGCCTTCTCG-3′	5′-CTCGTTCATCTGGGTGTAGTCC-3′
HMGCR	5'-GCACCTTTCTCTGCATTC C-3'	5'-CGAGAAAGAAAAGTTGAGGT-3'
Il-6	5'-CTACTCTCAAATCTGTTCTGG-3'	5'-GGATTCAATGAGGAGACTTG-3'
LDLr	5'-AGTGCGGGACCAACGAA-3'	5'-ATGGAGCCCACAGCCTT-3'
NQO1	5'-AGGGTCCTTCAGTTTACCTGTG-3'	5'-GGTGGTGGAGTCGGACCTCTA-3'
Nrf-2	5'-CATTGTCATCTACAAACGGGAA-3'	5'-AACTACTCCCAGGTTGCCCA-3'
PPARα	5'-GAATCGCGTTGTGTGACATG-3'	5'-AGG CTGCAAGGGCTTCTTTC-3'
Occludin	5'-TCTTCCTATAAATCCACG-3'	5'-TTGACCTTCCTGCTCTTC-3'
SOD2	5'-CTACTCTCAAATCTGTTCTGG-3'	5'-GGATTCAATGAGGAGACTTG-3'
SREBP1	5'-TCCTTCAGAGATTTGCTTTTG-3'	5'-TGAGGCAAAGCTGAATAAATC-3'
TNFα	5'-CACGATCAGGAAGGAGAAGA-3'	5'-TCTGGCCCAGGCAGTCAGAT-3'
UCP2	5'-TTACGAGCAACATTGGGAGAG-3'	5'-GCTGGAGGTGGTCGGAGATA-3'

Statistical Analysis

Data were expressed as mean ± standard deviation (Mean ± SD). Statistical analysis was performed using GraphPad Prism 5 Software, Inc. (San Diego, CA, USA) and p values ≤ 0.05 were considered as statistically significant.

Results

CAE and SAE reduced lipid accumulation in OA-treated HepG2 cells

HepG2 cells were exposed to OA and CAE or SAE for 24h and lipid accumulation was detected by oil red O staining. Oil red O is fat soluble diazo-dye used for staining

triglycerides and lipids. Oil red O stain protein bound lipid in paraffin sections. As shown in **Figure 4.10,** cells treated with oleic acid showed more lipid droplets than control cells. The extracts counteracted lipid accumulation induced by oleic acid, bringing back a less intense red color especially at highest dose.

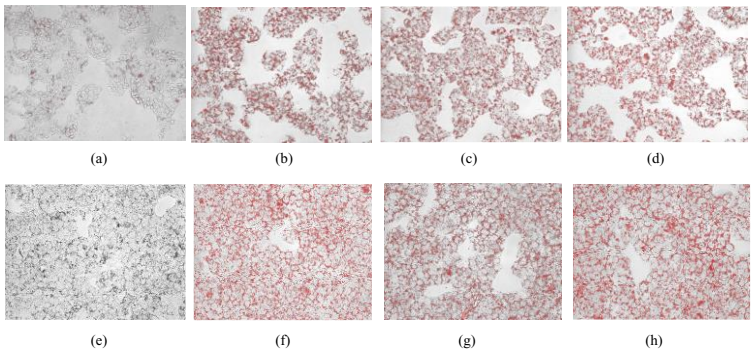

Figure 4.10. Effects of *C. annuum* L.cv Senise (CAE) and S. aethiopicum L. cv Rotonda (SAE) on lipid accumulation in HepG2 cells stimulated with oleic acid (OA) measured by staining with Oil-red-O. (**a**, **e**) untreated cells; (**b**,**f**) OA 0.3mM; (**c**) OA+ CAE 200µg/mL; (**d**) OA+ CAE 100µg/mL; (**g**) OA+ SAE 200µg/mL; (**h**) OA+ SAE 100µg/mL.

CAE and SAE influenced the expression of gene involved in fatty acid metabolism

The expression of several markers involved in lipid metabolism was analyzed in order to understand how the extracts reduced fat accumulation (**Figure 4.11-4.12**). Excess of fat promoted 3-hydroxy-3-methyl-glutaryl-CoA reductase (HMG-CoA reductase) expression and thus cholesterol synthesis. SAE and CAE decreased HMGCoA-reductase expression and especially CAE also sterol regulatory element-binding protein 1 (SREBP-1). Moreover, SAE promoted LDL uptake by increasing LDLR expression, otherwise CAE acted further on reverse cholesterol transport by enhancing ABCA1 expression. AMPK expression enhanced in cells treated with pepper extracts. Moreover, PPARα mRNA increased with treatment as well as uncoupling protein-2 (UCP2) and carnitine palmitoyl transferase 1A (CPT1A) expression which could promote fat oxidation.

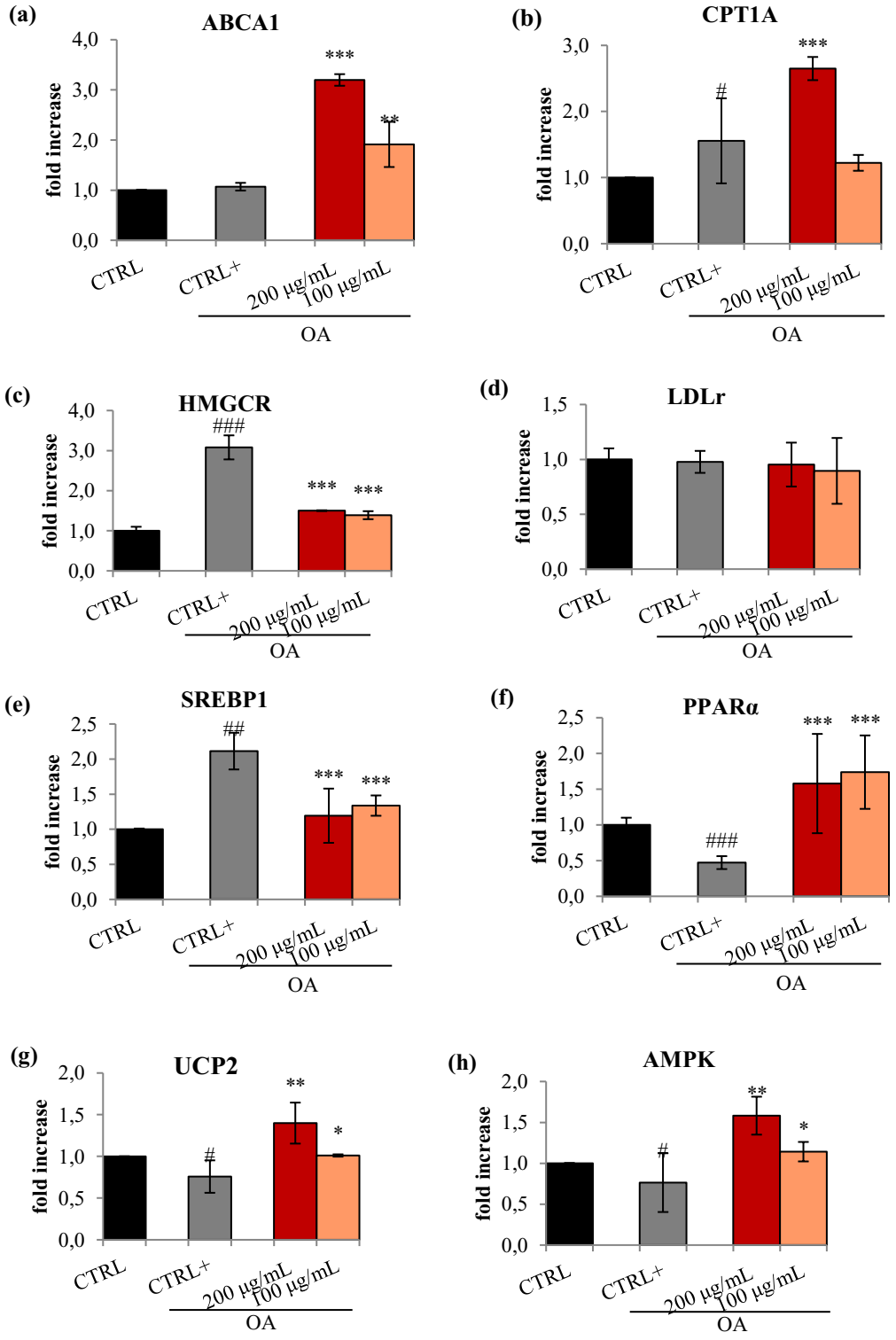

Figure 4.11 Effect of CAE (200 and 100 µg/mL) on the gene expression of (**a**) ATP-binding cassette transporter A1 (ABCA1), (**b**) carnitine palmitoyltrasferase 1A (CPT1A), (**c**) 3-hydroxy-3-methyl-glutaryl-coenzyme A reductase (HMGCR), (**d**) Low density lipoprotein receptor (LDLr), (**e**) Peroxisome proliferator activated receptor alpha (PPARα), (**f**) Sterol Regulatory Element-Binding Protein-1 (SREBP-1), (**g**) uncopling protein 2 (UCP-2), (**h**) AMP-activated protein kinase (AMPK) analysed by real-time q-PCR and normalized with the housekeeping gene, β-actin, in OA-treated HepG2 cell line. Data are expressed as mean ± standard deviation of three independent experiments (n=3). #$p<0.05$ ##$p<0.01$ *vs* untreated cells (CTRL); *$p<0.05$, **$p<0.01$, ***$p<0.001$ *vs* oleic acid (OA 0.3mM) treated cells (CTRL+)

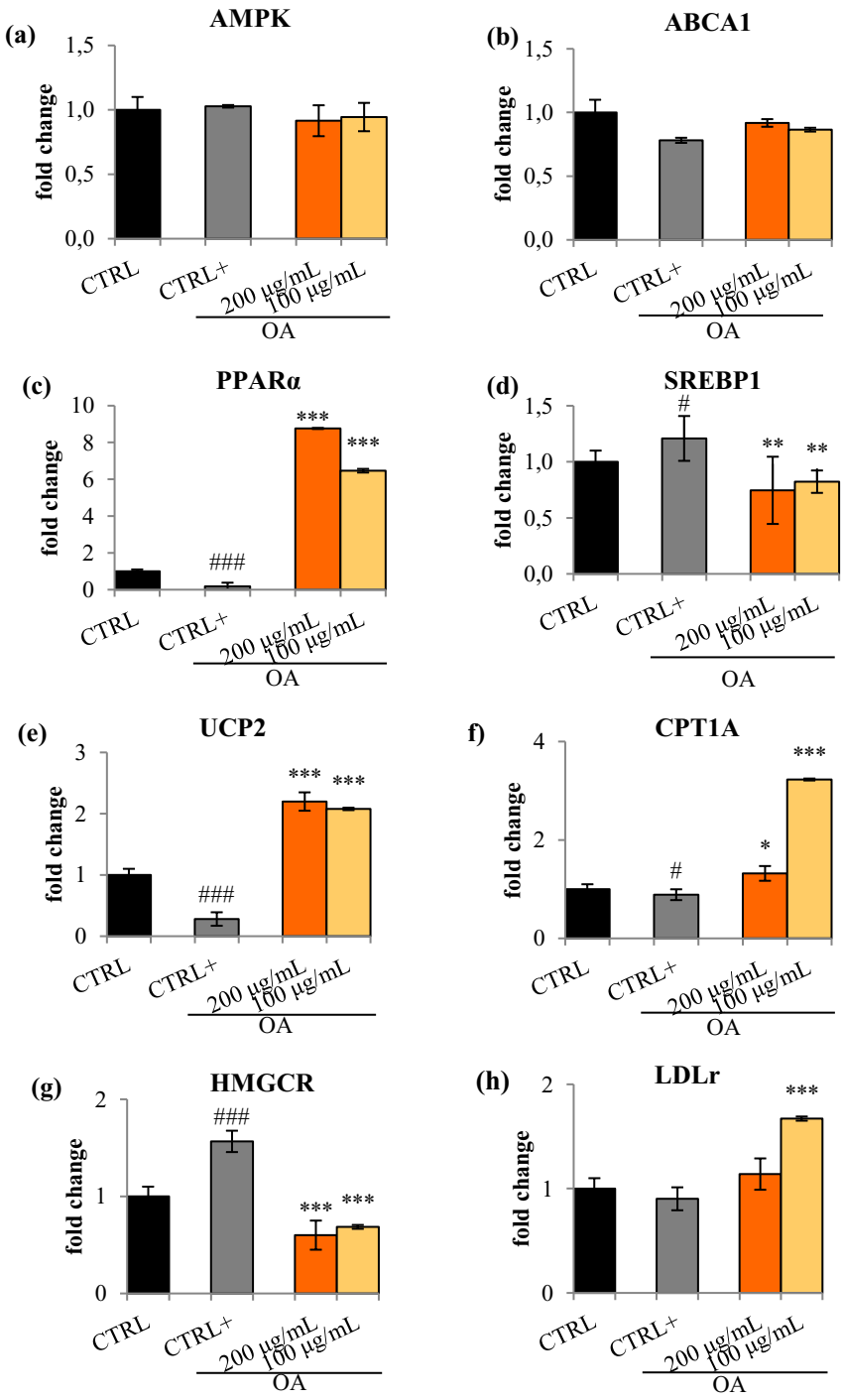

Figure 4.12 Effect of SAE (200 and 100 µg/mL) on the gene expression of (**a**) AMP-activated protein-kinase (**b**) ATP-binding cassette transporter A1 (ABCA1), (**c**) Peroxisome proliferator activated receptor alpha (PPARα), (**d**)Sterol Regulatory Element-binding Protein-1 (SREBP-1), (**e**) uncopling protein 2 (UCP-2) (**f**) carnitine palmitoyltrasferase 1A (CPT1A), (**g**) 3-hydroxy-3-methyl-glutaryl-coenzyme A reductase (HMGCR), (**h**) Low density lipoprotein receptor (LDLR), analyzed by real-time q-PCR and normalized with the housekeeping gene, *β*-actin, in oleic acid (OA 0.3mM)-treated HepG2 cell line. Data are expressed as mean ± standard deviation of three independent experiments (n=3). #$p<0.05$ ###$p<0.001$*vs* untreated cells (CTRL); *$p<0.05$, **$p<0.01$, ***$p<0.001$ *vs* oleic acid-treated cells (CTRL+).

CAE and SAE improved lipid absorption in Caco-2 cells

Caco-2 cells were treated with different doses of CAE or SAE for 24 and 48h and MTT assay was used to evaluate cell viability. As shown in **Figure 4.13**, CAE and SAE reported no cytotoxic effect at all doses tested after 24 and 48h of treatment. Moreover, especially SAE increased cell viability in a dose dependent manner after 48h.

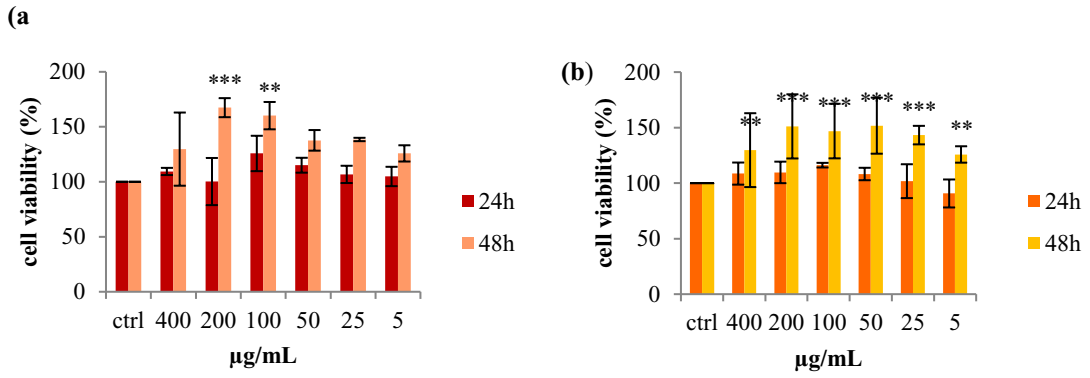

Figure 4.13 Cell viability of Caco-2 cells treated for 24 and 48 h with different concentrations of *Capsicum annuum* L. cv Senise extract (CAE) (**a**) or *Solanum aethiopicum* cv Rotonda peel extract (SAE) (**b**) evaluated by MTT assay. Data are expressed as the mean ± SD of three independent experiments (n = 3). ***$p<0.001$, **$p<0.01$ *vs* untreated cells (CTRL)

Caco-2 cell line were treated with OA (0.3mM) and CAE or SAE (200-100ug/mL) for 24h and the expression of gene involved in synthesis, uptake and efflux of cholesterol was evaluated. As shown in **figure 4.14**, OA up-regulated HMG-CoA reductase and could increase cholesterol synthesis; treatment with CAE drastically reduced its expression level. Moreover, CAE increased the expression of LDLr, ABCA1, ABCG5 and ABCG8, transporters involved in cholesterol absorption. According with previous study (Sinisgalli et al. 2020), CAE improved permeability of the barrier which is damaged by the excess of fat. CAE significantly increased occludin and *e*-cadherin expression, two proteins of cellular junctions. SAE had less influence on lipid trafficking improving only ABCA1 expression. In addition, SAE influenced also lipid synthesis by downregulation of SREBP1 and mainly of HMG-CoAr. Moreover, inflammatory status improved in cells treated with extract. IL-6 and TNF-a mRNA concentration was lower than OA-treated cells. (**Figure 4.15**).

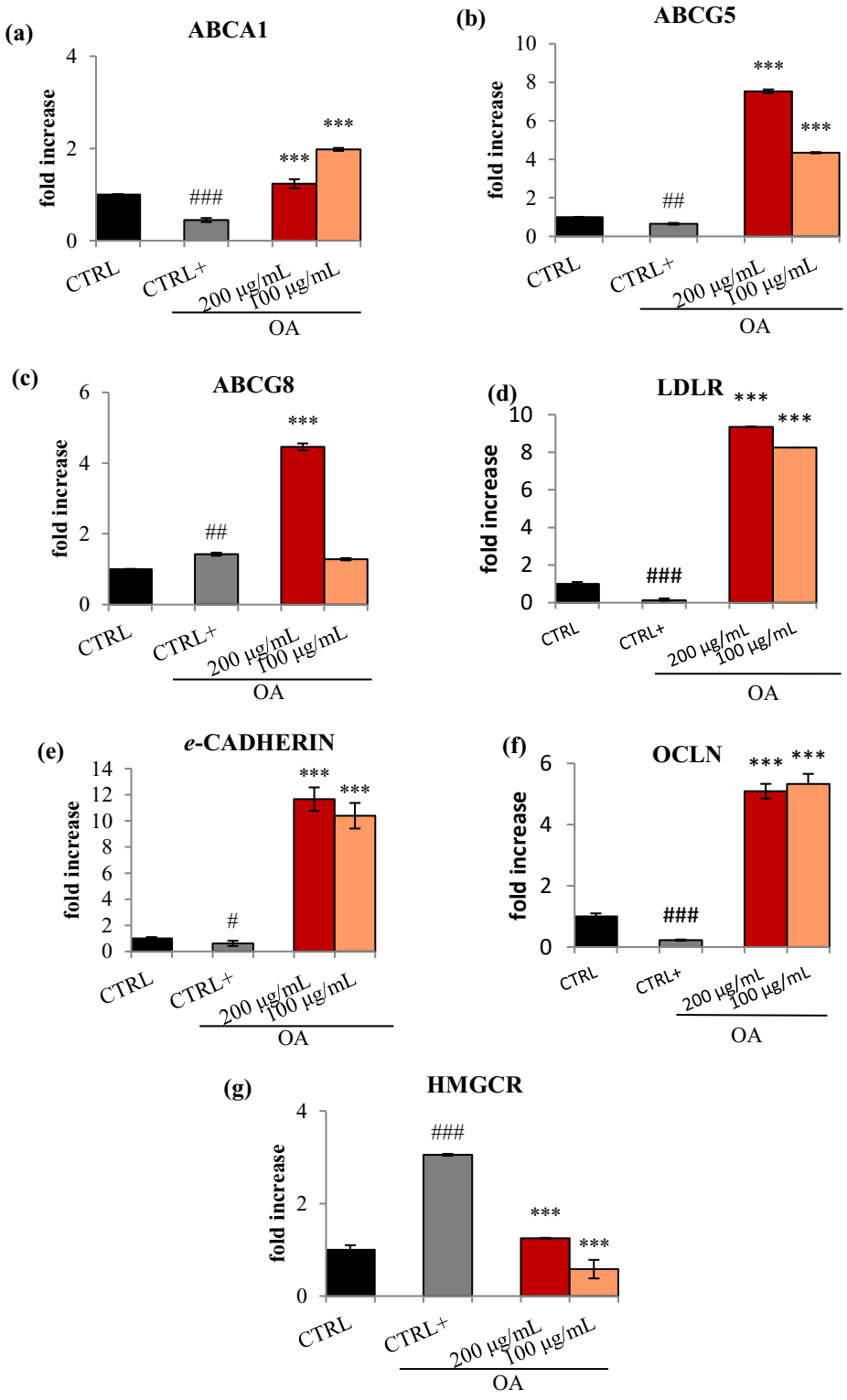

Figure 4.14 Effect of CAE (200 and 100 µg/mL) on the gene expression of (**a**) ATP-binding cassette transporter A1 (ABCA1), (**b**) ATP-binding cassette transporter G5 (ABCG5), (**c**) ATP-binding cassette transporter G8 (ABCG8)3-(**d**) *e*-cadherin, (**f**) occludin (OCLN), (**g**) hydroxy-3-methyl-glutaryl-coenzyme A reductase (HMGCR),) analyzed by real-time q-PCR and normalized with the housekeeping gene, *β*-actin, in HepG2 cell line. Data are expressed as mean ± standard deviation of three independent experiments (n=3).

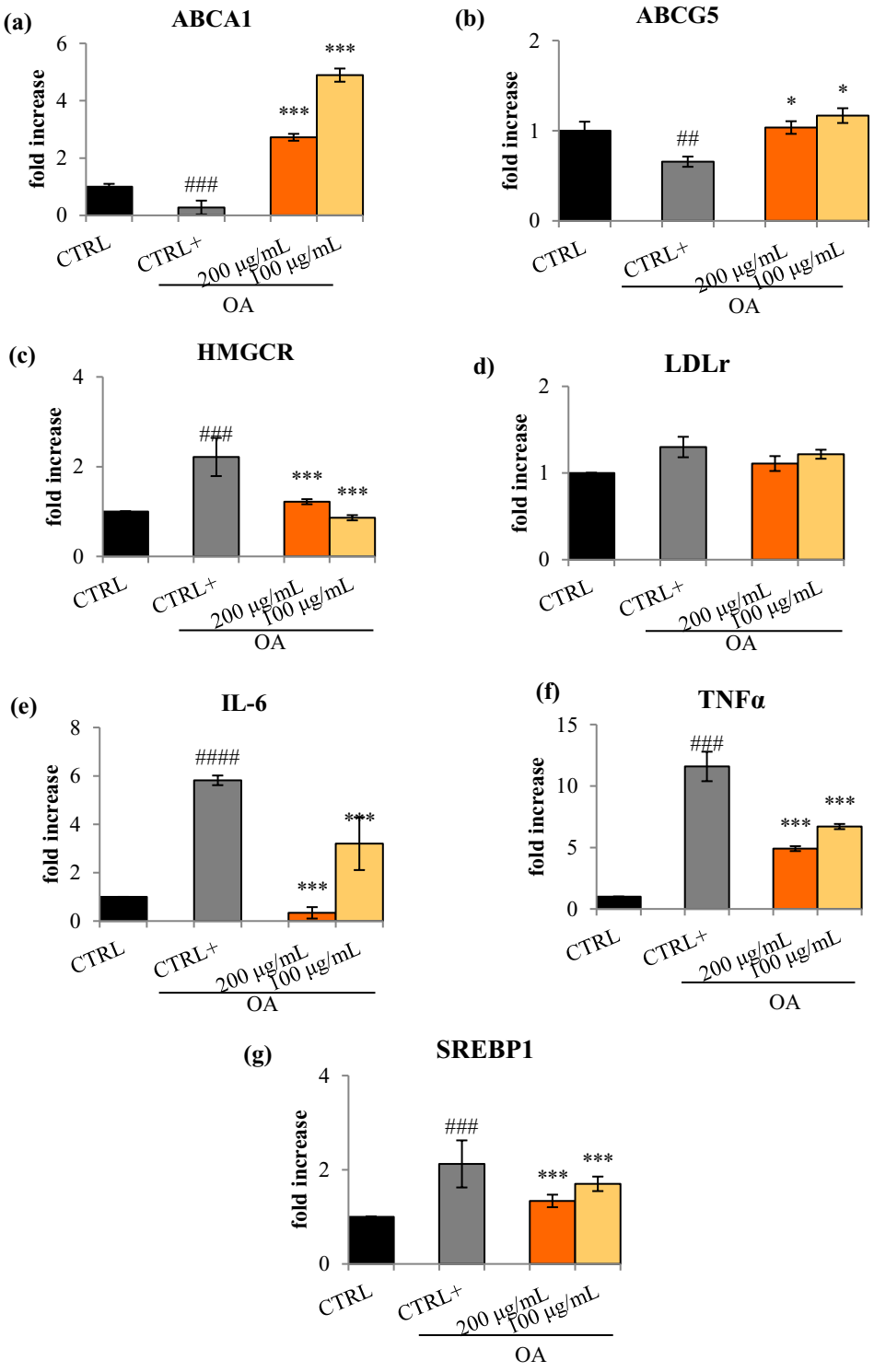

Figure 4.15 Effect of SAE (200 and 100 µg/mL) on the gene expression of (**a**) ATP-binding cassette transporter A1 (ABCA1), (**b**) ATP-binding cassette transporter G5 (ABCG5) (**c**) 3-hydroxy-3-methyl-glutaryl-coenzyme A reductase (HMGCR), (**d**) Low density lipoprotein receptor (LDLr), (**e**) inteleukine-6 (IL-6), (**f**) tumor necrosis factor α (TNFα), (**g**) sterol regulatory element-binding protein 1 (SREBP1) by real-time q-PCR and normalized with the housekeeping gene, *β*-actin, in oleic acid(OA 0.3Mm)-treated Caco-2 cell line. Data are expressed as mean ± standard deviation of three independent experiments (n=3). #p<0.05, ###p<0.001 *vs* untreated cells CTRL; ***p<0.001, *p<0.05 *vs* OA-treated cells (CTRL+)

Antioxidant activity of CAE and SAE in OA-treated HepG2 cells

Prolonged exposure to excess of fat induced ROS generation and pro-inflammatory cytokines production. HepG2 cell line were treated with OA and CAE or SAE for 24h and intracellular ROS were evaluated by flow cytometry. HepG2 cell line treated with oleic acid showed higher intensity fluorescence thus higher amount of ROS compared with control. CAE and SAE decreased OA-induced ROS generation restoring basal conditions (**Figure 4.16**).

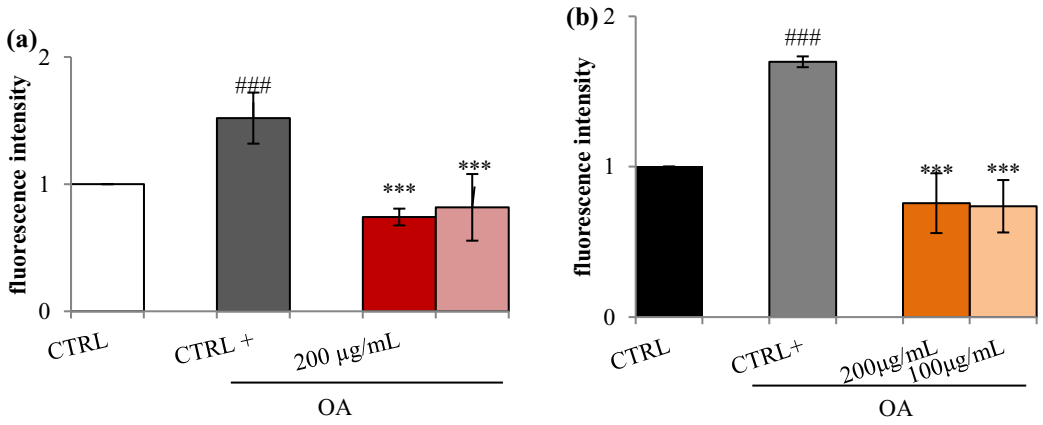

Figure 4.16 Effect of *C. annuum* L. cv Senise (CAE) (**a**) and *S. aethiopicum* L. cv Rotonda (SAE) (**b**) on oleic acid (OA)- induced intracellular reactive oxygen species (ROS) generation. Cells were treated with different concentrations of CAE or SAE (200-100 µg/mL) and oleic acid (OA 0.3mM) (CTRL+) for 24 h ROS generation was measured by DCFH-DA staining with flow cytometry analysis. Data are expressed as the mean ± SD of three independent experiments (n = 3). ###p< 0.001 *vs* untreated cells (CTRL), ***p<0.001 *vs* OA-treated cells (CTRL+).

The antioxidant activity resulted from different effects exerted by the extract on several markers. Both the extracts drastically reduced the expression of the pro-inflammatory cytokine IL-6. CAE promoted nuclear factor erythroid 2–related factor 2 (Nrf-2) and consequently superoxide dismutase (SOD-2), NADPH-quinone oxidase 1 (NQO1) expression. Moreover, CAE drastically up-regulated ATP-binding cassette transporter G2 (ABCG2). No statistical differences were reported on catalase and glutathione peroxidase-1 (GPx-1) expression (**Figure 4.17**). Higher levels of ROS induced endoplasmic reticulum stress (ER): CAE significantly reduced BIP and CHOP expression in OA-treated cells (**Figure 4.17**).

SAE increased the expression of Nrf-2 three times over the control exerting a greater effect than CAE. Furthermore, SAE promoted catalase, NQO1, SOD-2 and ABCG2 expression.As pepper extract, SAE reduced ER stress downregulating only BIP expression (**Figure 4.18**).

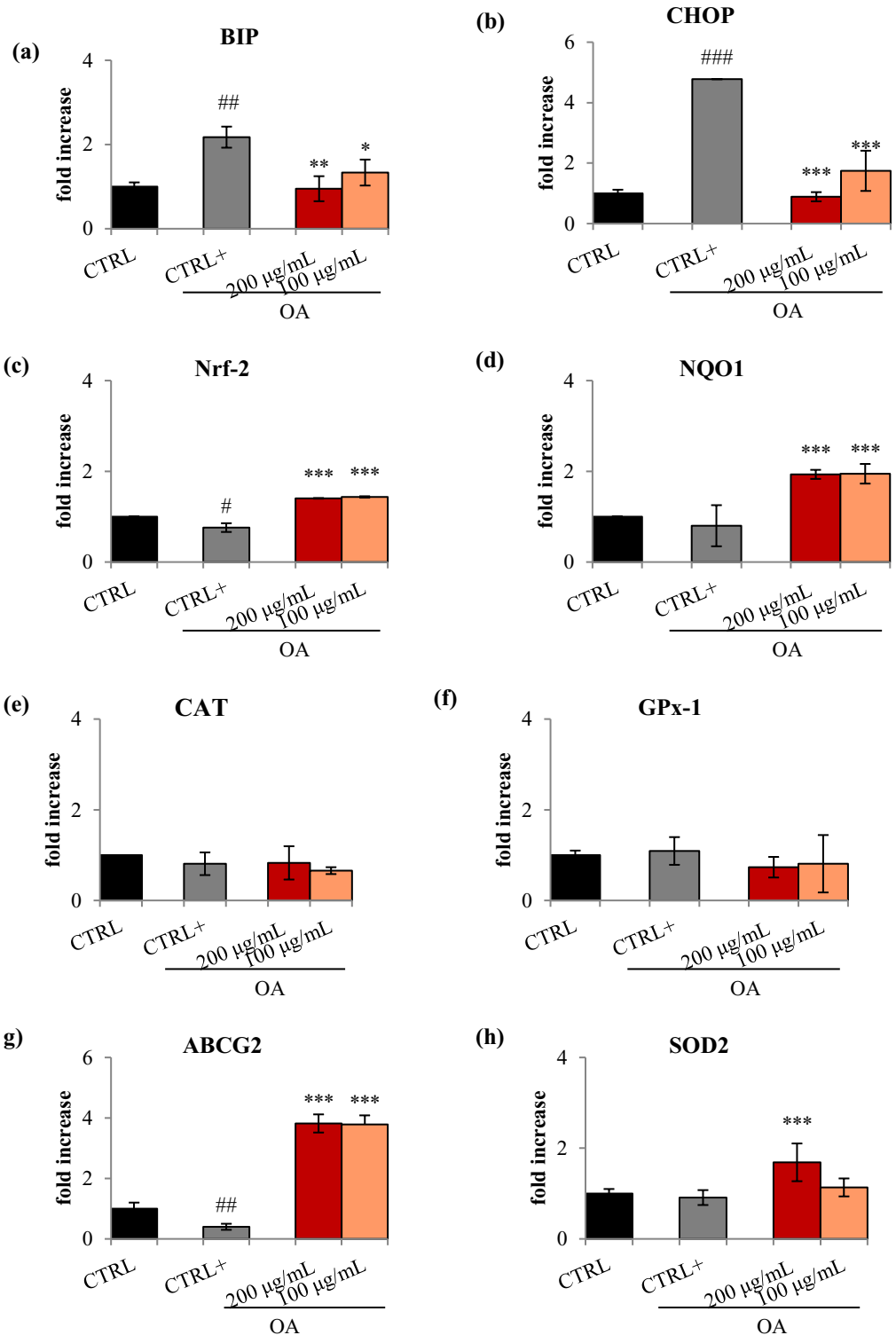

Figure 4.17 Effect of CAE (200 and 100 µg/mL) on the gene expression of (**a**) Binding Immunoglobulin Protein (BIP), (**b**) C/EBP homologous protein (CHOP), (**c**) nuclear factor erythroid 2-related factor 2 (Nrf-2), (**d**) NADPH-quinone oxidase (NQO1), (**e**) catalase (CAT), (**f**) glutathione peroxidase (GPx-1), (**g**)ATP-binding cassette transporter G2 (ABCG2), (**h**) superoxide dismutase (SOD-2) analyzed by real-time q-PCR and normalized with the housekeeping gene, *β*-actin, in oleic acid (OA 0.3mM)- treated HepG2 cell line. Data are expressed as mean ± SD of three independent experiments (n = 3). # $p < 0.05$, ##$p<0.01$, ###$p<0.001$ *vs* untreated cells (CTRL), *** $p < 0.001$ *vs*. OA-treated cells (CTRL+).

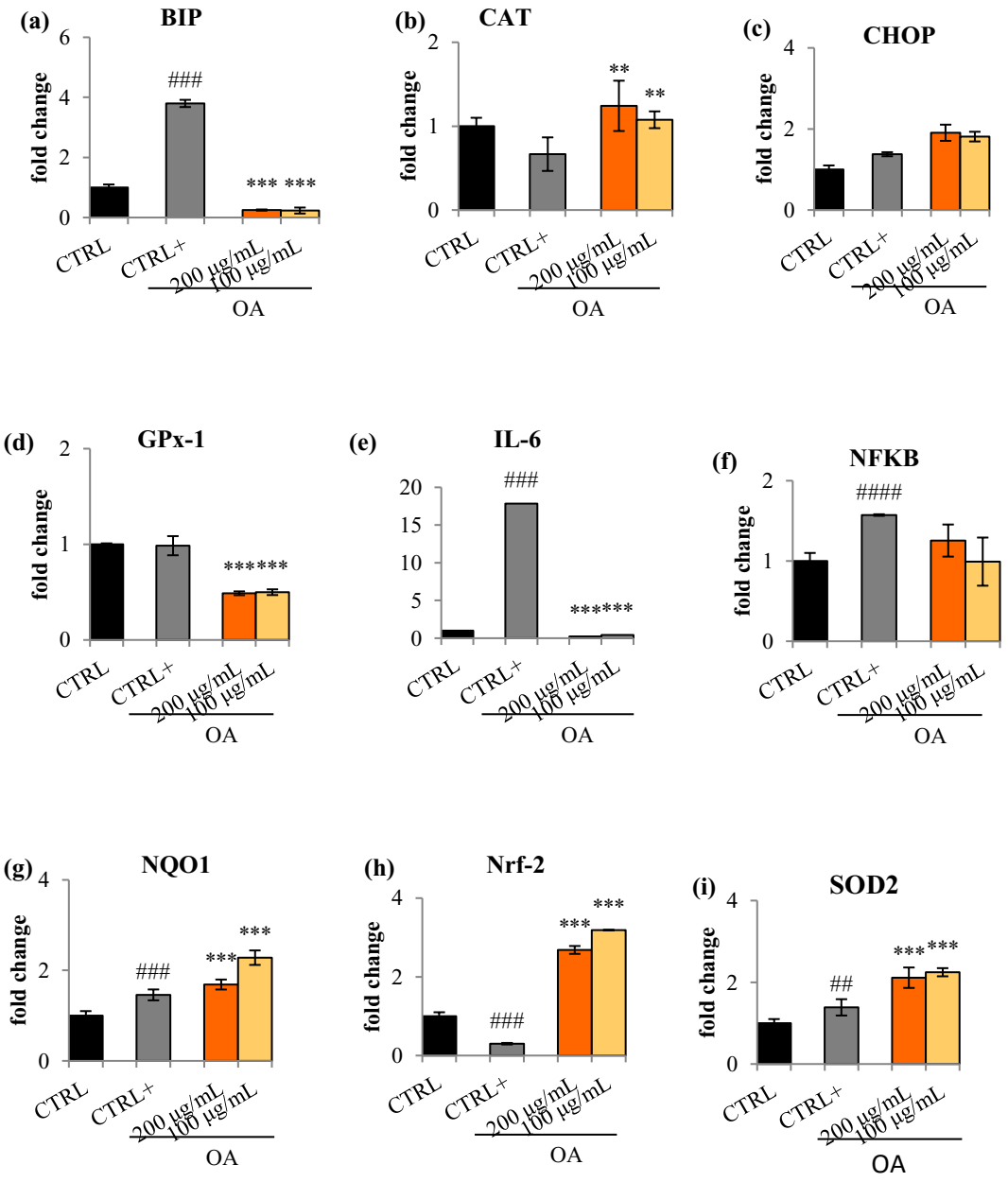

Figure 4.18 Effect of SAE (200 and 100 µg/mL) on the gene expression of (**a**) binding immunoglobulin protein(BIP) (**b**) catalase (CAT); (**c**) (CHOP) (**d**) ATP-binding cassette transporter A1 (ABCA1), (c) ATP-binding cassette transporter G2 (ABCG2) (d) glutathione peroxidase 1 (GPx-1); (**e**) interleukin-6 (IL-6); (**e**) nuclear factor kabba b (NFkB), (f) NADPH quinone dehydrogenase 1 (NQO1), (**g**) nuclear factor erythroid 2-related factor (Nrf2), (**i**) superoxide dismutase 2 (SOD-2) analyzed by real-time q-PCR and normalized with the housekeeping gene, *β*-actin, in oleic acid (OA 0.3 mM) treated HepG2 cells. Data are expressed as mean ± standard deviation of three independent experiments (n=3). ##p<0.01, ###p<0.001 *vs* CTRL, ***p<0.01, **p<0.001 *vs* OA-treated cells (CTRL+)

Discussion

The balance between fatty acid uptake, *de novo* lipogenesis, triglyceride synthesis and export and fatty acid oxidation determine the amount of fat stored in the liver. Thus, dysregulation in any of these processes leads to lipid imbalance and fatty acid diseases. Our previous study reported the ability of CAE to reduce LDL in plasma of obese mice (Sinisgalli et al. 2020). (Ogunka-Nnoka et al. 2018) demonstrated as an ethanol extract of *Solanum aethiopicum* stalks significantly reduced plasma cholesterol, triacylglycerol, LDL and VLDL cholesterol and increased HDL cholesterol in albino rats. Thus, the extract could have the capacity to improve the lipid profile of plasma thereby lowering the risk of cardiovascular disease (Ogunka-Nnoka, Onyegeme-Okerenta, and Omeje 2018). This action is caused by the composition of the same *S. aethiopicum* stalks and also fruits that are rich in saponins, alkaloids, flavonoids, and tannins as well as dietary fiber. Many studies have reported the ability of saponins to reduced plasma lipids, particularly it was seen that their hypolipidemic effect could be due to several mechanisms, which include the decrease of fatty acid, the increase of LDL receptors, the activation of LCAT and lipase and the inhibition of acetyl-CoA carboxylase (Elekofehinti et al. 2012).

In the present study CAE and SAE demonstrated hypolipidemic activity and reduced fat accumulation in OA-treated HepG2 cell line by influencing the expression of several markers involved in lipid metabolism. AMPK is a major sensor of the energy status which maintains energy homeostasis of the cell by activating catabolic pathways. AMPK inhibits *de novo* lipogenesis by phosphorylating and inhibiting SREBP1, a transcription factor promoting the expression of several lipogenic genes like FAS, SCD-1 and DGAT (Ferre and Foufelle 2010). Both the extracts reduced SREBP1 expression together with that of HMG-CoA reductase, a key enzyme in cholesterol synthesis and targets of statins, drugs commonly used in dyslipidemia treatment. As a result, endogenous cholesterol synthesis is reduced and cholesterol is mobilized by extra-hepatic liver tissues for the biosynthesis of bile acid. This is often indicated by an increase in HDL-cholesterol. Mainly, CAE promoted ABCA1 expression in OA-treated HepG2 cell line involved in cholesterol reuptake from peripheric tissues unable to degrade excess cholesterol.

Carotenoids, found in Senise pepper and Rotonda eggplant, are natural source of vitamin A (or retinol) which is metabolized to all-*trans* retinoic acid or 9-*cis* retinoic acid. These metabolites are high affinity ligands for retinol X receptors (RXRs) which binds and activates nuclear receptors like PPAR-α (Ziouzenkova and Plutzky 2008). CAE and SAE

could promote the expression of PPAR-α and consequently that of CPT1 and UCP2, involved in fat oxidation. RXR activation is also responsible of ABCA1 expression which is involved in reverse cholesterol transport and in cholesterol efflux from basolateral intestinal membrane promoting the formation of HDL (Ziouzenkova and Plutzky 2008; Fitzgerald et al. 2010). In addition to synthesis and oxidation, elimination of cholesterol is essential for hepatic cholesterol homeostasis. CAE mainly influenced lipid transport through intestinal barrier compared with SAE. In fact, pepper extract drastically up-regulated ABCA1 together with ABCG5 and ABCG8, two ABC transporters which play a key role in efflux of cellular cholesterol to intestinal lumen (Gil-Ramírez et al. 2016; Repa et al. 2002).. In addition, CAE promoted the expression of LDL receptor contributing to reduce LDL plasma concentrations. Polyphenol compounds can reduce plasma lipids, which might be due to the up-regulation of LDL receptor expression, inhibition of hepatic lipid synthesis and lipoprotein secretion, and an increase in cholesterol elimination via bile acids (Ogunka-Nnoka et al. 2018). Otherwise, SAE exerted hypolipidemic effect in intestinal cells acting mainly on lipid synthesis. Many studies reported as soluble fibers could be fermented in the colon into short-chain fatty acids, which in turn lower the synthesis of cholesterol and triacylglicerols.

Prolonged exposure to excess of fat induces the production of pro-inflammatory cytokines like TNFα, IL-1 and IL-6, first in adipose tissue and then in liver causing a state of chronic inflammation. These cytokines are potent stimulators for the production of reactive oxygen and nitrogen by macrophages and monocytes; therefore, a rise in the concentration of cytokines could be also responsible for the increased oxidative stress. The expression of IL-6 was decreased in HepG2 cell line treated with OA and extracts. Moreover, peel extract confirmed anti-inflammatory activity also in OA-treated Caco-2 cells by reducing IL-6 and TNFα mRNA amount. Superoxide dismutase (SOD), catalase (CAT) and glutathione peroxidase (GPx) are key enzymes in antioxidant defense which respectively dismutase superoxide radical, breakdown hydrogen peroxides to harmless molecules. The superoxide radical (O_2) or singlet oxygen radical (O_2^-) generated in tissues through metabolism or reactions in cells is catalytically converted to hydrogen peroxide (H_2O_2) and molecular oxygen (O_2) by superoxide dismutase. H_2O_2 when accumulated is toxic to body tissues or cells and in the presence of Fe^{2+} is converted to deleterious hydroxyl radical (OH) through Fenton reaction. Catalase, abundant in peroxisomes, and glutathione peroxidase (GPx) in mitochondria prevent this phenomenon break down H_2O_2 into water and molecular oxygen.

The activity of this enzymes diminished in obese (Albuali 2014; Ighodaro and Akinloye 2018). Both the extracts reduced ROS generation in OA-treated HepG2 cells by promoting several markers involved in antioxidant defense. Particularly, CAE and SAE increased SOD2 expression together with NQO1, which catalyzes the detoxification of quinones and their derivatives, preventing their participation in redox cycling and oxidative stress, and ABCG2 via Nrf-2 pathway. In this way the extracts improved the oxidative stress induced by OA in HepG2 cells used as model. ROS are positively correlated with endoplasmic reticulum (ER) stress: radicals can oxidize nascent proteins and increase misfolded and unfolded proteins in the ER. Furthermore, they promote calcium release from the ER by acting on calcium channels. Decreased concentration of the total calcium in the ER lumen ultimately impairs protein folding of nascent proteins. In cells treated with CAE, BIP expression was drastically reduced thus suggesting that antioxidant activity of the extract also improved ER stress compared with OA-treated cells. CAE also reduced CHOP expression.

C. annuum and S.aethiopicum are source of polyphenols known as antioxidant but previous study (Yahfoufi et al. 2018) also showed their anti-inflammatory activity due to their capacity to repress monocytes/macrophages by inhibiting adhesion molecules like intercellular adhesion molecule-1 (ICAM-1) and vascular cell adhesion molecule-1 (VCAM-1), cyclooxygenase-2 (COX-2), inducible nitric oxide synthase (iNOS), and reducing the production of TNF-α, IL-1-β and IL-6 expression.

Conclusion

Capsicum annum L. cv Senise and *Solanum aethiopicum* L. cv Rotonda peel extract counteracted fat accumulation by promoting lipolysis and lipid elimination instead of lipogenesis. It is interesting to underline that extracts also reduced oxidative stress and inflammatory status caused by prolonged exposure to excess of fat. Thus, for disease like obesity in which more than one molecular mechanism is involved *Capsicum annum* L. cv Senise and *Solanum aethiopicum* cv Rotonda could represent new multitarget therapeutic strategy.

4.3 *Capsicum annuum* L. *cv* Senise: improvement of endothelial dysfunction

Introduction

Obesity represents the most important risk factor for the development of hypertension and other cardiovascular diseases (Artham et al. 2009). The activation of the rennin-angiotensin system (RAS) has been reported as one of the possible mechanisms through which obesity could lead to hypertension and higher cardiovascular risk (Segura and Ruilope 2007). In the RAS, angiotensin 1-converting enzyme (ACE) plays a key role in the regulation of blood pressure and normal cardiovascular function. It catalyzes the conversion of angiotensin I to angiotensin II, which is known to increase the blood pressure. Hence inhibition of ACE is an important strategy for the treatment and management of obesity-related hypertension. Endothelial dysfunction is involved in pathophysiology of hypertension. It is an impairment of endothelium-dependent vasodilatation due to reduction of bioavailability of vasodilators, particularly nitric oxide, and/or an increase in endothelium-derived contracting factors. Reactive oxygen species (ROS) increased in obese patients and are positively correlated with endothelial dysfunction by decreasing nitric oxide production (Incalza et al. 2018, Fernández-Sánchez et al. 2011). NADPH oxidase represent the major source of ROS in endothelium (Toral et al. 2015). Immune cell-derived cytokines such as IFN-γ have been shown to activate and increase the expression of NADPH oxidase and contribute to vascular oxidative stress (Fernández-Sánchez et al. 2011, Wolfort et al. 2008). Obesity induces changes in spleen, the immune organ involved in filtering the blood, capturing pathogens and activating adaptative immune response. Changes in spleen structure like enlargement, sinusoidal dilatation and intracellular and intercellular deposits, cellular distribution, were found in obese patients (Abd El-Aziz, Naguib, and Rashed 2018). The change of spleen structure affects the immune function of the organism. Moreover, obesity induced changes also in splenocytes cytokine profile increasing production of pro-inflammatory cytokines, like IL-6 and INF-Y, and decreasing that of anti-inflammatory cytokines like IL-10 (DeFuria et al. 2013).

Thus, oxidative stress and inflammation play key role in the development of obesity and associated cardiovascular diseases.

Previously, we have demonstrated antioxidant and anti-inflammatory activity of CAE in OA-treated HepG2 cell used as steatosis model. In the present study we would evaluate biological activity also in splenocytes and in arteria of obese mice as potential cardioprotective effect.

Material and methods

Chemicals

Absolute ethanol, Dulbecco's Modified Eagle Medium (DMEM), dimethyl sulfoxide (DMSO), [3-(4,5-dimethyl-2-thiazolyl)-2,5-diphenyl-2H-tetrazolium bromide] (MTT) and 2′,7′-dichlorodihydrofluorescein diacetate (DCFH-DA), captopril, hippuryl-*L*-histidyl-*L*-leucine (HLL), hippuric acid (HA), Angiotensin converting enzyme (ACE) were purchased from Sigma Aldrich S.p.A. (Milan, Italy). Trypsin-EDTA solution, fetal bovin serum (FBS), glutamine, penicillin-streptomycin, and phosphate saline buffer (PBS) were purchased from Euroclone (Milan, Italy). Reagents used for RT-PCR were purchased from Euroclone (Milan, Italy).

Angiotensin converting enzyme (ACE) inhibition in vitro assay

ACE inhibitory activity of CAE was performed using an HPLC-DAD as reported by (Ranilla et al. 2010) with some modifications. The method used is based on the determination of the hippuric acid (HA) formed by hippuryl-*L*-histidyl-*L*-leucine (HLL) in the reaction catalyzed by ACE:

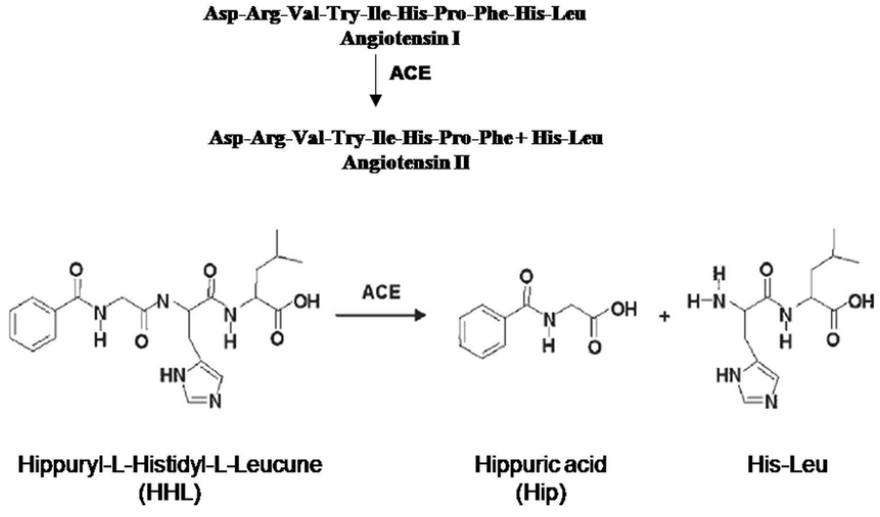

For the assay, 50µL of sample was pre-incubated with 200 µL of ACE enzyme (2 mU/mL in 0.1M NaCl-borate buffer) at 25°C for 10 min. Then, the mixture was incubated with 100 µL of substrate (HHL 0.5 mM in 0.1M NaCl-borate buffer) at 37°C for 60min. The reaction was stopped by adding 150 µL of HCl 0.5 M and the percentage of ACE inhibition was determined by an HPLC system. An aliquot of 20 µL from the reaction mixture was analyzed on a Kinetex C18 column (100 × 4.6 mm, 5 µm particle size; Phenomenex, Macclesfield, UK) using an isocratic elution of MeOH (60:100 v/v) at a flow rate of 1 mL/min. HA and HHL were detected by UV at 228 nm. The percentage of ACE inhibition was calculated as follow:

$$\%\text{inhibition} = (([HA]_{control}-[HA]_{sample})/[HA]_{control})*100$$

Captopril was used as a positive control.

Cell study

Cell culture

Splenocytes were freshly isolated from the mouse spleen. Male C57BL/6 mice were sacrificed by cervical dislocation. Their spleens were aseptically removed using autoclaved forceps and stored in cold sterile R10 (RPMI 1640 (Roswell Park Memorial Institute) with L-glutamine and sodium bicarbonate, Sigma Aldrich, St. Louis, USA supplemented with 10% FBS, 10 000 U/mL Penicillin and 10 mg/mL streptomycin). Single-cell suspensions were prepared by gently homogenizing the spleens through a cell strainer. The cells were washed three times in cold R10 (1500 rpm, 5 min, 4 °C). The pellet was resuspended in R10 and cells were counted using a Bürker chamber after Turk solution staining. The grow factor β-mercaptoethanol (BME), was added to the cell culture at a final concentration of 50 µM.

MTT assay

Murine splenocytes were seeded in flat-bottomed micro-culture plates ($2*10^6$ cells/mL) and treated with different doses of CAE (12,5-25-50-100-200 µg/mL) or Concanavalin A (5 µg/mL) as positive control for 24 h and 48 h. Cell viability was evaluated by MTT assay as described previously in section 4.1.

Intracellular ROS determination

Splenocytes were seeded in 6-well plates (3mil/mL) and treated with different doses of CAE (200-100-50 ug/mL) or *N*-acety-*L*-cysteine (NAC 2.5mM) for 24h. Then, cells were stressed with LPS (100ng/mL) for 6h and stained with the fluorescent dye CellROX® Green Reagent. Splenocytes were stimulated with LPS for 6h and then treated with CAE or NAC for 24h. In order to evaluate possible preventive effects of the extract, cells were pretreated first with CAE for 24h and then stressed with LPS for 6h. Afterwards, cells were stained. The production of ROS was evaluated using the fluorescent dye CellROX® Green Reagent and fluorescence was measured by flow cytometer LSR II with HTS.

Cytokine detection in murine splenocytes by an ELISA assay

The concentration of IL-4 and IFN-γ was measured by commercial Enzyme Linked ImmunoSorbent Assay (ELISA) kits (Biolegend, USA). Splenocytes were treated with CAE or Con A as followed:

a) Splenocytes were seeded in 24-well plate ($3*10^6$ cells/mL) and treated with different concentrations of CAE (12.5-25-50-100-200 µg/mL) or Con A (5 µg/mL) as positive control for 24h
b) Splenocytes were seeded in 24-well plate ($3*10^6$ cells/mL) pre-treated with ConA (5 µg/mL) for 24h and then treated with CAE (12.5-25-50-100-200 µg/mL) for 24h;
c) Splenocytes were seeded in 24-well plate ($3*10^6$ cells/mL) pretreated with CAE (12.5-25-50-100-200 µg/mL) for 3h and then they were stimulated with ConA (5 µg/mL) for 24h.

After treatment, cells were collected and centrifuged (800rpm, 5min, RT). Supernatants were harvested and the amount of cytokines were measured by using ELISA MAX kit (Biolegend, USA) according to the manufacture instructions. Briefly, 100 µL of coating buffer solution containing a capture antibody was added to each well of the 96-well plate and incubated overnight. Then, 100 µL of assay diluent was added to block any remaining binding sites on the well. After 1 h incubation at RT, the sample prepared in assay diluent (1:2) was added to each well and incubated for 2 h at RT. At the same time, standards, positive and negative controls were plated. 100 µL of detection antibody solution was then added to each well and incubated 1 h at RT. Wash buffer was used to wash the wells at each step. After that 100 µL of Avidin-HRP solution was added to each well for 30 min and then 100 µL of TMB substrate solution was added. After 30 min of incubation in the dark, the stop solution was

added. Absorbance was read at 450nm (reference at 570nm) by an absorbance reader (Tecan i-control 1.10, Austria Gmbh). Results are expressed as pg/mL, using the following standard curves: IFN-γ: $y = 0.0032x + 0.0305$, $R^2 = 0.9973$; IL-4: $y = 0.0017x + 0.077$, $R^2 = 0.9952$

Detection of IL-4 and IFN-γ secreting cells

Production of IFN-γ and IL-4 was evaluated in splenocytes treated with CAE by using ImmunoSpot kits according to the manufacturer's protocol (Double colour IFN-γ/IL-4, CTL, Germany). 96-well polyvinylidene difluoride-backed microtiter plates were activated with 15 µL of 70% ethanol for less than one minute and washed 3 times with sterile PBS. Plates were coated with 80 µL of murine IFN-γ/IL-4 capture antibodies solution and incubated overnight at 4°C. Plate was washed one time with 150 µL PBS and 0.5 mil/mL of splenocytes from homogenized spleen of healthy C57Bl/6 mouse were seeded. Cells were incubated with different doses of CAE (12.5-25-50-100-200 µg/mL) or Con A (5µg/mL) alone and together at 37°C and 5% CO_2 for 24h. Plates were washed with PBS and wash buffer to remove cells and 80 µL/well of anti-murine IFN-γ/IL-4 detection antibodies solution were added and incubated for 2h at RT. After 3 washing with wash buffer, 80 µL/well of a solution containing enzymatic conjugates were added and the plate was incubated for 1 h at RT. Plates were washed two times with wash buffer and distilled water and 80µL/well of Blue Developer Solution were added and incubated for 15 min at RT. The reaction was stopped by gently rinsing membrane with tap water. The same steps were repeated for Red developer solution. After 24h of air-drying at RT, the plate was scanned with Immunospot software.

In vivo study

Vascular reactivity study in high fat diet (HFD) fed mice treated with CAE

The study was carried out in accordance with the 'Guide for the Care and Use of Laboratory Animals' as promulgated by the National Institute of Health, and the protocols approved by the Ethic Committee of Laboratory Animals of the University of Granada (Spain) (Ref. No. 28/03/2016/030). Male 5-week-old C57BL/6J mice (Janvier, St Berthevin, Cedex, France) were housed in standard condition (12-hour light/dark cycle, temperature 22 ± 1°C, 55 ± 10% relative humidity) with free access to food and water. The mice were divided into four groups (n=10): control, control-treated with CAE (25 mg/kg), obese control and obese-treated with CAE at different doses (1, 10 and 25 mg/kg). Pepper extract was administered daily by oral gavage for six weeks. Control mice received a standard diet (13% calories from

fat, 20% calories from protein and 67% calories from carbohydrate) (Global diet 2014; Harlan Laboratories, Barcelona, Spain) whereas obese mice were fed a high-fat diet (HFD) in which 60% of its caloric content was derived from fat (Purified diet 230 HF; Scientific Animal Food & Engineering, Augy, France). At the end of the treatment, mice were sacrificed under isoflurane anaesthesia.

Descending thoracic aortic rings were dissected from animals and were suspended in a wire myograph (model 610M, Danish Myo Technology, Aarhus, Denmark) for isometric tension measurement as previously described (Toral et al. 2015). The organ chamber was filled with Krebs solution (NaCl 118 mM, KCl 4.75 mM, $NaHCO_3$ 25 mM, $MgSO_4$ 1.2 mM, $CaCl_2$ 2 mM, KH_2PO_4 1.2 mM, and glucose 11 mM) at 37°C and gassed with 95% O_2 and 5% CO_2 (pH~7.4). Length–tension characteristics were obtained via the myograph software (Myodaq 2.01) and the aortae were loaded to a tension of 5mN. After 90 min of stabilization period, cumulative concentration-response curves to acetylcholine (10^{-9} M-10^{-5} M) were performed in intact rings pre-contracted by U46619 (10^{-8} M). Relaxant responses to acetylcholine were expressed as a percentage of precontraction (Toral et al. 2015).

NADPH oxidase activity

The lucigenin-enhanced chemiluminescence assay was used to determine NADPH oxidase activity in intact aortic rings, as previously described (Toral et al. 2015). Aortic rings from all experimental groups were incubated for 30 minutes at 37ºC in HEPES-containing physiological salt solution (NaCl 119 mM, HEPES 20 mM, KCl 4.6 mM, $MgSO_4$ 1 mM, Na_2HPO_4 0.15 mM, KH_2PO_4 0.4 mM, $NaHCO_3$ 1 mM, $CaCl_2$ 1.2 mM and glucose 5.5 mM, pH 7.4). Aortic production of O_2 was stimulated by addition of NADPH (100 μM). Rings were then placed in tubes containing physiological salt solution, with or without NADPH and lucigenin was injected automatically at a final concentration of 5 μmol/L to avoid known artefacts when used a higher concentration. NADPH oxidase activity were determined by measuring luminescence over 200 s in a scintillation counter (Lumat LB 9507, Berthold, Germany) in 5-s intervals and was calculated by subtracting the basal values from those in the presence of NADPH. Vessels were then dried, and dry weight was determined. NADPH oxidase activity is expressed as relative luminescence units (RLU)/min/mg dry aortic ring.

Statistical analysis

Data were expressed as mean ± standard deviation (Mean ± SD). Statistical analysis was performed using GraphPad Prism 5 Software, Inc. (San Diego, CA, USA) and p values ≤ 0.05 were considered as statistically significant.

Results

ACE inhibitory activity of CAE

Angiotensin 1-converting enzyme (ACE) plays a key role in the regulation of blood pressure and normal cardiovascular function. It catalyzes the conversion of angiotensin I to angiotensin II, which is known to increase the blood pressure. CAE inhibited the enzyme in a dose-dependent manner reporting 86% of inhibition at 1 mg/mL. At this concentration the HA formation was reduced compared to negative control (**Figure 4.1**).

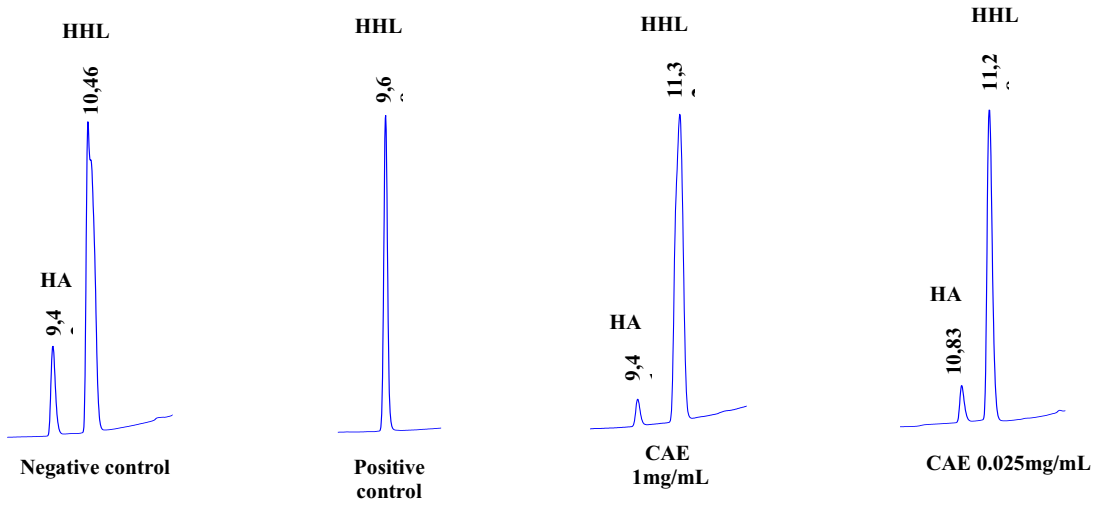

Figure 4.19 Representative chromatograms of angiotensin-I converting enzyme (ACE) reaction mixture using CAE extract at different concentration (1-0.025 mg/mL) compared with positive control captopril and negative control (HHL plus ACE without inhibitor)

MTT assay

Splenocytes were treated with different doses of CAE and cell viability was evaluated by MTT assay. CAE was dissolved in EtOH/DMSO and the final concentration (1.6% and 0.4%, respectively) of solvent demonstrated no cytotoxic effect. As shown in **Figure 4.19**,

the extract had no effect on cell viability after 3, 24 and 48h. Con A, a well-known T cell mitogen, promoted cell proliferation especially after 24 and 48h (**Figure 4.19**).

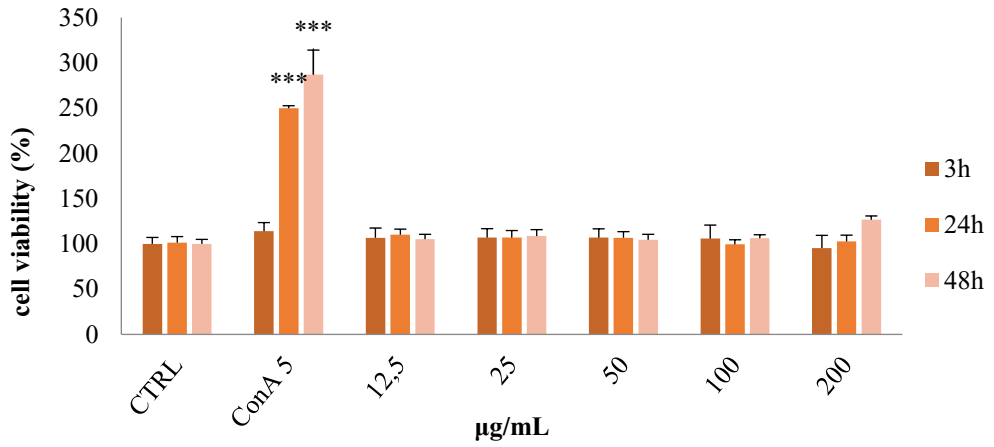

Figure 4.20 Cell viability, evaluated by MTT assay, in murine splenocytes treated with different doses of *Capsicum annuum* L. cv Senise (CAE) and Concanavalin A (5 µg/mL) for 3,4 and 48 h.***$p<0.001$ *vs* untreated cells (CTRL).

CAE inhibits intracellular ROS generation in LPS-stimulated immune cells

Prolonged exposure to high doses of LPS trigger excessive production of inflammatory mediators, which might lead to a deleterious condition of oxidative stress, due to excessive generation of radicals (Noworyta-Sokołowska et al. 2013). Murine splenocytes were treated with different doses of CAE (200-50 µg/mL) and antioxidant activity was evaluated in basal or stressed conditions.

Intracellular ROS were analysed by flow cytometry, using CellROX® Green Reagent, a DNA dye that after oxidation, binds to DNA and produce fluorescence measured by flow cytometer.

Morphological characteristic and fluorescence of cell population can be observed on dot plots generated (**Figure 4.21a**). Forward scatter (FSC) and side scatter (SSC) refer to the size or to granularity and complexity of the cells, respectively. In this way different cell populations can be distinguished: the dots with low FSC and SSC signal represent cell debris; dots with high FSC signal and low SSC represent cells with low internal complexity or granularity like lymphocytes/monocytes; cells like granulocytes, generate high FSC and SSC signals since they are large cells with high internal complexity/granularity. However, granulocytes (neutrophils, basophils, and eosinophils) are very similar in size and structure,

giving them similar light- scattering properties, so without any probe it is impossible to distinguish between them.

As shown in **Figure 4.21**, a gate was drawn around the population of interest (dot plot on the left). Cells were staining with CellROX® Green Reagent for measuring oxidative stress in live cells. This cell-permeant dye is non-fluorescent in a reduced state, instead exhibits orange fluorescence upon oxidation by ROS. Fluorescence was detected by flow cytometer using the filter Alexa Fluor. As shown in dot plots correlating fluorescence intensity with

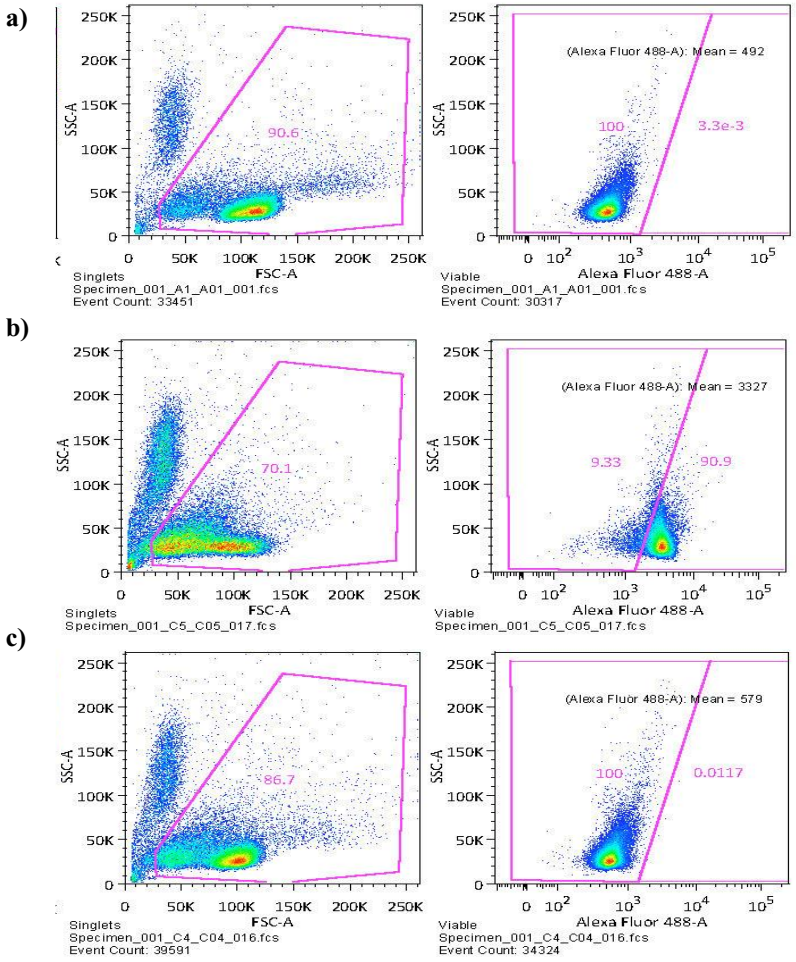

Figure 4.21 Dot plots charts for controls, representative of the method: (a) untreated cells (CTRL), (b) LPS-stressed cells, (c) NAC-treated cells

cell morphology (AlexaFluor *vs* SSC-A), fluorescence emitted by untreated cells as well as by NAC-treated cells (**Figure 4.20a-c**) (<10^3) was lower than stressed cells (**Figure 4.21b**). The position of the cells changed depend on fluorescence emitted.

LPS induced oxidative stress in immune cells reported 2-fold increase in fluorescence intensity compared with control. The pre-treatment with extract for 24h decreased ROS amount reporting a fluorescence value lower than LPS-stressed cells and also than NAC, a

known antioxidant (**Figure 4.22**). CAE did not affect endogenous ROS: fluorescence intensity of CAE-treated cells was not statistically different from untreated cells (CTRL). CAE was able to counteract oxidative stress induced by LPS in a dose-dependent manner. In fact, cells treated with CAE after stimulation with LPS had fluorescence intensity value similar to untreated cells.

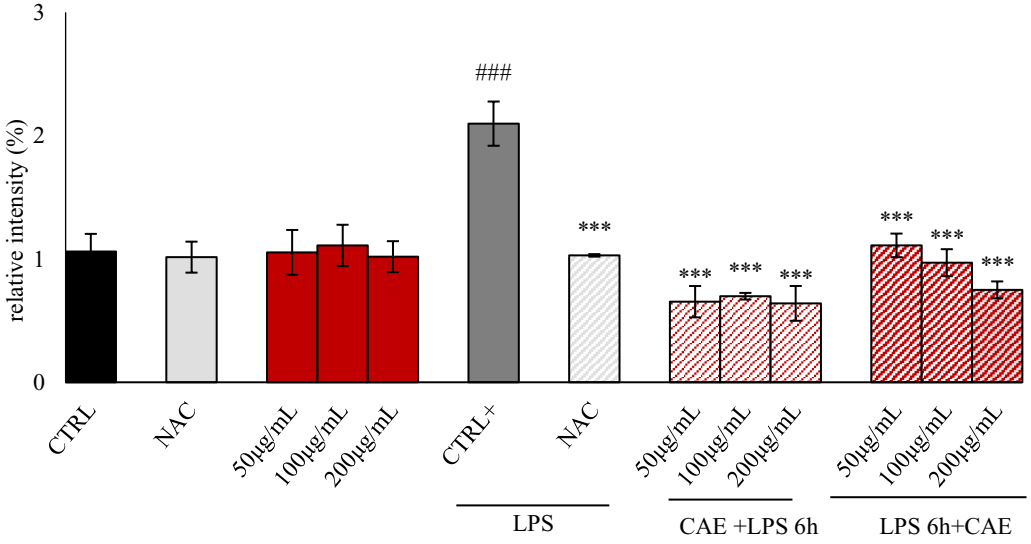

Figure 4.22 Effects of CAE on endogenous and LPS- induced intracellular reactive oxygen species (ROS) generation. Data are expressed as the mean ± SD of three independent experiments (n = 3). ###p< 0.001 *versus* CTRL, *** p<0.001 *vs* LPS-treated cells.

Anti-inflammatory activity of CAE in immune cells

ELISA assay

Murine splenocytes were treated with CAE, and IFN-γ and IL-4 production in basal or stressed conditions was evaluated by ELISA assay. Cytokines were evaluated on supernatant of cells treated with different doses of CAE alone for 24 and 48h, cells previously stimulated with ConA for 24h and then treated with CAE, cells treated with CAE for 24h and then stimulated with ConA.

As regards IL-4 **(Figure 4.22)**, the cytokine is spontaneously secreted by the control (CTRL, untreated splenocytes). CAE influenced IL-4 amount in a dose-dependent manner. After 24h, CAE did not affect IL-4 concentrations at highest doses (200-50µg/mL) reporting

amounts similar to the CTRL. The lowest doses increase IL-4 amount. The effect was significantly after 48h of the treatment. As shown in **Figure 4.22**, IL-4 was reduced by highest doses of the extract (200-50 μg/mL). Con A stimulated IL-4 production after 24 h. Pre-treatment with CAE, protect cells from inflammatory effect induced by ConA the highest doses drastically inhibited IL-4 production reporting a value of 16.74±1.2 pg/mL lower also then untreated cells (89.74±5.36 pg/mL). Moreover, the extract demonstrated good activity also in splenocytes stimulated with Con A. All doses of extract reduced IL-4 production of more than three times compared to ConA (167.41±5.46 pg/mL) reporting values ranged from 39.38±3.18 to 55.71±1.51 pg/mL.

IFN-γ was not produced by splenocytes as well as CAE-treated cells after 24 and 48h (**Figure 4.22**). Con A stimulated IFN-γ production after 24h which decreased in cells pre-treated with the highest dose of the extract (200μg/mL) (figure 7). CAE inhibited pro-inflammatory stimuli in cells treated with ConA only at 200μg/mL by halving IFN- γ concentration (**Figure 4.22**).

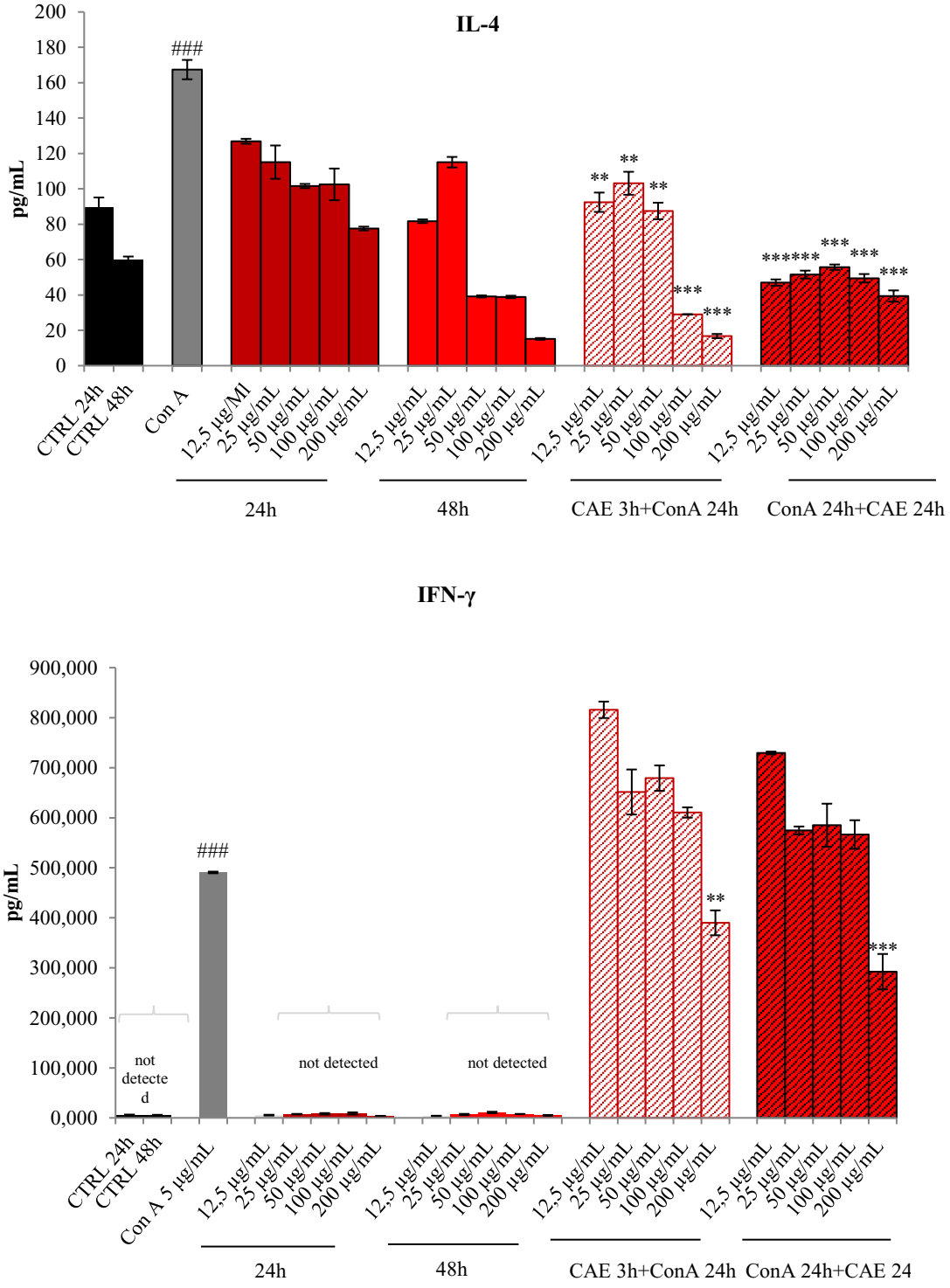

Figure 4.23 Enzyme-linked immunosorbent (ELISA) assay to detecting IL-4 and IFN-γ in cell culture of splenocytes treated with different concentration of CAE (200-12.5 ug/mL) in presence or not of ConA (5µg/mL). ###p<0.001 *vs* CTRL, *p<0.05, **p<0.01, ***p<0.001 *vs* ConA.

ELISpot assay

In order to evaluate the possible effect of CAE on the T cell response and to validate ELISA results, an ELISpot assay was carried out. IFN-γ and IL-4 production was evaluated in murine splenocytes treated with CAE in presence or not of an inflammatory stimulus (**Figure 4.24**).

The evaluation was done after 24 h of treatment. The assay was carried out three times on different days, with cells tested in duplicates to determine the reproducibility of the assay. Spots were counted with Immunospot software. Each spot is the "footprint" of a single cell that has released a relatively high number of cytokines. Thus, the number of spots is representative of the size of the population that secreted the cytokine, is not representative of the amount of cytokine produced **(Figure 4.24).**

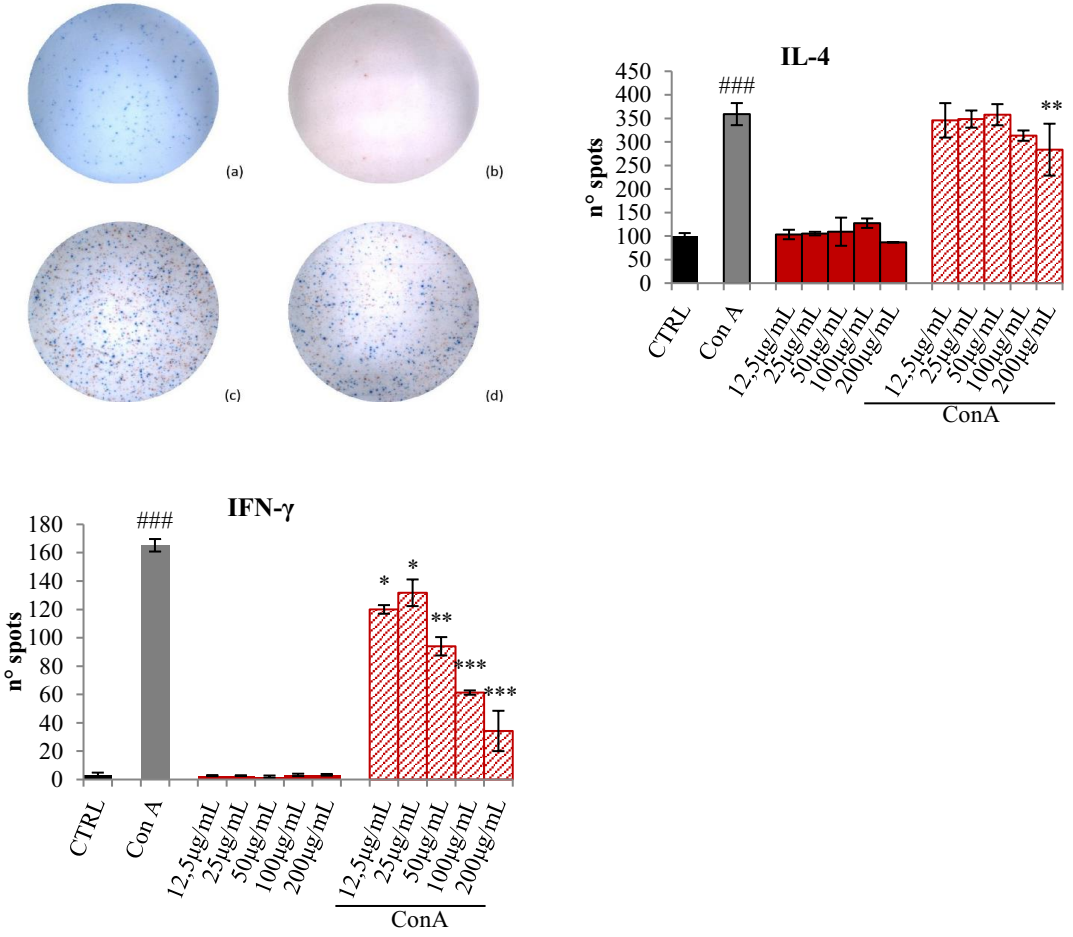

Figure 4.24 Enzyme-linked immunosorbent spot (ELISPOT) assay of detecting interferon (IFN)-γ or IL-4 secreting T cells. 1.ELISPOT wells: blue spots represent IL-4, red spots represent IFN- γ. (**a**) IL-4 production from untreated cells; (**b**) IFN-γ production from untreated cells; (**c**) IL-4 and IFN-γ production from Con A-stimulated cells; (**d**) IL-4 and IFN-γ production from cells stimulated with 100 µg/mL of ethanol extract of *Capsicum annuum* L. Senise extract (CAE) and 5 µg/mL of Con A for 24h; 2. Spot count of IFN-γ or IL-4 secreting splenocytes after CAE treatment alone and after addition of ConA. Data are expressed as the mean of spots ± standard deviation of three experiments. ###$p<0.001$ vs control; *** $p<0.001$, ** $p<0.01$, * $p<0.05$ vs ConA

According with ELISA assay, IFN-γ was not produced in untreated and CAE treated cells. ConA stimulated IFN- γ production reporting a number of spots one-hundred higher than CTRL. CAE treatment counteract inflammatory activity of ConA in a dose dependent manner. The highest doses reported the lowest number of spots.

About IL-4 production, a limited population of cells secrete the cytokine in basal condition (CTRL). Number of spots in CAE-treated cells was not significantly different compared to control. When CAE is administered together with Con A reduced cell activation only at 200 µg/mL reporting a number of spots lower than ConA.

Effect of CAE on endothelial disfunction

Obese mice were treated with different doses (25-1 mg/Kg) of CAE for 6-weeks and then endothelial function was evaluated. Aortae from HFD-mice showed reduced endothelium-dependent vasodilator response to acetylcholine which is considered as an index of endothelial function compared with control group (**Figure 4.25a**). Treatment improved vasodilatation induced by acetilcoline in obese mice without statistical differences with non obese mice (**Figure 4.25a**). Moreover, CAE reduced NADPH oxidase activity restoring basal conditions (**Figure 4.25b**).

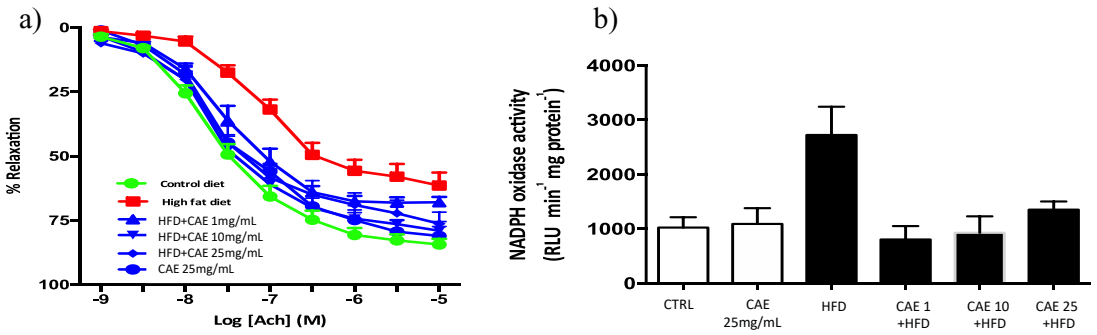

Figure 4.25 (**a**) Effects *C.annuum* L. cv Senise (CAE)(1-25mg/kg) administration on endothelial function. (**b**) Effects of *C.annuum* L. cv Senise (CAE)(1-25mg/kg) on aortic NADPH activity in mice fed with high fat diet (HFD)

Discussion

Obesity is a multifactorial disease which involved several tissues and induced different metabolic disorders. Excess of fat induces weight gain but also the production of ROS and pro-inflammatory. In Chapter 2 we have demonstrated as CAE enhanced antioxidant defense

in OA-treated HepG2 cells used as steatosis model. In the present study, antioxidant activity of CAE was confirmed also in splenocytes stressed with LPS. ROS and inflammatory cytokines are closely related and their production increased in several pathological conditions like obesity. CAE exerted anti-inflammatory activity and reduced IL-4 and IFN-γ production in splenocytes stimulated with Con A.

Antioxidant and anti-inflammatory activity demonstrated in hepatocytes and splenocytes could be the molecular mechanism responsible of improvement endothelial dysfunction in obese mice. Many studies reported as ROS and proinflammatory cytokines induce NADPH oxidase, which contributes to the impairment of endothelium-dependent vasodilatation by inactivating nitric oxide. NADPH oxidase, a multienzyme complex, is considered the major source of superoxide anion in the vascular wall of obese mice. Superoxide anion reacts and inactivates NO, a key cell-signaling molecule in regulation of vasomotor tone and blood flow. CAE inhibits NADPH oxidase and improves endothelial dysfunction in mice fed with high fat diet.

Red peppers bioactive compounds have shown a potent capability to attenuate oxidative stress and improve endothelial function through their different properties, among them, anti-inflammatory, anti-platelet aggregation, antioxidant properties in the vascular wall, anti-atherogenic activity and pro-apoptotic activity(Ranilla et al. 2010). Particularly their main constituent capsaicin exerted antihypertensive effect through the transient receptor potential vanilloid subtype 1 (TRPV1) activation (Yang et al. 2010). TRPV1 is a non-selective calcium influx channel which releases calcitonin-gene-related peptide (CGRP) from sensory nerves when activated by capsaicin and causes vasodilatation and depressurization. Thus, it represents potential target to improve hypertension. Red peppers are also a source of many antioxidant compounds like carotenoids, polyphenols flavonoids which can reduce oxidative stress and improve vasodilatation. Capsaicinoids and capsinoids, analogues non-pungent of capsaicin, as well as polyphenols and carotenoids were found also in Senise pepper.

Conclusions

Antioxidant and anti-inflammatory activity of *Capsicum annuum* L. cv Senise are involved in its cardioprotective effect in obese mice. Decrease of ROS and pro-inflammatory cytokines production counteracted oxidative stress and inflammatory status in hepatocytes and splenocytes but also inhibited NADPH oxidase involved in impairment endothelium-dependent vasodilatation by inactivating nitric oxide synthase.

4.4 *Capsicum annuum* L. cv Senise: improvement in insulin resistance of OA-treated HepG2 cell line

Introduction

Blood glucose homeostasis is maintained by the coordinated control of cytokines and several hormones like insulin and glucagon. Prolonged exposure to a diet rich in fat or sugar and physical or mental stress can alter glucose homeostasis and therefore can cause hyperglycaemia (Newgard et al. 2009). Excess of fat increase the production of ROS and pro-inflammatory cytokines which can interfere with insulin signalling pathway and alter glucose metabolism (Nagle et al. 2009).

The insulin signalling starts when insulin binds to insulin receptor (IR) which results in IR auto-phosphorylation of key tyrosine residues. Tyrosine residues of insulin receptor substrate are subsequently phosphorylated by the IR kinase which can further trigger the sequential activation and phosphorylation of downstream signalling molecules, including insulin receptor substrate (IRS), phosphoinositide 3-kinase (PI3K) and the protein kinase AKT. This, in turn, results in the translocation of intracellular glucose transporter (GLUT) vesicles to the plasma membrane for the transportation of extracellular glucose into cells. Activated Akt plays a pivotal role in the glucose metabolism which can activate insulin-stimulated glucose transport and regulates glycogen synthesis by GSK-3α and β inactivation (Luo et al. 2015). Protein tyrosine phosphatase 1B (PTP1B) is a negative regulator of insulin signalling transduction by inhibiting phosphorylation of IR and IRS Fatty acids like palmitic acid promoted PTP1B expression (Yang et al. 2018).

In previous pages we have demonstrated that hypolipidemic activity of CAE is associated to a decrease of fat accumulation and also to an improvement of other secondary effects caused by prolonged exposure to excess of fat like oxidative stress and endothelial dysfunction. Thus, we questioned if the extract improved also insulin resistance associated to obese liver. HepG2 cell line treated with oleic acid were used as model of fatty liver and some markers involved in insulin resistance were evaluated through different cell-based assays

Materials and methods

Chemicals and reagents

Acarbose, potassium phosphate monobasic, sodium chloride, starch, chloridric acid, iodine-potassium iodide, sodium potassium tartrate, sodium phosphate monobasic, iodine, potassium iodide, α-amylase from hog pancreas (CAS number: 9000-90-2), sodium carbonate, 3,5-dinitrosalicylic acid, 4-p-nitrophenyl-α-d-glucopyranoside, and α-glucosidase from Saccharomyces cerevisiae (CAS number: 9001-42-7), 2-[N-(7-Nitrobenz-2-oxa-1,3-diazol-4-yl)amino]-2-deoxy-D-glucose (2-NBDG), oleic acid were purchased from Sigma-Aldrich (Milan, Italy). Dulbecco's Modified Eagle Medium (DMEM), Trypsin-EDTA solution, fetal bovin serum (FBS), glutamine, penicillin-streptomycin, and phosphate saline buffer (PBS) were purchased from Euroclone (Milan, Italy).

Potential hypoglycaemic activity

α-Amylase inhibition assay

The *α*-amylase inhibition assay was performed using the iodine/ potassium iodide method (Santoro et al. 2020). 25 µL of each sample was mixed with *α*-amylase solution (50 µL, 5U/mL) in phosphate buffer (pH 6.9 with 6 mM sodium choride) in a 96-well microplate and incubated for 10 min at 37°C. Then, the reaction was initiated with the addition of starch solution (100 µL, 0.1%). Similarly, a blank was prepared by adding sample solution to all reaction reagents without enzyme solution. The reaction mixture was incubated for 10 min at 37°C. The reaction was then stopped with the addition of HCl (25 µL, 0.1M). This was followed by the addition of the iodine- potassium iodide (KI /0.5 mM) solution (100 µL). The sample and blank absorbance was read at 630 nm for 10 min. Results are expressed as IC_{50} (mg/mL) values determined by GraphPad Prism 5 Software (San Diego, CA, USA).

α-Glucosidase inhibition assay

Different concentrations of each sample were incubated with *α*-glucosidase solution (40 µL, 0.1 U/mL) in phosphate buffer (50 µL, 0.1 M, pH 7) for 10 min. Then, 40 µL of 0.5 mM 4-nitrophenyl *α*-D-glucopyranoside were added and incubated for 15 min. The reaction was stopped by adding 100 µL of 0.2 M sodium carbonate solution. The enzymatic hydrolysis of substrate was monitored by the amount of *p*-nitrophenol released in the reaction mixture at 405 nm (Braca et al. 2018). Results are expressed as IC_{50} (mg/mL for extracts and for pure compounds) values determined by GraphPad Prism 5 Software (San Diego, CA, USA).

Cell culture

Human hepatocellular carcinoma cell line (HepG2) was cultured in DMEM supplemented with 10% fetal bovine serum, 2 mM glutamine, 100 U/mL penicillin, and 100 µg/mL streptomycin and maintained at 37°C in a humidified atmosphere containing 5% CO_2.

Glucose uptake assay by 2-NBDG

Glucose uptake assay was performed according to the method of Chen et al. 2010. HepG2 cell line were plated in 24-well plates (1×10^5 cells/well) and treated with oleic acid (OA 0.3mM) and different doses of CAE (200-100 µg/mL) for 24h. Then, media was removed and cells washed twice with phosphate buffer (PBS). The fluorescent analogue of glucose, 2-NBDG (50 µM) was added and incubated for 30 min. The 2-NBDG uptake was stopped by removing the incubation medium and cells were washed twice with PBS. Cells were trypsinized and re-suspended in 300 µl of PBS. Fluorescence was measured by BD FACSCanto II (BD Pharmigen, San Jose, CA, US) (λ_{ex} 465 nm and λ_{em} 540 nm).

Quantitative RT-PCR

HepG2 cells were seeded in 6-well plates ($8.5*10^5$ cells/well) and treated with different doses of pepper extract (200-100µg/mL) and oleic acid (OA) 0.3mM for 24h. RNA extraction and qRT-PCR were performed as described in section 4.1.

Table 4.7 Forward and reverse primers

Gene	Forward primer	Reverse primer
β-actin	5′-CCTGGCACCCAGCACAAT-3′	5′-GCCGATCCACACGGAGTACT-3′
GLUT-1	5’-GCCAAGAGTGTGCTAAAGAAG-3’	5’-TGGAGTAATAGAAGACAGCGT-3’
GSK	5’-AGTGCAAAGCAGCTGGTCCG-3’	5’-GGAGTTCCCAGGACCTTGAT-3’
IRS-1	5’-CGAGAACGAGAAGAAGTGG-3’	5’-GTGCTTGTTCTTGGAGTCAG-3’
PT1B	5’-CGTGCAGGATCAGTGGAAGG-3’	5’-GCTTCCTTTTTCTTCCTTGA-3’

Sample Preparation for NMR Analysis

The HepG2 cell line was cultured in 6-well plates at a density of 8.5×10^5/well and treated with OA (0.3mM) and CAE (200-100 µg/mL). After 24 h, culture medium and cells (≈5 million of cells per treatment) were collected and preserved at −80 °C until use. For the metabolite extraction, cells were suspended in phosphate buffer saline (500 uL, PBS, pH 7.4) w/o Ca^{2+} and Mg^{2+} and kept on ice for 30 min. Then, cells were lysed through sonication (37%, 30 s) and centrifuged (10 min, 4 °C, 13,000 rpm) to remove precipitated cellular

debris. The supernatant was transferred to a fresh extraction tube, followed by the addition of methanol, chloroform and distilled water in the ratio of 4:4:2.85. The aqueous phases were transferred to a new tube and lyophilized for NMR analysis (Aftab et al. 2014) Lyophilized samples were mixed with 600 µL of D_2O and 5 µL of TSP (3-trimethylsilyl propionic acid-d_4 sodium salt) and placed in a 5 mm NMR tube. TSP was used as both chemical shift reference and internal standard for quantitative analysis. All samples were at pH 7. The NMR spectra were acquired on a Varian Unity Inova 500 MHz spectrometer. The spectrometer was equipped with a 5-mm triple resonance pulsed field z-axis gradient probe, operating at 499.96 MHz for 1H. The temperature during all experiments was kept at 25 °C. No sample rotation was applied.

The 1D ^{1}H NMR spectra were acquired using a solvent suppression pulse sequence to saturate the residual ^{1}H water proton signal. One hundred and twenty-eight transients were acquired with a spectral width of 5995 Hz and an acquisition time of 4 s. A recycle delay of 1 s was selected. VNMRJ 2.1B software (Agilent Technologies, Santa Clara, CA, USA) was used to acquire all the spectra. Spectra were processed using NMR SUITE 8.0 (Chenomx Inc., Edmonton, AB, Canada). 1D spectra were Fourier transformed with a FT size of 32 k and a 1 Hz line-broadening, phased and a polynomial baseline correction was applied over the whole spectral range. The PROFILER module was used to identify metabolites by fitting the compound signatures from the spectral Chenomx NMR Suite library. Metabolite concentrations were calculated by determining the heights of the signatures best fitting the experimental signals.

Results

Potential hypoglycemic activity by in vitro assay

Key enzymes as *α*-glucosidase and *α*-amylase are involved in the dietary carbohydrate digestion in humans. Inhibitors of these enzymes may be effective in retarding carbohydrate digestion and glucose absorption to suppress postprandial hyperglycaemia (Tundis, Loizzo, and Menichini 2010). The extract CAE demonstrated good activity *vs* *α*-amylase enzyme reported an IC_{50} value of 11.91±2.05 µg/mL close to IC_{50} value of acarbose (7.51±0.74 µg/mL); no activity was registered *vs* glucosidase enzyme at tested concentrations

Effect of CAE improved insulin signaling in OA-treated HepG2 cells

HepG2 cells were seeded and treated with CAE (200-100 µg/mL) and OA (0.3 mM). After 24h, the expression level of several markers was analyzed by qRT-PCR (**Figure 4.26**). CAE decreased protein tyrosine phosphatase 1B (PT1B) and enhanced the expression of insulin receptor substrate-1 (IRS-1) compared to oleic acid. As result of insulin signaling improvement, GLUT1 expression increased with treatment. In addition, CAE reduced glycogen synthase kinase (GSK3) expression.

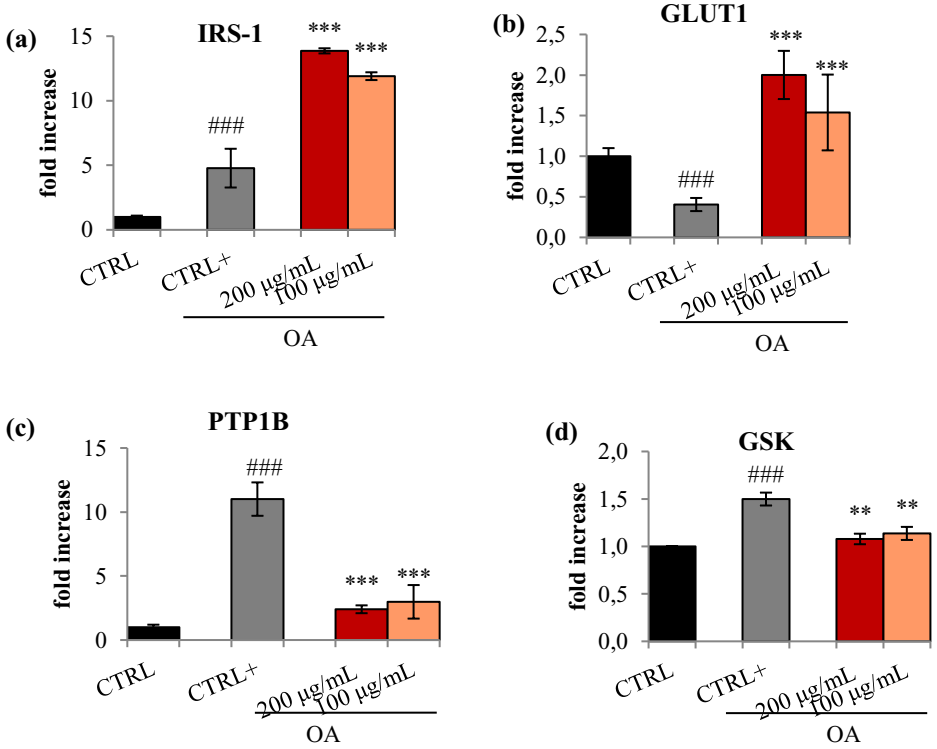

Figure 4.26 Effect of CAE (200 and 100 µg/mL) on the gene expression of (**a**) insulin receptor substrate 1 (IRS-1), (**b**) glucose transporter type 1 (GLUT1), (**c**) protein tyrosine phosphatase 1B (PTP1B), (**d**) glycogen synthase β3 (GSK) analyzed by real-time q-PCR and normalized with the housekeeping gene, *β*-actin, in oleic acid (OA 0.3mM)-treated HepG2 cell line. Data are expressed as mean ± standard deviation of three independent experiments (n=3). ###$p<0.001$ *vs* untreated cells (CTRL) **$p<0.01$***$p<0.001$ *vs* oleic acid treated cells (CTRL+)

CAE increased glucose uptake in OA-treated HepG2 cells

Increased fatty acids has been shown to impair insulin signaling and glucose metabolism in the liver. The effect of CAE on glucose uptake was evaluated by using 2- [N -(7-nitrobenz-2-oxa-1,3-diazol-4-yl) amino]-2-deoxyglucose (2-NBDG) a fluorescent analogue of glucose in OA-treated cells (**Figure 4.27**). This dye could be incorporated by glucose transporting systems and immediately be converted to another fluorescent derivative by phosphorylation

on C6 and formation of phospho derivative 2-NBDG 6-phosphate (Leira et al. 2002). The extract promoted 2-NBDG influx in fact an increase in fluorescence was observed. In addition, CAE promoted GLUT1 expression involved in glucose transport (**Figure 4.26**).

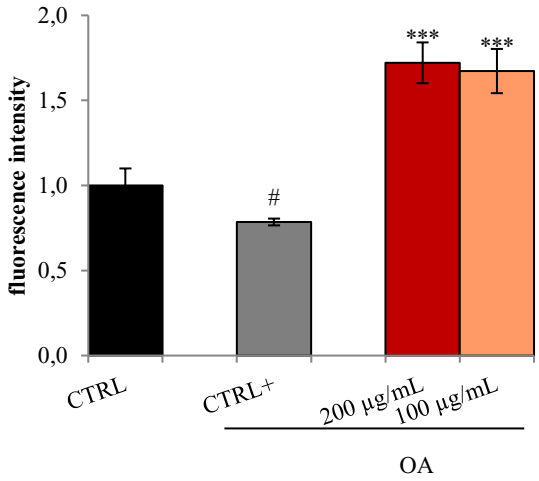

Figure 4.27 Glucose uptake of 2-NBDG assays from HepG2 cells treated with OA (CTRL+) in presence or not of CAE (200-100 µg/mL). #p<0.05 *vs* CTRL ***p<0.001 *vs* CTRL+

^{1}H-NMR analysis of cell culture media and cellular lysate

Cell culture media were collected from HepG2 cell line treated with OA and different doses of CAE (200-100µg/mL) for 24h. Untargeted NMR-based metabolomic profile was performed in order to evaluate intracellular and extracellular metabolic perturbation caused by different treatment. Some metabolites were identified: ten amino acids (alanine, leucine, lysine, histidine, methionine, phenylalanine, threonine, tyrosine, valine, glutamate) and three intermediates of glycolysis or Krebs cycle (glucose, pyruvate and lactate). As shown in **Figure 4.28** amino acid concentrations decreased in culture media of cells treated with CAE compared with oleic acid. On the contrary, increases on intracellular amounts of amino acids were observed with both CAE doses (200-100µg/mL) although the highest increase was not observed for all the amino acids with the same doses of the extract. Moreover, CAE reduced extracellular glucose, pyruvate and lactate concentration compared to OA. These metabolites increased in cells treated with the highest dose of extract (200 µg/mL).

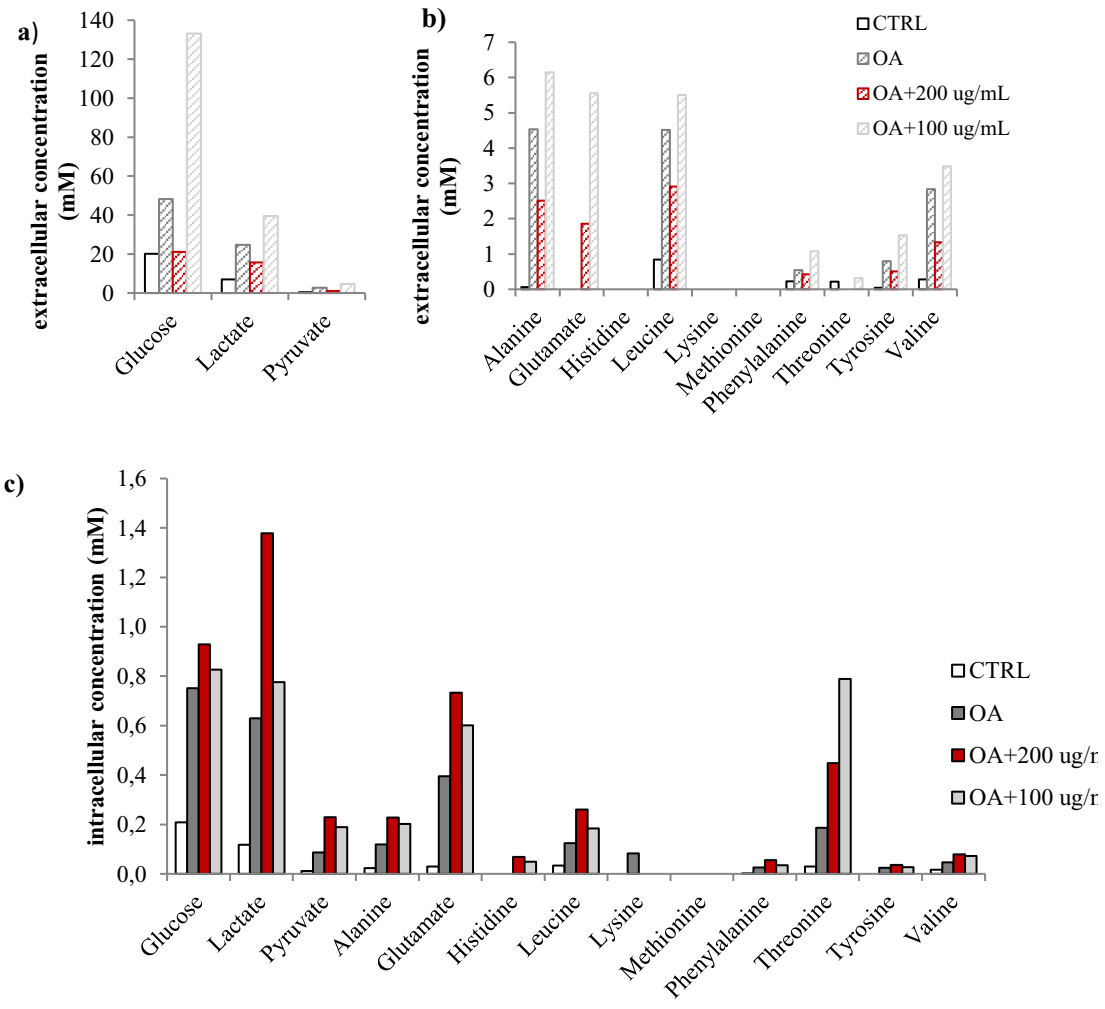

Figure 4.28 Metabolites identified in HepG2 cells (a-b) and their culture media (c). Concentration data (mM) were obtained by Chenomx Profiler

Discussion

Potential hypoglycemic activity of CAE was evaluated through α-amylase and *α*-glucosidase *in vitro* assay. *α*-amylase is involved in starch digestion by acting upon *α* -1,4 glycosidic linkages and producing glucose as final product. Increased activity of the enzyme, due to insulin deficiency or resistance, caused hyperglycemia. Inhibitors of *α*-amylase like acarbose, miglitol and voglibose are normally used in treatment of hyperglycemia but they induced several side effects like bloating and abdominal uneasiness (Sales et al. 2012). Therefore, the administration of natural products could be a promising strategy in diabetes treatment. According with previous study CAE reported good inhibition vs *α*-amylase. The activity was better than that evaluated by Loizzo et al 2013 (Loizzo et al. 2013) on the same

cultivar, but similar to *C. annuum* var. *acuminatum* from Calabria which exhibited an IC_{50} of 6.9 μg/mL (Tundis et al. 2011).

The hypoglycemic activity was confirmed also in OA-treated HepG2 cell line used as model. Excess of fat induced pro-inflammatory cytokines and ROS which can interfere with insulin signaling pathway and increase plasma glucose. Protein tyrosine phosphatase 1B (PT1B) is a key negative regulator of the insulin signaling pathways and its increased activity and expression are implicated in the pathogenesis of insulin resistance (Liu et al. 2015). Some studies have shown that PTP1B overexpression inhibits phosphorylation of insulin receptor (IR) and its substrate(Brandt et al. 2004) leading to insulin resistance (Liu et al. 2015). PTP1B inhibitor increased tyrosine phosphorylation of IR and activated the downstream molecules of insulin signaling like IRS-1, Akt and Erk1 /2. In the present study CAE drastically downregulated PTP1B in OA-treated cells and enhanced IRS-1 expression. The improvement of insulin signaling enhance glucose uptake, glycolysis and glycogen synthesis. CAE enhanced the expression of GLUT-1 and thus glucose transport inside the cells. As demonstrated by 2-NBDG assay, glucose uptake was higher in cells treated with extract. This was confirmed also by NMR analysis which showed as Senise pepper reduced glucose amounts in culture media of OA-treated cells, while increased intracellular content compared with OA. Moreover, intracellular pyruvate increased in HepG2 cell line treated with extract suggesting an improvement of glycolysis. In addition, the extract reduced GSK expression, a serine/threonine protein kinase which leads to an increase in glycogen synthesis (Henriksen and Dokken 2006). Many studies reported as plasma levels of some amino acids are associated with obesity, diabetes and insulin resistance. Studies on rat obese model exhibited enhanced protein degradation and reduced catabolism of branched-chain amino acids (BCAAs) which could increase their plasma levels. The BCAAs isoleucine, leucine, and valine together with alanine, glutamate, proline, and tyrosine are positively correlated with homeostasis model assessment of insulin resistance (HOMA-IR) (Wurts et al. 2013) In addition, studies on BCAA supplementation in both animals and humans demonstrated that these amino acids may directly promote insulin resistance through chronic phosphorylation of mTOR, JNK, and $IRS1_{Ser307}$ (Newgard et al. 2009). Tyrosine is a precursor of catecholamines and could promote an increase in blood glucose level through the anti-insulin action of catecholamines. By contrast, other studies have demonstrated improved glucose homeostasis in animals fed a diet specifically enriched in leucine (Wang et al. 2011). Concentrations of alanine, leucine, phenylalanine, tyrosine were reduced in

culture media of HepG2 cell line treated with OA and CAE, especially the highest dose (200 µg/mL) compared to OA alone.

Conclusions

Capsicum annuum cv Senise strongly up-regulated PTP1B expression, a phosphatase inhibitor of signaling pathway. In this way the extract promoted glucose uptake as demonstrated by high expression of GLUT1 and higher concentration of intracellular glucose. Moreover, the extract promoted glycogen synthesis by reducing GSk3β expression and reduced protein degradation. These effects also confirmed that CAE promoted the utilization of fatty acid as source of energy reducing in this way fat accumulation as previously demonstrated (section 4.1.1).

Chapter 5

CONCLUSIONS

Phytochemical profile and biological activity of *Capsicum annuum* L. cv Senise and *Solanum aethiopicum* cv Rotonda, typical products of Basilicata region, were investigated in this thesis for the first time.

Senise dried pepper fruits and Rotonda eggplant peel were extracted by exhaustive maceration with absolute ethanol and biological activity was evaluated on different cell model.

Both the extracts exerted good antioxidant activity on HepG2 cell line used as model. Pre-treatment with extracts protected cell from oxidative stress induced by *t*-BOOH. Senise pepper and eggplant extracts reduced ROS generation by promoting the expression of markers involved in antioxidant pathway via Nrf-2 pathway.

To improved biovailibity and thus efficacy, both the extracts were loaded in liposomes. These nanoformulations improved antioxidant activity of the extracts: cells treated with extract loaded in liposomes showed lower amount of ROS compared to raw extract. In this way the same or stronger beneficial effect can be achieved with lower doses reducing costs and possible side effects.

This effect was more evident for Senise pepper.

Antioxidant activity was confirmed also in OA-treated HepG2 cell line. The extracts reduced ROS generation caused by excess of fat promoting the expression of markers involved in antioxidant defence. ROS and pro-inflammatory cytokines are highly produced by the excess of fat.

Both the extract demonstrated anti-inflammatory activity: SAE especially in OA-treated Caco-2 cell line by downregulating NF-Kb and consequently IL-6 and TNFα expression; CAE inhibited IL-4 and IFN-γ production in splenocytes which together to reduction of ROS improved endothelial dysfunction in obese mice by inhibiting NADPH oxidase.

Oxidative stress and inflammatory status are consequence of fat accumulation due to prolonged exposure to excess of fat. Both extracts promoted lipolysis instead of *de novo* lipogenesis influencing the expression of PPARα and SREBP1 respectively.

Biological activities observed are due to health promoting compounds found in the fruits of investigated plant species. Twenty-four and thirteen compounds were identified in *C. annuum* cv Senise and *S. aethiopicum* cv Rotonda respectively, by LC-MS belonging to different structure class live flavonoids, phenolic acids, sesquiterpens, carotenoids and capsinoids. All of these compounds are already known for their antioxidant activity, but they exerted also anti-aging, anti-diabetic, anticancer, anti- inflammatory effect.

Unlike synthetic drugs, *C. annuum* L. cv Senise and *S. aethiopicum* L. cv Rotonda extracts exerted beneficial activity not on single but on multiple target sites due to synergistic and additive effects of different compounds present.

References

Abd El-Aziz, Rokaya, Mervat Naguib, and Laila A Rashed. 2018. 'Spleen size in patients with metabolic syndrome and its relation to metabolic and inflammatory parameters', *The Egyptian Journal of Internal Medicine*, 30: 78-82.

Aftab, Obaid, Mikael KR Engskog, Jakob Haglöf, Albert Elmsjö, Torbjörn Arvidsson, Curt Pettersson, Ulf Hammerling, and Mats G Gustafsson. 2014. 'NMR spectroscopy-based metabolic profiling of drug-induced changes in vitro can discriminate between pharmacological classes', *Journal of chemical information and modeling*, 54: 3251-58.

Albuali, Waleed H. 2014. 'Evaluation of oxidant-antioxidant status in overweight and morbidly obese Saudi children', *World journal of clinical pediatrics*, 3: 6.

Amorati, R.; Valgimigli, L. 2015. 'Advantages and limitations of common testing methods for antioxidants', *Free Radical Research*, 49, 633–649.

Anosike, Chioma A, Onyechi Obidoa, and Lawrence US Ezeanyika. 2012. 'The anti—inflammatory activity of garden egg (Solanum aethiopicum) on egg albumin—induced oedema and granuloma tissue formation in rats', *Asian Pacific Journal of Tropical Medicine*, 5: 62-66.

Armentano, M.F.; Caterino, M.; Miglionico, R.; Ostuni, A.; Pace, M.C.; Cozzolino, F.; Monti, M.; Milella, L.; Carmosino, M.; Pucci, P.; et al. 2018. 'New insights on the functional role of URG7 in the cellular response to ER stress', *Biology of the cell* , 110, 147–158.

Artham, Surya M, Carl J Lavie, Richard V Milani, and Hector O Ventura. 2009. 'Obesity and hypertension, heart failure, and coronary heart disease—risk factor, paradox, and recommendations for weight loss', *Ochsner Journal*, 9: 124-32.

Aversano, R.; Contaldi, F.; Adelfi, M.G.; D'Amelia, V.; Diretto, G.; De Tommasi, N.; Vaccaro, C.; Vassallo, A.; Carputo, D. 2017. 'Comparative metabolite and genome analysis of tuber-bearing potato species', *Phytochemsitry*, 137, 42–51.

Bozzuto, G.; Molinari, A. 2015.'Liposomes as nanomedical devices', *International Journal of Nanomedicine* , 10, 975–999.

Bonomo, M.G.; Di Tomaso, K.; Calabrone, L.; Salzano, G. 2018. 'Ethanol stress in Oenococcus oeni: Transcriptional response and complex physiological mechanisms', *Journal of Applied Microbiology*, 125, 2–15.

Brechbuhl, H.M.; Gould, N.; Kachadourian, R.; Riekhof, W.R.; Voelker, D.R.; Day, B.J. 2010. 'Glutathione Transport Is a Unique Function of the ATP-binding Cassette Protein ABCG2*. *Journal of Biological Chemistry*, 285, 16582–16587.

Braca, Alessandra, Chiara Sinisgalli, Marinella De Leo, Beatrice Muscatello, Pier Luigi Cioni, Luigi Milella, Angela Ostuni, Sergio Giani, and Rokia Sanogo. 2018. 'Phytochemical profile, antioxidant and antidiabetic activities of Adansonia digitata L.(Baobab) from Mali, as a source of health-promoting compounds', *Molecules*, 23: 3104.

Brandt, Kirsten, Lars Porskjær Christensen, J Hansen-Møller, SL Hansen, J Haraldsdottir, L Jespersen, S Purup, A Kharazmi, Vibeke Barkholt, and Hanne Frøkiær. 2004. 'Health promoting compounds in vegetables and fruits: A systematic approach for identifying plant components with impact on human health', *Trends in food science & technology*, 15: 384-93.

Briskin, Donald P. 2000. 'Medicinal plants and phytomedicines. Linking plant biochemistry and physiology to human health', *Plant physiology*, 124: 507-14.

Caddeo, C.; Nacher, A.; Vassallo, A.; Armentano, M.F.; Pons, R.; Fernàndez-Busquets, X.; Carbone, C.; Valenti, N.; Fadda, A.M.; Manconi, M. 2016. 'Effect of quercetin and resveratrol co-incorporated in liposomes against inflammatory/oxidative response associated with skin cancer', *International Journal of Pharmacology*, 513, 153–163.

Cherchar, H.; Faraone, I.; D'Ambola, M.; Sinisgalli, C.; Piaz, F.D.; Oliva, P.; Kabouche, A.; Kabouche, Z.; Milella, L.; Vassallo, A. 2019. 'Phytochemistry and Antioxidant Activity of Aerial Parts of Phagnalon sordidum L.', *Planta Medica*, 85, 1008–1015.

Cottiglia, F.; Bonsignore, L.; Casu, L.; Deidda, D.; Pompei, R.; Casu, M.; Floris, C. 2005. 'Phenolic constituents from Ephedra Nebrodensis', *Natural Product Research*, 19, 117–123.

Cooray, H.C.; Janvilisri, T.; Van Veen, H.W.; Hladky, S.B.; A Barrand, M. 2004. 'Interaction of the breast cancer resistance protein with plant polyphenols', *Biochemical and Biophysical Research Communications*, 317, 269–275.

DeFuria, Jason, Anna C Belkina, Madhumita Jagannathan-Bogdan, Jennifer Snyder-Cappione, Jordan David Carr, Yanina R Nersesova, Douglas Markham, Katherine J Strissel, Amanda A Watkins, and Min Zhu. 2013. 'B

cells promote inflammation in obesity and type 2 diabetes through regulation of T-cell function and an inflammatory cytokine profile', *Proceedings of the National Academy of Sciences*, 110: 5133-38.

Devari, S.; Jaglan, S.; Kumar, M.; Deshidi, R.; Guru, S.; Bhushan, S.; Kushwaha, M.; Gupta, A.P.; Gandhi, S.G.; Sharma, J.P.; et al. 2014. 'Capsaicin production by Alternaria alternata, an endophytic fungus from Capsicum annum; LC–ESI–MS/MS analysis', *Phytochemistry*, 2014, 98, 183–189.

Elekofehinti, OO, IG Adanlawo, JA Saliu, and SA Sodehinde. 2012. 'Saponins from Solanum anguivi fruits exhibit hypolipidemic potential in Rattusnovergicus', *Der Pharmacia Lettre*, 4: 811-14.

Flora, S. 2007. 'Role of free radicals and antioxidants in health and disease', *Cellular and Molecular Biology*, 53, 1–2.

Faraone, I.; Rai, D.K.; Russo, D.; Chiummiento, L.; Fernandez, E.; Choudhary, A.; Milella, L. 2019. Antioxidant, Antidiabetic, and Anticholinesterase Activities and Phytochemical Profile of Azorella glabra Wedd', *Plants*, 8, 265.

Faraone, Immacolata, Dilip K Rai, Daniela Russo, Lucia Chiummiento, Eloy Fernandez, Alka Choudhary, and Luigi Milella. 2019. 'Antioxidant, antidiabetic, and anticholinesterase activities and phytochemical profile of Azorella glabra Wedd', *Plants*, 8: 265.

Fernández-Sánchez, Alba, Eduardo Madrigal-Santillán, Mirandeli Bautista, Jaime Esquivel-Soto, Ángel Morales-González, Cesar Esquivel-Chirino, Irene Durante-Montiel, Graciela Sánchez-Rivera, Carmen Valadez-Vega, and José A Morales-González. 2011. 'Inflammation, oxidative stress, and obesity', *International journal of molecular sciences*, 12: 3117-32.

Ferre, P, and F Foufelle. 2010. 'Hepatic steatosis: a role for de novo lipogenesis and the transcription factor SREBP-1c', *Diabetes, obesity and metabolism*, 12: 83-92.

Fitzgerald, Michael L, Zahedi Mujawar, and Norimasa Tamehiro. 2010. 'ABC transporters, atherosclerosis and inflammation', *Atherosclerosis*, 211: 361-70.

Forbes-Hernández, Tamara Y, Francesca Giampieri, Massimiliano Gasparrini, Sadia Afrin, Luca Mazzoni, Mario D Cordero, Bruno Mezzetti, José L Quiles, and Maurizio Battino. 2017. 'Lipid accumulation in HepG2 cells is attenuated by strawberry extract through AMPK activation', *Nutrients*, 9: 621.

Gil-Ramírez, Alicia, Víctor Caz, Roberto Martin-Hernandez, Francisco R Marín, Carlota Largo, Arantxa Rodríguez-Casado, María Tabernero, Alejandro Ruiz-Rodríguez, Guillermo Reglero, and Cristina Soler-Rivas. 2016. 'Modulation of cholesterol-related gene expression by ergosterol and ergosterol-enriched extracts obtained from Agaricus bisporus', *European journal of nutrition*, 55: 1041-57.

Henriksen, Erik J, and Betsy B Dokken. 2006. 'Role of glycogen synthase kinase-3 in insulin resistance and type 2 diabetes', *Current drug targets*, 7: 1435-41.

Herzig, Sébastien, and Reuben J Shaw. 2018. 'AMPK: guardian of metabolism and mitochondrial homeostasis', *Nature reviews Molecular cell biology*, 19: 121.

Higashikuni, Y.; Sainz, J.; Nakamura, K.; Takaoka, M.; Enomoto, S.; Iwata, H.; Tanaka, K.; Sahara, M.; Hirata, Y.; Nagai, R.; et al. 2011.'The ATP-Binding Cassette Transporter ABCG2 Protects Against Pressure Overload-Induced Cardiac Hypertrophy and Heart Failure by Promoting Angiogenesis and Antioxidant Response', *Arteriosclerosis Thrombosis Vascular Biology*, 32, 654–661.

Hwang, Yu-Jin, Hae-Ri Wi, Haeng-Ran Kim, Kye Won Park, and Kyung-A Hwang. 2014. 'Pinus densiflora Sieb. et Zucc. alleviates lipogenesis and oxidative stress during oleic acid-induced steatosis in HepG2 cells', *Nutrients*, 6: 2956-72.

Hayes, J.; Allen, P.; Brunton, N.; O'Grady, M.; Kerry, J.P. 2011. 'Phenolic composition and in vitro antioxidant capacity of four commercial phytochemical products: Olive leaf extract (Olea europaea L.), lutein, sesamol and ellagic acid' *Food Chemistry*, 126, 948–955.

Ighodaro, OM, and OA Akinloye. 2018. 'First line defence antioxidants-superoxide dismutase (SOD), catalase (CAT) and glutathione peroxidase (GPX): Their fundamental role in the entire antioxidant defence grid', *Alexandria journal of medicine*, 54: 287-93.

Incalza, Maria Angela, Rossella D'Oria, Annalisa Natalicchio, Sebastio Perrini, Luigi Laviola, and Francesco Giorgino. 2018. 'Oxidative stress and reactive oxygen species in endothelial dysfunction associated with cardiovascular and metabolic diseases', *Vascular pharmacology*, 100: 1-19.

Jiang, Ping, Jia Xiong, Fei Wang, Mary H Grace, Mary Ann Lila, and Rui Xu. 2017. 'α-Amylase and α-Glucosidase Inhibitory Activities of Phenolic Extracts from Eucalyptus grandis× E. urophylla Bark', *Journal of Chemistry*.

Kanuri, Giridhar, and Ina Bergheim. 2013. 'In vitro and in vivo models of non-alcoholic fatty liver disease (NAFLD)', *International journal of molecular sciences*, 14: 11963-80.

Kaulmann, A.; Bohn, T. Carotenoids, inflammation, and oxidative stress—Implications of cellular signaling pathways and relation to chronic disease prevention. Nutr. Res. 2014, 34, 907–929.

Kawaguchi, Y.; Ochi, T.; Takaishi, Y.; Kawazoe, K.; Lee, K.-H. 2004. 'New Sesquiterpenes from Capsicum annuum', *Journal of Natural Products*, 67, 1893–1896.

Lekala, C.S.; Madani, K.S.H.; Phan, A.D.T.; Maboko, M.M.; Fotouo, H.; Soundy, P.; Sultanbawa, Y.; Sivakumar, D.; Fotouo, H. 2019. 'Cultivar-specific responses in red sweet peppers grown under shade nets and controlled-temperature plastic tunnel environment on antioxidant constituents at harvest', *Food Chemistry*, 275, 85–94.

Lamorte, Daniela, Immacolata Faraone, Ilaria Laurenzana, Luigi Milella, Stefania Trino, Luciana De Luca, Luigi Del Vecchio, Maria Francesca Armentano, Chiara Sinisgalli, and Lucia Chiummiento. 2018. 'Future in the Past: Azorella glabra Wedd. as a source of new natural compounds with antiproliferative and cytotoxic activity on multiple myeloma cells', *International journal of molecular sciences*, 19: 3348.

Lea, Tor. 2015. 'Caco-2 cell line', *The impact of food bioactives on health*: 103-11.

Leira, F, MC Louzao, JM Vieites, LM Botana, and MR Vieytes. 2002. 'Fluorescent microplate cell assay to measure uptake and metabolism of glucose in normal human lung fibroblasts', *Toxicology in vitro*, 16: 267-73.

Lima, C.F.; Fernandes-Ferreira, M.; Pereira-Wilson, C. 2006. 'Phenolic compounds protect HepG2 cells from oxidative damage: Relevance of glutathione levels', *Life Sciences*, 79, 2056–2068.

Liu, Qing, Stig Bengmark, and Shen Qu. 2010. 'The role of hepatic fat accumulation in pathogenesis of non-alcoholic fatty liver disease (NAFLD)', *Lipids in health and disease*, 9: 1-9.

Liu, Zhi-Qin, Ting Liu, Chuan Chen, Ming-Yan Li, Zi-Yu Wang, Ruo-song Chen, Gui-xiang Wei, Xiao-yi Wang, and Du-Qiang Luo. 2015. 'Fumosorinone, a novel PTP1B inhibitor, activates insulin signaling in insulin-resistance HepG2 cells and shows anti-diabetic effect in diabetic KKAy mice', *Toxicology and Applied Pharmacology*, 285: 61-70.

Loizzo, Monica R, Rosa Tundis, Federica Menichini, Giancarlo A Statti, and Francesco Menichini. 2008. 'Influence of ripening stage on health benefits properties of Capsicum annuum var. acuminatum L.: in vitro studies', *Journal of Medicinal Food*, 11: 184-89.

Loizzo, Monica Rosa, Alessandro Pugliese, Marco Bonesi, Damiano De Luca, Nora O'Brien, Francesco Menichini, and Rosa Tundis. 2013. 'Influence of drying and cooking process on the phytochemical content, antioxidant and hypoglycaemic properties of two bell Capsicum annum L. cultivars', *Food and chemical Toxicology*, 53: 392-401.

Luo, Jiao, Ning Wu, Bo Jiang, Lijun Wang, Shuaiyu Wang, Xiangqian Li, Baocheng Wang, Changhui Wang, and Dayong Shi. 2015. 'Marine bromophenol derivative 3, 4-Dibromo-5-(2-bromo-3, 4-dihydroxy-6-isopropoxymethyl benzyl) benzene-1, 2-diol Protects Hepatocytes from Lipid-Induced Cell Damage and Insulin Resistance via PTP1B Inhibition', *Marine drugs*, 13: 4452-69.

Marincas, O.; Feher, I.; Magdas, D.A.; Puşcaş, R. 2018. 'Optimized and validated method for simultaneous extraction, identification and quantification of flavonoids and capsaicin, along with isotopic composition, in hot peppers from different regions', *Food Chemistry*, 267, 255–262.

Marín, A.; Ferreres, F.; Tomás-Barberán, F.A.; Gil, M.I. 2004. 'Characterization and Quantitation of Antioxidant Constituents of Sweet Pepper (Capsicum annuumL.)', *Journal of Agricolture Food Chemistry*, 52, 3861–3869.

Mbondo, Naomi N, Willis O Owino, Jane Ambuko, and Daniel N Sila. 2018. 'Effect of drying methods on the retention of bioactive compounds in African eggplant', *Food science & nutrition*, 6: 814-23.

Miglionico, R.; Ostuni, A.; Armentano, M.F.; Milella, L.; Crescenzi, E.; Carmosino, M.; Bisaccia, F. 2017. 'ABCC6 Knockdown in HepG2 Cells Induces a Senescent-like Cell Phenotype', *Cellular Molecular Biology Letters*, 22, 517–526.Mignet, N.; Seguin, J.; Chabot, G.G. 2013. 'Bioavailability of Polyphenol Liposomes: A Challenge Ahead', *Pharmaceutics*, 5, 457–471.

Mohd Hassan, Norazian, Nurul Asyiqin Yusof, Amirah Fareeza Yahaya, Nurul Nasyitah Mohd Rozali, and Rashidi Othman. 2019. 'Carotenoids of capsicum fruits: Pigment profile and health-promoting functional attributes', *Antioxidants*, 8: 469.

Moudache, M.; Colon, M.; Nerín, C.; Zaidi, F. 2016. 'Phenolic content and antioxidant activity of olive by-products and antioxidant film containing olive leaf extract', *Food Chemistry*, 212, 521–527.

Muhammad, A.; Anis, I.; Ali, Z.; Awadelkarim, S.; Khan, A.; Khalid, A.; Shah, M.R.; Galal, M.; Khan, I.A.; Choudhary, M.I. 2012. 'Methylenebissantin: A rare methylene-bridged bisflavonoid from Dodonaea viscosa which inhibits Plasmodium falciparum enoyl-ACP reductase', *Bioorgoranic and Medicinal Chemistry Letters*, 22, 610–612.

Muhammad, A.; Tel-Çayan, G.; Öztürk, M.; Duru, M.E.; Nadeem, S.; Anis, I.; Ng, S.W.; Shah, M. 2016. 'Phytochemicals from Dodonaea viscosa and their antioxidant and anticholinesterase activities with structure–activity relationships', *Pharmaceutical Biology*, 54, 1–7.

Nagle, Cynthia A, Eric L Klett, and Rosalind A Coleman. 2009. 'Hepatic triacylglycerol accumulation and insulin resistance', *Journal of lipid research*, 50: S74-S79.

Newgard, Christopher B, Jie An, James R Bain, Michael J Muehlbauer, Robert D Stevens, Lillian F Lien, Andrea M Haqq, Svati H Shah, Michelle Arlotto, and Cris A Slentz. 2009. 'A branched-chain amino acid-related

metabolic signature that differentiates obese and lean humans and contributes to insulin resistance', *Cell metabolism*, 9: 311-26.

Noworyta-Sokołowska, Karolina, Anna Górska, and Krystyna Gołembiowska. 2013. 'LPS-induced oxidative stress and inflammatory reaction in the rat striatum', *Pharmacological reports*, 65: 863-69.

Nwanna, Esther E, Adeniyi A Adebayo, Ayokunle O Ademosun, and Ganiyu Oboh. 2019. 'Phenolic distribution, antioxidant activity, and enzyme inhibitory properties of eggplant (Solanum aethiopicum) cultivated in two different locations within Nigeria', *Journal of food biochemistry*, 43: e12797.

Ogunka-Nnoka, CU, BM Onyegeme-Okerenta, and HC Omeje. 2018. 'Effects of ethanol extract of S. aethiopicum stalks on lipid profile and haematological parameters of Wistar albino rats', *Int J Sci Res Methods Hum*, 10: 215-29.

Pascale, Raffaella, Maria A Acquavia, Tommaso RI Cataldi, Alberto Onzo, Donatella Coviello, Sabino A Bufo, Laura Scrano, Rosanna Ciriello, Antonio Guerrieri, and Giuliana Bianco. 2020. 'Profiling of quercetin glycosides and acyl glycosides in sun-dried peperoni di Senise peppers (Capsicum annuum L.) by a combination of LC-ESI (-)-MS/MS and polarity prediction in reversed-phase separations', *Analytical and Bioanalytical Chemistry*: 1-11.

Plazas, Mariola, Jaime Prohens, Amparo Noelia Cuñat, Santiago Vilanova, Pietro Gramazio, Francisco Javier Herraiz, and Isabel Andújar. 2014. 'Reducing capacity, chlorogenic acid content and biological activity in a collection of scarlet (Solanum aethiopicum) and gboma (S. macrocarpon) eggplants', *International journal of molecular sciences*, 15: 17221-41.

Ranilla, Lena Galvez, Young-In Kwon, Emmanouil Apostolidis, and Kalidas Shetty. 2010. 'Phenolic compounds, antioxidant activity and in vitro inhibitory potential against key enzymes relevant for hyperglycemia and hypertension of commonly used medicinal plants, herbs and spices in Latin America', *Bioresource technology*, 101: 4676-89.

Repa, Joyce J, Knut E Berge, Chris Pomajzl, James A Richardson, Helen Hobbs, and David J Mangelsdorf. 2002. 'Regulation of ATP-binding cassette sterol transporters ABCG5 and ABCG8 by the liver X receptors α and β', *Journal of Biological Chemistry*, 277: 18793-800.

Sales, Paloma Michelle, Paula Monteiro Souza, Luiz Alberto Simeoni, Pérola Oliveira Magalhães, and Dâmaris Silveira. 2012. 'α-Amylase inhibitors: a review of raw material and isolated compounds from plant source', *Journal of Pharmacy & Pharmaceutical Sciences*, 15: 141-83.

Salvia, A.M.; Cuviello, F.; Coluzzi, S.; Nuccorini, R.; Attolico, I.; Pascale, S.P.; Bisaccia, F.; Pizzuti, M.; Ostuni, A.2017. 'Expression of Some ATP-Binding Cassette Transporters in Acute Myeloid Leukemia', *Hematology Reports* , 9, 137–141.

Santoro, Valentina, Valentina Parisi, Massimiliano D'Ambola, Chiara Sinisgalli, Magnus Monné, Luigi Milella, Rosario Russo, Lorella Severino, Alessandra Braca, and Nunziatina De Tommasi. 2020. 'Chemical Profiling of Astragalus membranaceus Roots (Fish.) Bunge Herbal Preparation and Evaluation of Its Bioactivity', *Natural Product Communications*, 15: 1934578X20924152.

Segura, Julian, and Luis M Ruilope. 2007. 'Obesity, essential hypertension and renin–angiotensin system', *Public health nutrition*, 10: 1151-55.

Shen, S.; Callaghan, D.; Juzwik, C.; Xiong, H.; Huang, P.; Zhang, W. 2010. 'ABCG2 reduces ROS-mediated toxicity and inflammation: A potential role in Alzheimer's disease', *Journal of Neurochemistry*, 114, 1590–1604.

Sinisgalli, Chiara, Immacolata Faraone, Antonio Vassallo, Carla Caddeo, Faustino Bisaccia, Maria Francesca Armentano, Luigi Milella, and Angela Ostuni. 2020. 'Phytochemical Profile of Capsicum annuum L. cv Senise, Incorporation into Liposomes, and Evaluation of Cellular Antioxidant Activity', *Antioxidants*, 9: 428.

Sinisgalli, Chiara, Teresa Vezza, Patricia Diez-Echave, Angela Ostuni, Immacolata Faraone, Laura Hidalgo-Garcia, Daniela Russo, Maria Francesca Armentano, José Garrido-Mesa, and Maria Elena Rodriguez-Cabezas. 2020. 'The Beneficial Effects of Red Sun-Dried Capsicum annuum L. cv Senise Extract with Antioxidant Properties in Experimental Obesity are Associated with Modulation of the Intestinal Microbiota', *Molecular Nutrition & Food Research*: 2000812.

Speranza, G.; Scalzo, R.L.; Morelli, C.F.; Rabuffetti, M.; Bianchi, G. 2019. 'Influence of drying techniques and growing location on the chemical composition of sweet pepper (Capsicum annuum L., var. Senise)', *Journal of Food Biochemistry*, 43, e13031.

Sricharoen, P.; Lamaiphan, N.; Patthawaro, P.; Limchoowong, N.; Techawongstien, S.; Chanthai, S. 2017. 'Phytochemicals in Capsicum oleoresin from different varieties of hot chilli peppers with their antidiabetic and antioxidant activities due to some phenolic compounds', *Ultrasonics Sonochemistry*, 38, 629–639.

Stefan, Norbert. 2020. 'Causes, consequences, and treatment of metabolically unhealthy fat distribution', *The Lancet Diabetes & Endocrinology*, 8: 616-27.

Toral, Marta, Manuel Gómez-Guzmán, Rosario Jiménez, Miguel Romero, María José Zarzuelo, María Pilar Utrilla, Carlos Hermenegildo, Ángel Cogolludo, Francisco Pérez-Vizcaíno, and Julio Gálvez. 2015. 'Chronic

peroxisome proliferator-activated receptorβ/δ agonist GW0742 prevents hypertension, vascular inflammatory and oxidative status, and endothelial dysfunction in diet-induced obesity', *Journal of hypertension*, 33: 1831-44.

Tuberoso, C.; Serreli, G.; Montoro, P.; D'Urso, G.; Congiu, F.; Kowalczyk, A. 2018. 'Biogenic amines and other polar compounds in long aged oxidized Vernaccia di Oristano white wines', *Food Research International Journal*, 111, 97–103.

Tundis, R, MR Loizzo, and F Menichini. 2010. 'Natural products as α-amylase and α-glucosidase inhibitors and their hypoglycaemic potential in the treatment of diabetes: an update', *Mini reviews in medicinal chemistry*, 10: 315-31.

Tundis, Rosa, Monica R Loizzo, Federica Menichini, Marco Bonesi, Filomena Conforti, Giancarlo Statti, Damiano De Luca, Bruno de Cindio, and Francesco Menichini. 2011. 'Comparative study on the chemical composition, antioxidant properties and hypoglycaemic activities of two Capsicum annuum L. cultivars (Acuminatum small and Cerasiferum)', *Plant foods for human nutrition*, 66: 261.

Yahfoufi, Nour, Nawal Alsadi, Majed Jambi, and Chantal Matar. 2018. 'The immunomodulatory and anti-inflammatory role of polyphenols', *Nutrients*, 10: 1618.

Yang, Dachun, Zhidan Luo, Shuangtao Ma, Wing Tak Wong, Liqun Ma, Jian Zhong, Hongbo He, Zhigang Zhao, Tingbing Cao, and Zhencheng Yan. 2010. 'Activation of TRPV1 by dietary capsaicin improves endothelium-dependent vasorelaxation and prevents hypertension', *Cell metabolism*, 12: 130-41.

Yang, Ruiyi, Lu Wang, Jie Xie, Xiang Li, Shan Liu, Shengxiang Qiu, Yingjie Hu, and Xiaoling Shen. 2018. 'Treatment of type 2 diabetes mellitus via reversing insulin resistance and regulating lipid homeostasis in vitro and in vivo using cajanonic acid A', *International journal of molecular medicine*, 42: 2329-42.

Wahyuni, Y.; Ballester, A.R.; Sudarmonowati, E.; Bino, R.J.; Bovy, A.G. 2011. 'Metabolite biodiversity in pepper (Capsicum) fruits of thirty-two diverse accessions: Variation in health-related compounds and implications for breeding', *Phytochemistry*, 72, 1358–1370.

Wang, Thomas J, Martin G Larson, Ramachandran S Vasan, Susan Cheng, Eugene P Rhee, Elizabeth McCabe, Gregory D Lewis, Caroline S Fox, Paul F Jacques, and Céline Fernandez. 2011. 'Metabolite profiles and the risk of developing diabetes', *Nature medicine*, 17: 448-53.

Wang, X.; Hai, C.; Liang, X.; Yu, S.; Zhang, W.; Li, Y. 2010.'The protective effects of Acanthopanax senticosus Harms aqueous extracts against oxidative stress: Role of Nrf2 and antioxidant enzymes', *Journal of Ethnopharmacology*, 127, 424–432.

Watanabe, Ayako, Hiroaki Toshima, Hiroshi Nagase, Toshinori Nagaoka, and Teruhiko Yoshihara. 2001. 'Structural confirmation of 15-norlubiminol and 15-norepilubiminol, isolated from Solanum aethiopicum, by chemical conversion from lubimin and epilubimin, and their antifungal activity', *Bioscience, biotechnology, and biochemistry*, 65: 1805-11.

Wiciński, Michał, Maciej Socha, Maciej Walczak, Eryk Wódkiewicz, Bartosz Malinowski, Sebastian Rewerski, Karol Górski, and Katarzyna Pawlak-Osińska. 2018. 'Beneficial effects of resveratrol administration—Focus on potential biochemical mechanisms in cardiovascular conditions', *Nutrients*, 10: 1813.

Wlodek, Danuta, and Michael Gonzales. 2003. 'Decreased energy levels can cause and sustain obesity', *Journal of theoretical biology*, 225: 33-44.

Wong, Chin Piow, Toshio Kaneda, and Hiroshi Morita. 2014. 'Plant natural products as an anti-lipid droplets accumulation agent', *Journal of natural medicines*, 68: 253-66.

Wu, S.; Yue, Y.; Tian, H.; Li, Z.; Li, X.; He, W.; Ding, H. 2013. 'Carthamus red from Carthamus tinctorius L. exerts antioxidant and hepatoprotective effect against CCl4-induced liver damage in rats via the Nrf2 pathway', *Journal of Ethnopharmacology*, 148, 570–578.

Xavier, G.; Chandran, M.; George, T.; Beevi, S.N.; Mathew, T.B.; Paul, A.; Arimboor, R.; Vijayasree, V.; Pradeepkumar, G.T.; Rajith, R. 2014. 'Persistence and effect of processing on reduction of fipronil and its metabolites in chilli pepper (Capsicum annum L.) fruits', *Environmental Monitoring Assessment*, 186, 5429–5437.

Xia, Ning, Andreas Daiber, Ulrich Förstermann, and Huige Li. 2017. 'Antioxidant effects of resveratrol in the cardiovascular system', *British journal of pharmacology*, 174: 1633-46.

Yogendrarajah, P.; Van Poucke, C.; De Meulenaer, B.; De Saeger, S. 2013. 'Development and validation of a QuEChERS based liquid chromatography tandem mass spectrometry method for the determination of multiple mycotoxins in spices', *Journal of Chromatography A*, 1297, 1–11.

Zhao, Jian, Penghui Li, Tao Xia, and Xiaochun Wan. 2020. 'Exploring plant metabolic genomics: chemical diversity, metabolic complexity in the biosynthesis and transport of specialized metabolites with the tea plant as a model', *Critical reviews in biotechnology*, 40: 667-88.

Zhang, H.; Tsao, R. 2016. 'Dietary polyphenols, oxidative stress and antioxidant and anti-inflammatory effects', *Current Opinion Food Science*, 8, 33–42.

Ziouzenkova, Ouliana, and Jorge Plutzky. 2008. 'Retinoid metabolism and nuclear receptor responses: new insights into coordinated regulation of the PPAR–RXR complex', *FEBS letters*, 582: 32-38.